UNIVERSITY OF COPENHAGEN
FACULTY OF HEALTH AND MEDICAL SCIENCE

PhD thesis

Dorte Schou Nørøxe

DEPARTMENT OF ONCOLOGY, RIGSHOSPITALET

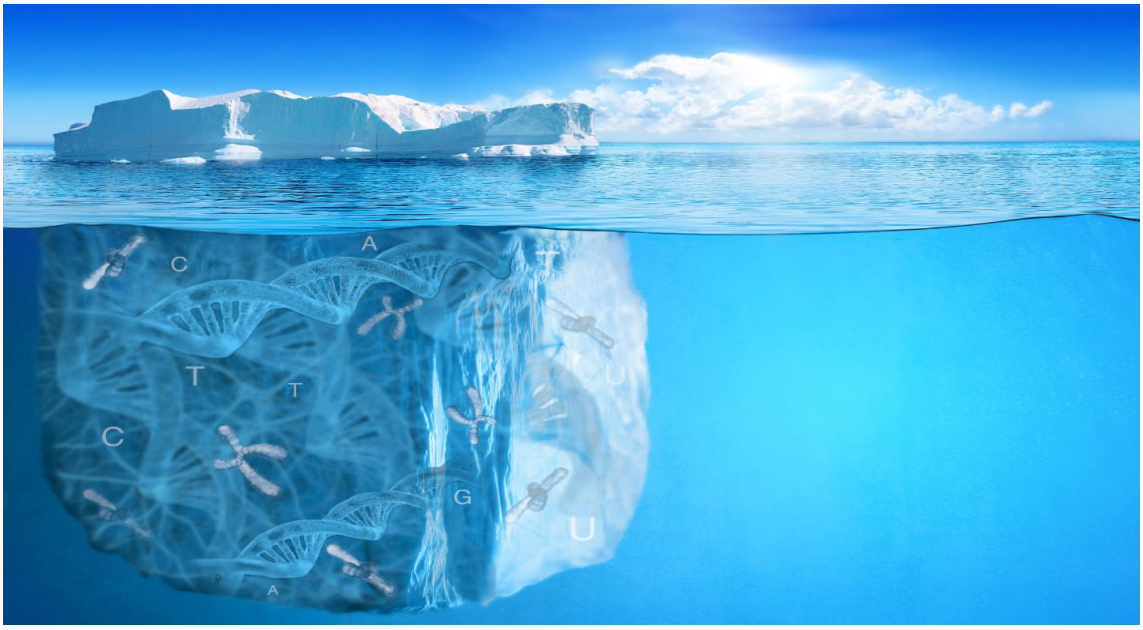

Genomic profiling and precision medicine in patients with glioblastoma

Translational oncology

This thesis has been submitted to the Graduate School of Health and Medical Science, University of Copenhagen, July 5th, 2019.

TITLE:	Genomic profiling and precision medicine in patients with glioblastoma Translational oncology
AUTHOR	Dorte Schou Nørøxe, MD
DEPARTMENT	Department of Oncology and Department of Radiation Biology Rigshospitalet, University of Copenhagen, Denmark
PRINCIPAL SUPERVISOR	Professor Ulrik Lassen, MD, PhD Department of Oncology, Rigshospitalet, University of Copenhagen, Denmark
CO-SUPERVISORS	Hans Skovgaard Poulsen, MD, DMSc Department of Oncology and Department of Radiation Biology, Rigshospitalet, University of Copenhagen, Denmark
	Professor Finn Cilius Nielsen, MD, DMSc Center for Genomic Medicine, Rigshospitalet, University of Copenhagen, Denmark
	Petra Hamerlik, MSc, PhD, associate professor Brain Tumor Group Danish Cancer Society Research Center
ASSESSMENT COMMITTEE	Professor Inge Marie Svane, MD, PhD, DMSc (Chairman) Department of Clinical Medicine, Herlev Hospital, University of Copenhagen, Denmark
	Professor Klaus Pantel, MD Center for Experimental Medicine, Institute of Tumor Biology, University Hospital Hamburg-Eppendorf, Germany
	Professor Bjarne Winther Kristensen, MD, PhD Department of Clinical Pathology, Odense University Hospital, University of Southern Denmark, Denmark
PHD PROGRAM	PCAP
PHD ENROLLMENT	April 1st, 2016
THESIS SUBMITTED	March 29th, 2019
THESIS RESUBMITTED	July 5th, 2019

Acknowledgements

Treatment of glioblastoma (GB) is truly multidisciplinary work as has also been the case with this PhD. I have worked with some inspiring people driven by curiosity and professionalism. I owe great thanks to my supervisors Ulrik Lassen, Hans Skovgaard, Petra Hamerlik and Finn Cilius Nielsen for making this large scaled project possible. Especially thank you to Ulrik and Hans for believing in me and facilitating the process by constructive talks, positive mindsets, incredible knowledge and professional supervision. I have had the pleasure of working with The Brain Cancer Research Group at The Danish Cancer Society headed by Petra Hamerlik. Christopher Meulengracht, Henriette Pedersen and lastly Monica Blomstrøm with whom I worked closely with by optimizing the system for the sample registration. Her approach to the work has been constructive and thorough. Also, a thank you to Mette Bruun-Pedersen for your nice and practical way of working. The learning curve has been steep in my daily contact with Center for Genomic Medicine with Christina Westmose Yde, Olga Østrup and Ane Yde Schmidt who have always been patient with a medical doctor like me, introducing me to a new field of research. They have contributed immensely in the labor-intensive work with the development of the genomic reports, helping to incorporate them into the clinic. Julie Buur Fisker, Maria Guschina, Aseeba Ayub and Miriam Yan Juk Guo from the laboratory and David Scheie and Heidi Ugleholdt from Department of Pathology have been essential in receiving, processing and analyzing the samples and have always been smiling and helpful. I came to work close with Joachim Weischenfeldt from The Finsen Laboratory and his postdoc Aidan Flynn. They have introduced me to new aspects of basic science in a friendly, patient and knowledgeable manner. I have also been fortunate by working closely together with the skilled neuro surgeons with Jane Skjøth-Rasmussen, Jannick Brennum and now Morten Ziebell. Jane has been my daily contact and I appreciate her as a person and as a colleague. I would also like to thank all the people around the patients; the CNS-team at Rigshospitalet, Hans Skovgaard, Aida Muhic, Søren Møller, Benedikte Hasselbalch, Henrik Roed and Thomas Urup for supporting this project that has included "their" patients. Vibeke Andrée-Larsen from Department of Neuro Radiology who took the time to help with imaging, also in the CheckMate trials. The radiation radiography staff who have all been helpful when I came to talk to the patients. Their curiosity for generating new knowledge for improving treatment in glioblastoma, has made the inclusion uncomplicated. A special thank you goes to Department of Radiation Biology where I have spent many hours through the years: Kirsten Grunnet, helping both in science and as a nurse at the CNS-team, Signe Regner Michaelsen for many talks, both serious and not so serious ones, plus constructive collaboration on the manuscripts, Mette Villingshøj for always taking time to talk and help, Camilla Bjørnbak Holst, Sarah Chehri, Maria Dinche Johansen, Mikkel Staberg, Simone Bendix Eibye, Ole Didrik Lærum and my office buddy Vinicius Araújo Barbarosa de Lima for pleasant company. I have also spent many hours at my desk in the basement which have been fun, enjoyable and educating by being surrounded by different fields in oncology; MDs, physicists and engineers, with each of their specific areas, making it a very diverse and stimulating place. Thank you to Line, Katrine, Thomas, Anne, Malene, Mikkel, Anne Sofie, Mirjana, Ivan, Mikkel, Michael, Anni,

Karin, Jacob, Katrin, Charlotte, Daniel, Christina, Thomas, Michael and all the rest. I have really enjoyed your company. Hugs to my office buddies in the basement, Gry Assam Taarnhøj, Lise Brehm Omland, Ida Viller Tuxen, Signe Skriver, Cecilie Hollænder-Mieritz, Lise Barlebo Ahlborn and Lotte Nygård. We have helped each other both personally and professionally. You are inspiring people and I look forward to working with you in the clinic. I send a special thank you to the patients. They have accepted inclusion even though they knew that the personal gain was minimal. Still, they wanted to help future patients by providing their tissue for scientific use. During the > 100 patient consultations I have had throughout this project, I have experienced another dimension of the physician-patient relationship since I was not the treating physician and I am glad that I could maintain the connection to the patients during three years of absence from the clinic. Lastly but not least, I owe a great thank you to my surroundings, family and friends, who have acted as an adjuvant for me, making this project an experience of a common goal. My family has always been and is everything for me. My three children, Agnethe, Naja and Ella have supported me in their own special ways, cheering on me without exactly knowing for what but always enthusiastic. And my husband, Kim who is a part of me, always supportive, ready to listen, participate in a qualified discussion, give a smile or a hug. Qujanaq, asavakkit.

Dorte Schou Nørøxe
29th of March 2019

Contents

SUMMARY IN ENGLISH 7

DANSK RESUMÉ 8

MANUSCRIPTS 10

ABBREVIATIONS 11

INTRODUCTION 13

1.1 Hypothesis and aims 14

BACKGROUND 15

2.1 Glioblastoma in the traditional context 15

2.1.1 Evaluation 17

2.2 Glioblastoma in the molecular context 18

2.2.1 Main scientific and translational results from genomic data 19

2.2.2 The 2016 WHO classification of brain tumors 21

2.2.3 Immuno therapy 21

2.2.4 Tumor growth, heterogeneity and clonal evolution 23

2.3 Biomarkers and liquid biopsies 25

2.3.1 Blood as a biomarker 25

2.4 Clinical impact of molecular biology 26

2.5 The molecular paradox 28

MATERIALS AND METHODS 29

3.1 The Copenhagen Glioblastoma Cohort 29

3.2 Patients and clinical information 30

3.3 Pathological analyses 31

3.4 Genomic analyses 31

3.5 Tumor size determination (study III) 36

3.6 Tumor board meeting (Study I and II) **36**

3.7. Statistical analyses **36**

SUMMARY OF RESULTS **37**

4.1 STUDY I: Genomic profiling in patients with newly diagnosed glioblastoma – a prospective, translational study **38**

4.2 STUDY II: Tumor mutational burden before and after treatment with Temozolomide in paired samples of glioblastoma **41**

4.3 STUDY III: Cell-free DNA in newly diagnosed patients with glioblastoma – a clinical prospective feasibility study **43**

DISCUSSION **45**

5.1 Genomic profiling gains access to trials **45**

5.2 Tumor mutational burden and chromosomal instability as prognostic markers **46**

5.3 Tumor heterogeneity and paired sampling (tumor purity) **46**

5.4 Tumor mutational burden and immunotherapy for a selected group **47**

5.5 Treatment monitoring using liquid biopsies **47**

5.6 Feasible and relevant in a daily clinical setting **48**

FUTURE PERSPECTIVES AND CONCLUSION **49**

REFERENCES **51**

FULL TEXT OF INCLUDED MANUSCRIPTS **55**

Summary in English

Glioblastoma (GB) is an incurable brain cancer with limited treatment options. GB can be diagnosed in the young as well and in the elderly, with a median age at diagnosis of approximately 65 years. For majority of cases, the etiology is unknown. GB has been studied extensively, including the comprehensive genomic profiling in 2008 by The Cancer Genome Atlas (TCGA) and many important projects have followed. Important prognostic and predictive biomarkers have been identified and incorporated in the clinic. Even though, first line treatment has not changed since 2005 and the overall survival (OS) remains 16-22 months. One explanation might be that projects have been carried out on archival tissue with insufficient or retrospectively collected information on previous treatment or isocitrate dehydrogenase (*IDH*) and/or O6-methyl-guanine-DNA-methyl-transferase (MGMT) status. Study I aimed at investigating the clinical utility of performing genomic profiling in newly diagnosed patients with GB with a clinical focus on targetable alterations and identification of patients for protocolled treatment. A total of 108 patients were included and we performed next generating sequencing analyses. All generated reports were discussed at biweekly tumor board meetings with participation of specialists involved in experimental treatment. The setup was clinically applicable with genomic results ready at first progression. Importantly, we identified one patient with a *NTRK2* fusion and the patient will be considered for a trial at our institution with a TRK inhibitor at progression. We fund that tumor mutational burden (TMB)-high and/or chromosomal instability (CI)-median was correlated with significantly worse survival. These results need validation but have potential for use in stratification in future clinical trials. Next, we investigated alterations in TMB/Megabase (Mb) and signature analyses in 35 paired samples before and after treatment with majority of patients receiving radio therapy/Temozolomide (TMZ). TMB increased with a factor 1.1 after treatment and no hypermutated samples were identified nor did we find evidence of development of a TMZ signature. Unsurprisingly, the most prevalent signature was the age-related AC1. Tumor purity in the relapse samples constituted a challenge when comparing TMB from the same patient and we had to exclude seven samples due to low tumor purity. Improved methods for optimizing sampling to ensure better tumor purity is needed as well as a standardized assay to analyze for TMB to better compare between studies and cancer types. Study III aimed at investigating the concentration of cell-free DNA (cfDNA) as a marker of response to treatment. Base-pair fragmentation analyses were performed, and we defined a base-pair peak ≤166 to have a high probability of containing tumor derived DNA. Eight patients were included, and plasma samples were collected prior to diagnostic surgery, prior to oncologic treatment, during treatment and until progression. We found that cfDNA increased before or at radiologic progression in 3/4 patients with progression and that cfDNA did not increase in 3/4 patients without progression. CfDNA levels could aid in all three cases of pseudo progression. CfDNA was an easy-accessible method with potential for further development as an add-on marker of response. In conclusion, we find that genomic profiling can improve treatment of GB and can be used for designing and stratifying patients for inclusion in experimental trials. We find that majority of patients with GB should enter clinical trials, preferably in an adaptive design with a marker-based approach due to the small number of patients.

Dansk resumé

Glioblastom (GB) er en uhelbredelig type hjernekræft med begrænsede behandlingsmuligheder. Den mediane alder ved diagnose er 65 år, men såvel unge som ældre kan få stillet diagnosen. For størstedelen af patienterne er ætiologien ukendt. Omfattende forskning er blevet udført indenfor GB, inklusive den første genomiske profilering udgået fra The Cancer Genome Atlas (TCGA) i 2008. Utallige banebrydende projekter er siden foretaget med identificering af prognostiske og prædiktive markører, der er implementeret i klinikken i dag. På trods af dette, har den primære behandling ikke ændret sig siden 2005 og overlevelsen er fortsat omkring 16-22 måneder. En af forklaringerne kan være, at tidligere projekter er udført på arkivvæv med utilstrækkelig information om tidligere givet behandling eller retrospektivt analyseret status for isocitrat dehydrogenase (*IDH*) og/eller O6-methyl-guanine-DNA-methyl-transferase (MGMT). Studie I undersøgte den kliniske anvendelighed af at udføre genomisk profilering i nydiagnosticerede patienter med GB. Vi fokuserede på genetiske ændringer, der kunne rammes med målrettet behandling i kliniske forsøg. Vi inkluderede i alt 108 patienter og alle patienter fik lavet en genomisk rapport baseret på next generation sequencing analyser. Rapporterne blev diskuteret hver anden uge på et tumor board møde med deltagelse af specialister involveret i eksperimentel behandling. Fremgangsmåden var mulig i en klinisk hverdag med resultater klar ved første tilbagefald. Vi identificerede en patient med en *NTRK2* fusion og patienten vil blive vurderet mhp indgang i et klinisk forsøg med en TRK-hæmmer ved progression. Vi fandt at høj tumor mutationsbyrde (TMB) og/eller median kromosomal instabilitet var signifikant korelleret til en dårligere overlevelse. Disse resultater skal valideres men har potentiale til brug for fremtidig stratificering i kliniske forsøg. Herefter undersøgte vi ændringer i TMB/Megabase (Mb) samt signatur analyser i 35 parrede prøver før og efter behandling hvor flertallet af patienterne havde modtaget radioterapi/Temozolomid (TMZ). TMB steg med en faktor 1,1 efter behandling uden identificering af hypermutation. Ligeledes fandt vi ikke udvikling af en TMZ-signatur. Ikke overraskende var den mest prævalente signatur, den aldersbetingede AC1. Det viste sig at nedsat tumor indhold i prøverne udgjorde en udfordring ved sammenligning af TMB fra hver patient og syv prøver blev ekskluderet alene pga manglende tumor indhold. Der er behov for at optimere indsamling af prøver for at sikre et renere indhold af tumor. Ligeledes er der behov for udvikling af en standardiseret måde hvorpå TMB kan måles, således at sammenligning mellem studier og mellem cancer typer bedre kan udføres. Studie III undersøgte hvorvidt koncentrationen af cellefrit DNA (cfDNA) var hensigtsmæssig som markør ved evaluering af behandlingsrespons. Vi udførte fragmentbestemmelse på basepar længde i hver prøve og definerede et cut-off ≤166 som værende stor sandsynlighed for at prøven indeholdt DNA fra tumor. Vi inkluderede i alt otte patienter og plasma prøver blev taget før diagnostisk operation, før start på onkologisk efterbehandling, under den onkologiske behandling og indtil patienten fik tilbagefald. Vi fandt at cfDNA koncentrationen steg før eller ved radiologisk tilbagefald i 3/4 patienter. Ligeledes steg koncentrationen af cfDNA ikke i 3/4 patienter uden tilbagefald og i alle tre tilfælde af pseudoprogression, kunne cfDNA koncentrationen guide i rigtig retning. CfDNA er en lettilgængelig metode med klinisk potentiale som tillæg til vurdering af behandlingsrespons. Vi konkluderer at genomisk profilering kan forbedre behandlingen af patienter med GB og kan bruges til at

stratificere patienter til kliniske lægemiddelforsøg. Størstedelen af patienter med GB bør indgå i kliniske forsøg med en markør-baseret tilgang og fortrinsvis i adaptive designs pga de små grupper af patienter.

Manuscripts

This thesis contains three manuscripts with one published, one in preparation for resubmission and one manuscript in preparation

STUDY I **Dorte Schou Nørøxe,** Christina Westmose Yde, Olga Østrup, Savvas Kinalis, Signe Regner Michaelsen, Jane Skjøth-Rasmussen, Jannick Brennum, Petra Hamerlik, Hans Skovgaard Poulsen, Ulrik Lassen. **Genomic profiling in newly diagnosed patients with glioblastoma – a prospective translational study.**
In preparation for resubmission

STUDY II **Dorte Schou Nørøxe≠**, Aidan Flynn≠, Christina Westmose Yde, Olga Østrup, Finn Cilius Nielsen, Jane Skjøth-Rasmussen, Jannick Brennum, Petra Hamerlik, Joachim Weischenfeldt, Hans Skovgaard Poulsen, Ulrik Lassen. **Tumor mutational burden before and after treatment with Temozolomide in paired samples of glioblastoma.**
≠Shared first authorship. Manuscript in preparation

STUDY III **Dorte Schou Nørøxe,** Olga Østrup, Christina Westmose Yde, Lise Barlebo Ahlborn, Finn Cilius Nielsen Signe Regner Michaelsen, Vibeke Andrée Larsen, Jane Skjøth-Rasmussen, Jannick Brennum, Petra Hamerlik, Hans Skovgaard Poulsen, Ulrik Lassen. **Cell-free DNA in newly diagnosed patients with glioblastoma – a clinical, prospective feasibility study.**
Published in Oncotarget 2019

REVIEW **Dorte Schou Nørøxe, Hans Skovgaard Poulsen, Ulrik Lassen. Hallmarks of glioblastoma: a systematic review.**
Published in Esmo Open 2016
Included as APPENDIX 1

Abbreviations

GB	Glioblastoma
WHO	World Health Organization
BBB	Blood Brain Barrier
RT	Radiotherapy
TMZ	Temozolomide
PFS	Progression-Free Survival
TCGA	The Cancer Genome Atlas
OS	Overall Survival
CI	Chromosomal Instability
TMB	Tumor Mutational Burden
WES	Whole Exome Sequencing
WGS	Whole Genome Sequencing
NGS	Next Generation Sequencing
cfDNA	Cell-free DNA
TTF	Tumor Treating Fields
EGFR	Epithelial Growth Factor Receptor
FDA	Food and Drug Administration
BEV	Bevacizumab
VEGFA	Vascular Endothelial Growth Factor A
IHC	Immunohistochemistry
RTK	Receptor Tyrosine Kinase
2-HG	2 Hydroxy-Glutarate
IT	Immuno Therapy
PD1i	Programmed Death1 inhibitor
FET/PET	(18)F-fluoro-ethyl-l-tyrosine positron emission tomography
(i)RANO	(immune related) Response Assessment in Neuro Oncology
MSI	Micro Satellite Instability
NTRK	Neurotrophin Tyrosin Receptor Kinase
FFPE	Formalin-Fixed-Paraffin-Embedded
RBGB	Regionernes Bio- og Genom Bank
MLPA	Multiplex Ligation-dependent Probe Amplification
(dd)PCR	(digital droplet) Polymerase Chain Reaction
SCNA	Somatic Copy Number Alteration
LOH	Loss of Heterozygosity
SCA	Segmental Chromosomal Aberration
NCA	Numerical Aberration

TERTp	Telomerase Reverse Transcriptase promotor
CE	Contrast Enhanced
CSF	Cerebrospinal fluid
ctDNA	circulating tumor DNA
bp	base-pair
NSCLC	Non-Small-Cell Lung Cancer
CRC	Colorectal Cancer
CTC	Circulating Tumor Cell
SNV	Single Nucleotid Variation
RCT	Randomized Clinical Trial
DKFZ	Deutsches Krebsforschungszentrum

1

Introduction

Throughout the years, glioblastoma World Health Organization (WHO) grade IV (GB) has had a central role in the neuro oncology research community and the clinic due to its complexity. Practically all phases in GB are challenging from high-risk surgery to the correct diagnosis, treatment planning to evaluation to lack of effective treatment options and therapy delivery across the blood brain barrier (BBB). On top of this, GB is incurable, the etiology is unknown and despite strong efforts, the treatment has not changed significantly since the game changing phase III trial from 2005 with the introduction of concurrent radio therapy (RT)/Temozolomide (TMZ) and adjuvant TMZ [1]. The incidence is 3.2/100.000 [2] with 2-300 new cases each year in Denmark. The median progression-free survival (PFS) and overall survival (OS) is 7-8 months and 16-22 months, respectively, depending on prognostic and predictive factors [3]. These challenges and lack of progress caused The Cancer Genome Atlas Group (TCGA) to choose GB to be the first cancer to undergo comprehensive genomic characterization in 2008 [4] and the tremendous work achieved in international collaborations like the TCGA, COSMIC, 1000Genome project and more contributed to a paradigm shift towards defining cancer as a dynamic disease of the genome with both genetic and epigenetic aberrations [5]. However, these large-scale databases might encompass some limitations that may partly explain the lack of clinical impact on survival. E.g. changes in diagnostic criteria with majority of samples collected between 1989-2011 with unknown or retrospectively analyzed isocitrate dehydrogenase (*IDH*) and O6-methyl-guanine-DNA-methyl-transferase (MGMT) promotor status, advances in high through-put technologies and lack of complete clinical information. Lastly, demographic sampling bias can dilute results since different ethnic groups can have a heterogenous genetic composition.

1.1 Hypothesis and aims

We wished to conduct a prospective collection of tissue from newly diagnosed patients with GB with the purpose of performing next generation sequencing (NGS) after implementation of the 2016 WHO diagnostic criteria and to include relevant clinical information. We hypothesized that this prospective Copenhagen Glioblastoma Cohort would be less biased by historical limitations. We defined the following three questions:

1. How is the genomic composition in prospectively collected tissue from newly diagnosed GB patients and can the results be used in a daily clinical setting?
2. How is the clonal evolution and changes in tumor mutational burden (TMB) in paired samples from the same patient before and after treatment exposure?
3. Can a blood-based biopsy aid in treatment evaluation?

To answer these questions, we designed and performed the following three studies:

Study I aim:
To investigate the prevalence of specific molecular aberrations in newly diagnosed GB patients linked together with clinical information. To investigate for genetic and clinical predictive and prognostic variables for OS with focus on chromosomal instability (CI), TMB and sub class division.

Study II aim:
To investigate the clonal evolution and changes in TMB in paired samples of GB before and after treatment exposure.

Study III aim:
To investigate the feasibility of using cell-free DNA (cfDNA) in the treatment course from diagnosis to progression.

2

Background

2.1 Glioblastoma in the traditional context

GB was first described in terms of histomorphology in 1865 by Rudolf Virchow. In 1926 Percival Baily and Harvey Cushing developed the basis for classification of GB [6]. Until 2016, the diagnosis was based solely on histomorphology with immunohistochemistry (IHC) with localization of necrosis, microvascular proliferation and mitosis. With the introduction of computed tomography (CT) in 1971 and magnetic resonance imaging (MRI) in 1982, non-surgical visualization of GB became possible. Treatment advanced from surgical removal only to adding RT to concurrent RT/TMZ with the possibility of proton therapy. Proton treatment has been offered in Denmark since January 2019 with opening of the Danish Center for Particle Therapy. The most recent GB-specific treatment approval was granted in 2015 for tumor treating fields (TTF) which is available in Denmark [7] (*figure 1*).

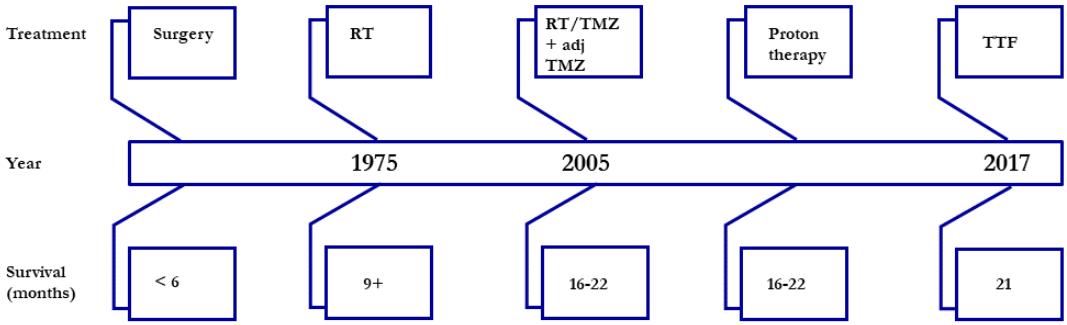

Figure 1. Timeline illustrating the most important historical development of treatment and survival for patients with glioblastoma. Abbreviations: RT: radio therapy; TMZ: Temozolomide; TTF: Tumor Treating Fields.

A list of selected pivotal trials that laid the basis for modern treatment in newly diagnosed GB patients can be seen in *table 1*.

Trial	**Phase / size**	**Primary endpoint**	**Intervention**	**PFS and OS (months)**	**Consequence**
Stupp (2005) [1, 3]	III / 573	OS	RT/TMZ+adj TMZ *vs.* RT	OS: 14.6 *vs.* 12.1	New first line
ACTIVATE (2010) [8]	II / 18	PFS and OS	Rindopepimut 4 weeks after RT/TMZ	OS: 26.0	Go for ACT III
ACT II (2011) [9]	II / 22	Immuno-genicity	Rindopepimut 4 weeks after RT/TMZ	PFS: 15.2 OS: 23.6	Go for ACT III
ACT III (2015) [10]	II / 65		Rindopepimut as add on to adj TMZ	PFS: 12.3 OS: 24.6	Go for ACT IV
ACT IV (2017) [11]	III / 745	OS	Rindopepimut as add on to adj TMZ	OS: 20.1 *vs.* 20.0	Terminated for futility
Nordic trial (2012) >60 years [12]	III / 291	OS	TMZ *vs.* 34Gy/10F *vs.* 60Gy/30F	TMZ/hypoRT/RT: 8.3 / 7.5 / 6.0 >70 years: TMZ+hypoRT> RT	Better treatment stratification (elderly)
AvaGlio (2014) [13]	III / 921	PFS and OS	BEV+RT/TMZ *vs.* placebo+RT/TMZ	PFS: 10.6 *vs.* 6.2 OS: 19.9 (not significant)	None (better QoL)
RTOG0825 (2014) [14]	III / 978	PFS and risk reduction for death	BEV+ RT/TMZ *vs.* placebo+RT/TMZ	PFS: 10.7 *vs.* 7.3 OS: 15.7 *vs.* 16.1	None (worse QoL)
Glarius (2016) [15]	II / 182	PFS rate at 6 months	BEV/RT plus adj BEV or Irinotecan *vs.* RT/TMZ plus TMZ	PFS (6): 79.3% *vs.* 42.6%. PFS 9.7 *vs.* 6.0 OS 17.5 *vs.* 16.6	None (no difference in QoL)
NeoTMZ (2017) ≤60 years [16]	Pilot / 114	OS	NeoTMZ/RT *vs.* RT	17.7 *vs.* 20.3	Terminated prematurely. OS longer in AA
Perry (2017) > 65 years [17]	III / 562	OS	40Gy/15F *vs.* RT/TMZ	OS: 7.6 *vs.* 9.3 MGMT predictive	Better treatment stratification (elderly)
TTF (2017) [7]	III / 695	PFS. OS secondary endpoint	TTF+TMZ after RT/TMZ *vs.* TMZ after RT/TMZ	PFS: 6.7 *vs.* 4.0 OS: 20.9 *vs.* 16.0	Approved for 1st line

Table 1. Selected pivotal trials in glioblastoma. Abbreviations: RT: radio therapy; adj: adjuvant; TMZ: Temozolomide; OS: overall survival; PFS: progression-free survival; BEV: Bevacizumab; QoL: quality of life; MGMT: O6-methul-guanine-DNA-methyl-transferase; TTF: tumor treating fields; neo: neoadjuvant; AA: anaplastic astrocytoma

Common for all the described treatment modalities are, that they are not targeted against specific alterations. Targeted treatment has been tested though, with the monoclonal antibody Cetuximab, targeting the epithelial growth factor receptor (EGFR) in relapse GB [18] or Bevacizumab (BEV), targeting the vascular endothelial growth factor A (VEGFA). BEV has been tried in different combinations in both first- and second line treatment but has only been approved for second line treatment by the Food and Drug Administration (FDA). We know that the treatment offered today is insufficient for cure and that a more stratified treatment approach is needed. Precision medicine based upon a personalized strategy seems promising.

2.1.1 Evaluation

Evaluation of GB was previously done by Response Evaluation Criteria in Solid Tumors (RECIST). In 1990 came the MacDonald criteria that incorporated 2D, contrast enhanced (CE) only, lesions [19]. With the introduction of antiangiogenic therapy such as BEV, limitations to the MacDonald criteria became evident since antiangiogenic therapy can reduce CE-lesions and cause non-CE lesions. Therefore, it was necessary to expand the evaluation criteria which was done in 2000 with the Response Assessment in Neuro Oncology (RANO) criteria [20] that are used today. RANO includes both CE and non-CE with ≥ 10 x 10 mm as defined to be measurable with a maximum of five target lesions. As was the case with the MacDonald criteria, both clinical condition and corticosteroid use is included (*table 2*). At our institution, we will consider using a (18)F-fluoro-ethyl-l-tyrosine positron emission tomography (FET/PET) if in doubt of progression to further evaluate and each case is discussed at a weekly multidisciplinary meeting with participation of neuro surgeons, neuro radiologists, neuro pathologists and neuro oncologists. Even though, interpretation can be difficult if there are many non-CE lesions on an MRI or to evaluate the degree of metabolic tissue on a FET/PET.

Criterion	**Complete response**	**Partial response**	**Stable disease**	**Progressive disease**
T1 – Gd+	None	≥50% ↓	<50% ↓ to <25% ↑	≥25% ↑
T2/FLAIR	Stable or ↓	Stable or ↓	Stable or ↓	↑
New lesions	None	None	None	Present
Corticosteroids	None	Stable or ↓	Stable or ↓	NA
Clinical status	Stable or ↑	Stable or ↑	Stable or ↑	↓
Requirement for response	All	All	All	Any

Table 2. Response assessment in neuro oncology (RANO) criteria for evaluation of glioblastoma patients using magnetic resonance imaging (MRI) [21].

2.2 Glioblastoma in the molecular context

Since the human genome project in 2001, the majority of human cancers have now been whole exome sequenced (WES) [22], resulting in targeted treatment across a variety of cancers. Tumor agnostic therapeutics have been approved for selected alterations like micro satellite instability (MSI)-high or *TRK*-fusions [23-25]. Targetable alterations have been identified in GB *(figure 2)*, but most are in preclinical trials and have not yet reached approval *(figure 3)* [22].

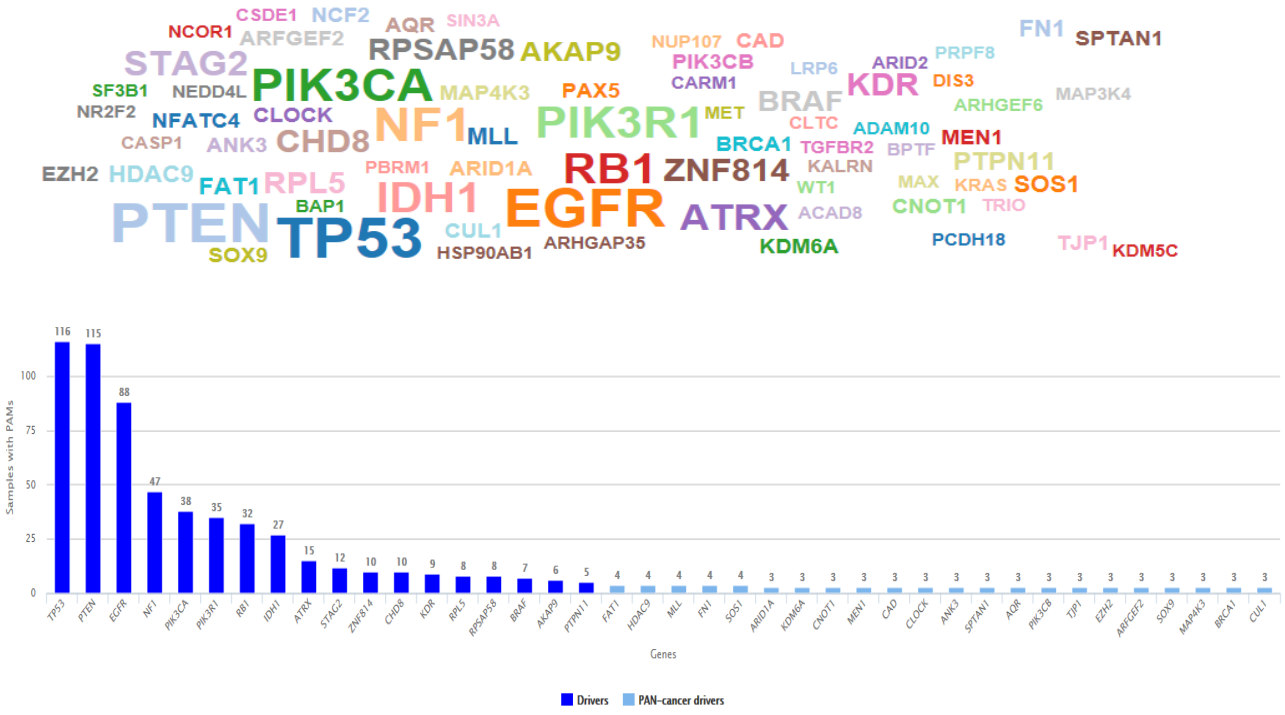

Figure 2.

Top: Driver cloud representing the prevalence of oncogenic drivers in glioblastoma. The size of the gene symbol is relative to the count of samples with a protein affecting mutation (PAM).

Bottom: Plot showing the same genes. Data based upon two projects with a total of 379 glioblastoma samples [26, 27]. *https://www.intogen.org/search?cancer=GBM#drivers* (*Assessed on the 20th of March 2019*)

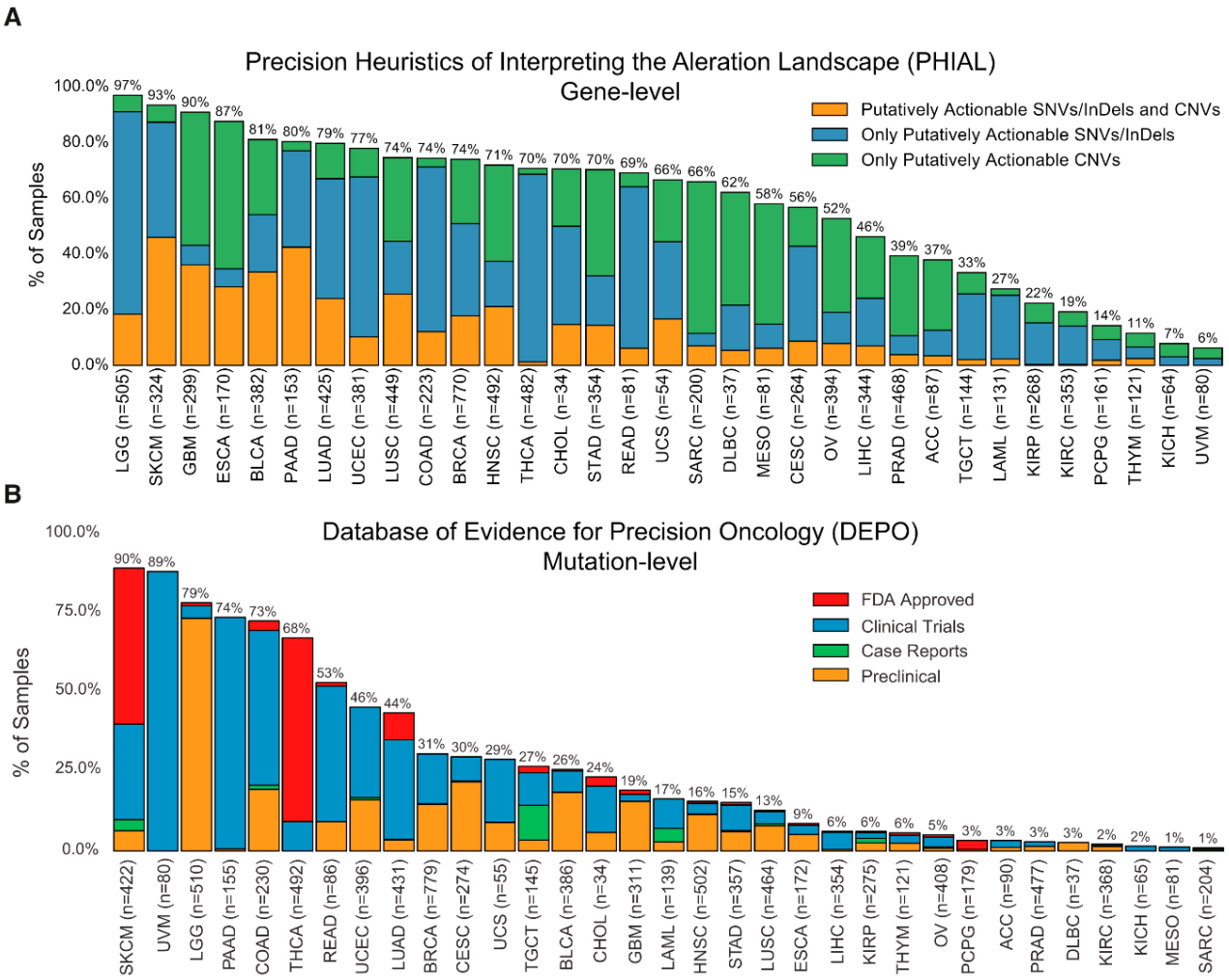

Figure 3. A: Putatively actionable single nucleotide variants (SN*Vs*)/Insertions/Deletions (InDels) and copy number variations (CN*Vs*) in different cancer types and it is illustrated that glioblastoma (GBM) has actionable alterations. B: Druggable mutations at different stages of approval by the Food and Drug Administration across different cancer types. Majority of the druggable mutations in glioblastoma is at the preclinical stage. Figure from [22] *[https://creativecommons.org/licenses/by-nc-nd/4.0/] (Assessed on the 28th of March 2019)*

2.2.1 Main scientific and translational results from genomic data

The greatest impact the genomic era has had on the way we define and treat cancer, is the shift to defining and treating cancer as a dynamic disease that is influenced by multiple factors, e.g. treatment pressure, viral exposure, the immune system, exogenous factors, hereditary cancer genes, the microbiome in the bowels and more. The impact of the omic-era in GB started with identification of MGMT-status as predictive of response to TMZ [3] which has had a key clinical impact and is used for inclusion criteria or stratification in clinical trials *(figure 4)*. Following, the identification of common altered genes like *PTEN, TP53, EGFR, NF1, PIK3CA, PIK3R1, RB1, IDH1* where most alterations

are deletions and/or loss of heterozygosity (LOH). *IDH*-status now defines a primary from a secondary GB with the latter occurring primarily in young patients and representing a better prognosis. *IDH*-mutated GB has a different biology with production of the oncometabolite 2-hydroxy-glutarate (2-HG) (*appendix 1*) which is being tested as a target in clinical trials. Until now, unfortunately with disappointing results. *IDH*-mutation is such a strong prognostic marker that the OS is worse in anaplastic astrocytoma (grade III), *IDH*-WT as compared to GB, *IDH*-mutated [28]. Pathway analyses have identified three core pathways affected, the receptor tyrosine kinase (RTK)/Ras/PI3K-signalling pathway, and the two tumor suppressor pathways p53 and RB1 [26, 29]. This work led to the identification of four subgroups based upon alterations in *PDGFRA, IDH1, EGFR* and *NF1* with the proneural-, classical-, mesenchymal- and neural subgroup [4]. The latter has since been categorized as normal brain tissue. Initially it was found that each subgroup responded differently to aggressive treatment, but later work found that the difference in response was mainly attributed to MGMT-status [29].

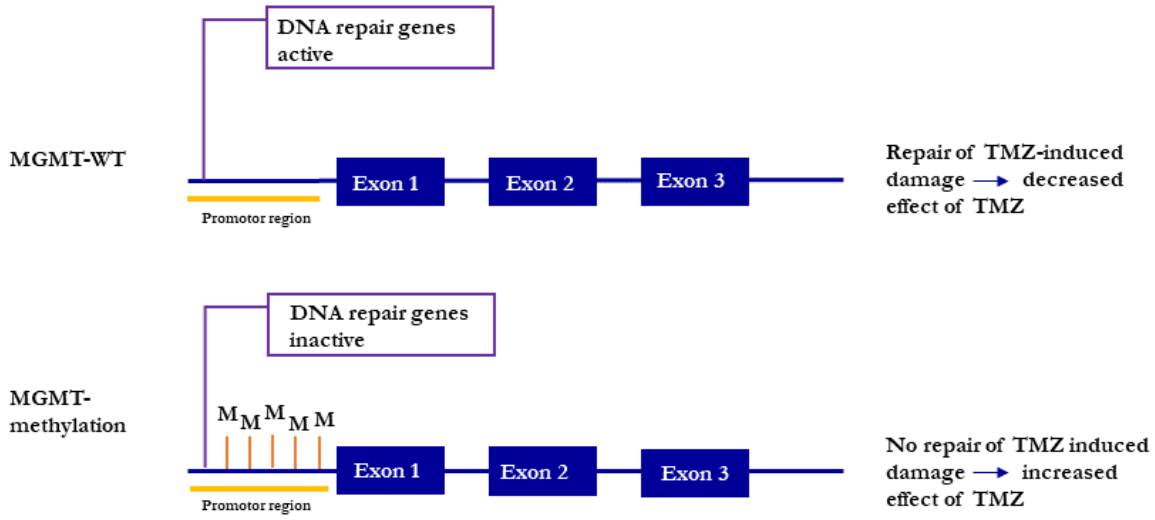

Figure 4. O6-methyl-guanine-DNA-methyl-transferase (MGMT) and transcription of DNA repair genes.
Top: The promotor region of MGMT is non-methylated causing an active gene transcription with DNA repair genes continuously repairing the DNA damage caused by Temozolomide (TMZ). This will decrease the effect of TMZ.
Bottom: The promotor region of MGMT is methylated causing an inactive transcription, why DNA repair genes cannot repair the damage caused by TMZ, increasing the effect of TMZ.

2.2.2 The 2016 WHO classification of brain tumors

With the growing advances in molecular genetics, a need for a more comprehensive diagnosis of brain tumors resulted in the 2016 WHO classification for brain tumors [5] with a layered diagnostic tool, beginning with the histomorphological diagnosis followed by a WHO grade and molecular analysis, resulting in an integrated diagnosis of GB into GB, *IDH*-WT, GB, *IDH*-mutated or GB, not otherwise specified (NOS) with the latter being reserved for laboratories without the necessary molecular analyses available. If discrepancy between the histomorphological and molecular diagnosis, the latter will dictate the diagnosis. New tools are being developed to aid in difficult cases with an important contribution being methylation profiling by 850K methylation, developed by the Heidelberg Group [30]. Cytosine-phosphate-Guanin (CpG) methylation is an epigenetic modification that serves as a regulator of gene transcription (illustrated by MGMT-status and DNA repair genes in *figure 4*) and the genome-wide methylation pattern from 850K methylation is compared to a continuously expanding reference and provides a likelihood of a diagnosis. The assay is especially helpful in rare entities and has been approved for difficult cases in Germany. It is being offered at two institutions in Denmark. The technology moves ahead so fast, that it is likely that suggestions for new brain tumor entities will be proposed continuously not waiting for a future revised WHO classification.

2.2.3 Immunotherapy

Immunotherapy (IT) has truly changed the clinical course for selected patients with melanoma, non-small-cell lung cancer (NSCLC) and kidney cancer and was granted breakthrough of the year in Science in 2013 [31]. TMB has been found predictive of response IT [32, 33] and TMB differs markedly in exogenous cancers like melanoma and NSCLC to endogenous cancers like GB which has a low TMB [34-36]. Until now, IT in GB has not had the same potential as in other cancer types but selected subgroups do show effect, e.g. patients with biallelic MMR deficiency [37, 38] and high TMB scores have been observed in some GB patients, making them potential candidates for IT. TMB is not (yet) approved as an indication for treatment with IT while the opposite is the case for Programmed Death1 Ligand (PDL1) expression in NSCLC in which a PDL1 expression $\geq$ 50% can lead to treatment with pembrolizumab in the first line setting and a PDL1 expression $\geq$ 1% can lead to treatment with nivolumab in the second line setting. However, there is a high degree of intra-observer variation when determining PDL1 expression with agreement rates of approximately 60% [39]. Unfortunately, there is also a high degree of assay-variability. The Blueprint Project therefore sought to compare four different assays [40]. The work has revealed both differences between the four assays but also great difference from cancer cells and immune cells making sampling bias relevant to consider when

interpreting a PDL1 result. PDL1 expression is currently the best marker available in the clinical setting but other markers must be evaluated, of which TMB is one candidate. Many IT-modalities for GB are available and have been tested, ranging from peptide and dendritic cell vaccines to viral therapy with polio to cytotoxic T-lymphocyte Antigen-4 (CTLA-4) to Programmed Death1 inhibitor (PD1i) *(appendix 1)*. Treatment with PD1i is being testing in two ongoing phase III trials for newly diagnosed GB *(table 3)*. A seen in other tumor types, pseudo progression during IT became a challenge due to influx of immune related cells and interpretation became insufficient with the RANO evaluation criteria. Hence, the iRANO criteria was developed and published in 2015 [41]. The most important information was that growth of (new) lesions, defined as progressive disease by the RANO-criteria, needs confirmation by a follow-up MRI, provided that the clinical condition of the patient is stable including a stable or decrease in corticosteroid dose.

Trial	Phase/study size	Primary endpoint	Intervention	Highlights (months)	Consequence
CA209-143 (2017) (NCT02017717)*	III / 369	OS	Nivo *vs.* BEV	PFS: 1.5 *vs.* 3.5 OS: 9.8 *vs.* 10.0	Exploratory for predictive value in subgroups
P*V*SRIPO (2018) [42]	I / 61	Toxicity and P2D	Intratumoral infusion of P*V*SRIPO	P2D: -1 OS. 12.5	Go for phase II
GAPVAC-101 ≠ (2019) [43]	**I / 15**	**Safety, tolerability, immunogenicity, feasibility**	**APVAC1 followed by APVAC2 with RT/TMZ**	**Safe and feasible OS: 29.0**	**Further development**
ReACT ≠ (ongoing) (NCT01498328) (EGFRvIII)	II / 127		BEV + Rindopepimut *vs.* standard	OS: 11.3 *vs* 9.3	Awaiting results
CA209-498 £ (ongoing) MGMT-WT (NCT02617589)	**III / 550**	**OS**	**RT/Nivo *vs.* RT/TMZ**	**Ended inclusion June 2017 (?).**	**Awaiting results**
CA209-548 £ (ongoing) MGMT-meth (NCT02667587)	**III / 693**	**OS and TMB**	**RT/TMZ plus Nivo/placebo**	**Ended inclusion May 2018 (?)**	**Awaiting results**

Table 3. Selected pivotal immunotherapy (IT) trials. Bold represents trials in newly diagnosed GB. *presented at the World Federation of Neuro-Oncology Societies (WFNOS) 2017. ≠Peptide vaccine. £ PD1i. Abbreviations: Nivo: Nivolumab; P*V*SRIPO: live attenuated poliovirus type 1 (Sabin) vaccine with its cognate internal ribosome entry site replaced with that of human (non-pathogenic) rhinovirus type 2; GAPVAC: Glioma Actively Personalized Vaccine Consortium; Programmed Death1 inhibitor: PD1i.

2.2.4 Tumor growth, heterogeneity and clonal evolution

A tumor evolves in a Darwinian manner and is largely dependent on the micro environment with proteins and cells supporting different levels of growth, migration and seeding [44, 45]. Since extracranial metastases are rare in GB [46], intracerebral spread occurs through invasion and migration to surrounding tissue with retrograde migration back to the tumor cavity after treatment. This is the main site of relapse [47, 48]. Before the possibility of genomic testing, cancers were essentially treated like a stable unit with a strategy of treating fast dividing cells, whether cancer cells or normal cells. Later it was appreciated that cancer is a dynamic, genomic and epigenomic disease and targeted treatment became preferable. However, resistance was developed, and strategies are now moving towards a combination of targeted plus non-targeted treatment. Still, treatment failure is happening and a major contributor to this is tumor heterogeneity and clonal evolution during treatment [49]. This was illustrated in the ACT-trials with the Rindopepimut vaccine. In these trials 67-97% of patients lost the expression of the targeted EGFRvIII after treatment [8, 10] and loss of MMR gene expression has been seen after RT/TMZ [50]. By performing multiple biopsies throughout a disease progression, it is possible to map the evolutionary process with detection of shared and/or private mutations for either the primary tumor or the metastatic site *(figure 5, unpublished data from study II)*. This might reveal genetic drivers for tumor formation, growth and migration. The TracerX and post mortem study PEACE and a renal cell carcinoma study are appropriate examples of heterogeneity studies with the latter demonstrating a private for primary, private for relapse or shared mutation profile of 23%, 20% and 22%, respectively [51, 52]. Hence, outgrowth of subclones or loss of targeted variants is possible. But multiple biopsies are not easily accessible in GB since brain tumor surgery is a high-risk procedure with risk of complications and is only performed for therapeutic indications. However, when performed, e.g. sampling bias and sequencing depth poses another obstacle since subclones can be present already at diagnosis but might not be surgically removed or not detected upfront by standard sequencing [53].

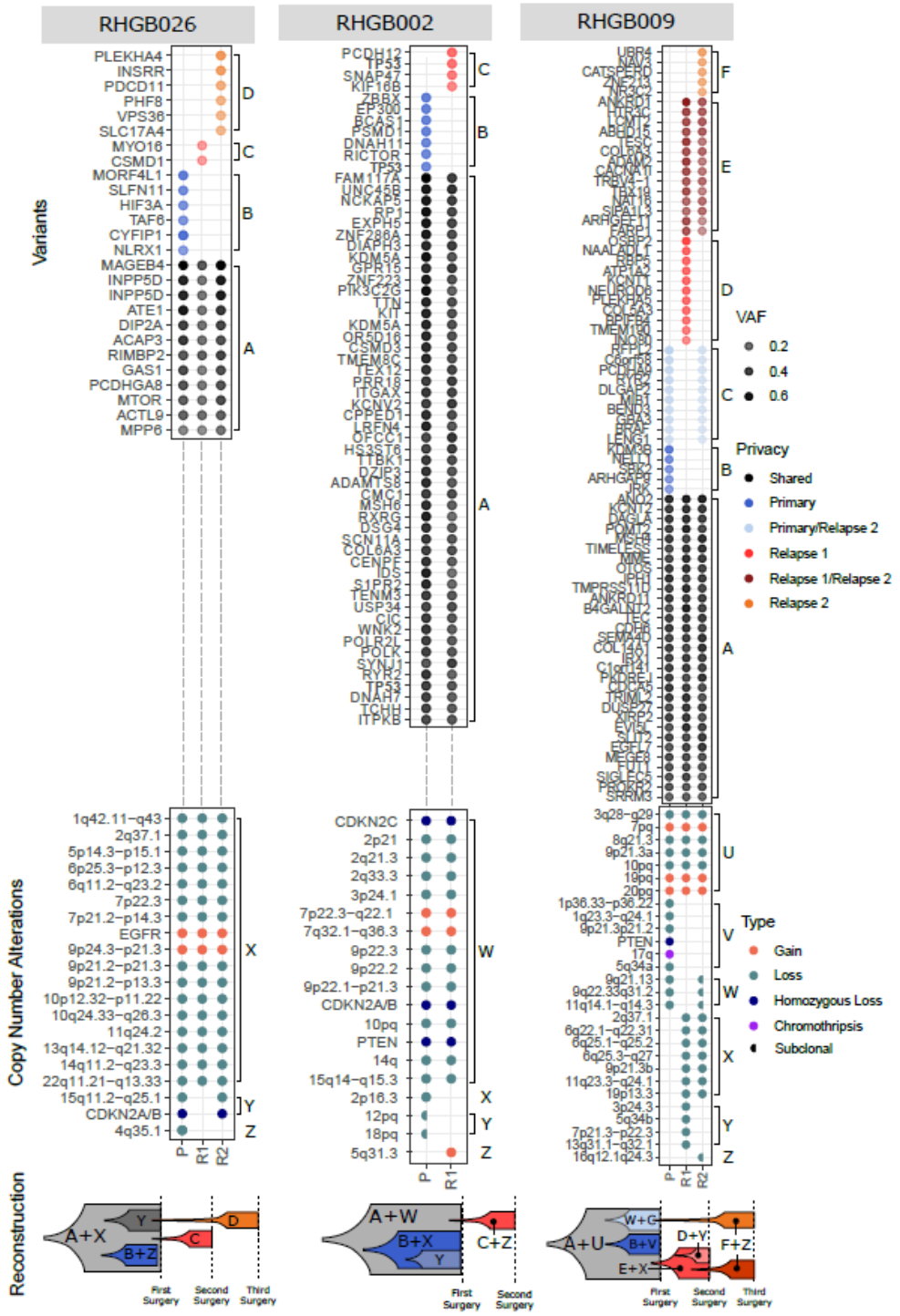

Figure 5. Clonal evolution in samples from three patients included in study II. Each column indicates a patient. RHGB026 had three surgeries (diagnostic and two relapse surgeries), RHGB002 had two surgeries (diagnostic and relapse) and RHGB009 had three surgeries (diagnostic and two relapse), respectively. In each column, variants (top) and copy number alterations (CNAs) are shown from each surgical procedure with shared *vs.* private alterations across the samples, indicated by colored dots as explained under "Privacy". Variant allele frequency (VAF) is indicated by the grey-scaled dots, as explained under "VAF". Types of CNAs are indicated by colored dots, as explained under "Type". *(Unpublished data.)*

2.3 Biomarkers and liquid biopsies

According to the REMARK guidelines, a biomarker should ideally reach abnormal levels in the development of GB, fluctuate during disease progression or regression and be predictive of treatment response [54]. For biomarker use, the cerebrospinal fluid (CSF) is an obvious example of a source for a liquid biopsy since the CSF circulates around the brain in close contact to the brain parenchyma and the tumor cells, especially if the tumor is adjacent to or is invading one of the ventricles. It is feasible to find GB-specific mutations in the CSF and it is more specific and sensitive than plasma samples [55-58]. A recently published study found a difference in sensitivity of 92.1% *vs.* 7.9% when detecting *TERT* promotor mutation in CSF *vs.* plasma, respectively [59] and *EGFR* could be detected with a sensitivity of 61% in extracellular vesicles in the CSF [60]. Other interesting fluids are urine or tear fluid which is even easier accessible than CSF or blood. Urine sampling though, is more relevant for extracranial cancers like bladder-, CRC or prostate cancer. Tear fluid is an interesting "liquid biopsy" and studies have shown difference in tear fluid proteins in patients with breast cancer as compared to healthy controls [61] but much research is still needed in this field.

2.3.1 Blood as a biomarker

A variety of methods are available to test for blood-based aberrations [62] and has already been evaluated in certain cancers like NSCLC with the *EGFR* T790M mutation or *ALK* translocation, cancer antigen (CA)-125 in ovary cancer, carcinoembryonic antigen (CEA) in colorectal cancer (CRC), the Philadelphia chromosome in chronic lymphatic leukemia and more [63-66]. Circulating tumor cells (CTCs) are new blood-based markers that represent an unbroken tumor cell with a retained cell membrane, cytoplasma and nucleus and thus a possibility to investigate both DNA, RNA and proteins. Minimal residual disease can be detected by the amounts of CTCs and it represent all detectable alterations in the tumor accounting for intra and inter tumor heterogeneity [67]. However, the amounts of CTCs in GB are limited to approximately 20-39% [68, 69]. A more accessible marker is the shedding of circulating cell free DNA (cfDNA), which includes DNA from normal cells as well as tumor cells [70-72] and is an easy, cost-effective method. Circulating tumor DNA (ctDNA) is costlier and requires complex, high through-put analyses. CtDNA measures specific tumor variants in the blood based upon e.g. single nucleotid variants (SN*Vs*), aneuploidy, amplifications or rearrangements and can be analyzed by e.g. digital droplet polymerase chain reaction (ddPCR) or WES. Several studies have shown that increased levels of a specific variant in the blood can be found significantly earlier than a radiologic or clinical progression, e.g. *BRAF, NRAS* and *KRAS* in solid tumors [73-75] but there is a distinct difference in detection levels for e.g. CRC and brain cancer.

However, ctDNA has been detected in brain cancer with *IDH* R132H or MGMT promotor methylation [76-78] but the greatest impact of both cfDNA/ctDNA has been in extracranial tumors [79]. Since cfDNA from tumor is more fragmented and shorter, size selection and -distribution can be used as strategies to distinguish tumor from normal DNA. [80-83]. Furthermore, in a sample with cfDNA, approximately 3-93% will come from tumor [84] and cfDNA can be used as a surrogate marker of tumor activity/burden. Shedding is increased according to tumor burden, necrosis and apoptosis [85] and sensitivity and specificity is important.

2.4 Clinical impact of molecular biology

As molecular genetics enters the daily clinical life, targeted trials are being offered. Below is a list of ongoing recruiting trials interesting for newly diagnosed GB patients *(table 4)*.

Trial (NCT)	Phase/study size	Primary endpoint	Intervention	Country
DEN-STEM	II/III / 60	PFS	DC-IT against cancer stem cell as add-on to RT/TMZ	Norway
EORTC-BTG-1709 (NCT03345095)	III / 750	OS	Marizomib/RT/TMZ *vs* RT/TMZ	Norway, Switzerland, Belgium, Netherlands, England, Spain, France
Intellance1 (NCT02573324) EGFR-amp	III / 640 (closed) Sub study phase I open for patients with hepatic impairment	OS	ABT-414/RT/TMZ *vs* RT/TMZ	Austria, Switzerland, Germany, Italy, Portugal, Ireland, Belgium, Netherlands, England, Spain, France
STEAM (NCT03224104) Elderly	I / 36	MTD and RP2D PFS (6 months)	TG02/RT *vs* TG02/TMZ	Switzerland, France
BGB290 (NCT03150862) Primary and relapse	Ib/II / 300	DLT, PFS and ORR	BGB290 as add on to RT or RT/TMZ	Switzerland, France
MRZ-112 (NCT02903069)	Ib / 72	MTD and RP2D	Marizonib as add on to RT/TMZ	Switzerland
GlioVax (NCT03395587)	II / 136	OS	DC vaccine as add on to RT/TMZ	Germany
N^2M^2 (NCT03158389)	I/II / 350	PFS (6 months)	Umbrella trial with 7 arms	Germany
AMG596 (NCT03296696) EGFRvIII pos Primary and relapse	I / 82	AE	Maintenance AMG596 after SOC	Germany, Netherlands, Spain, France
GBMTMZ/DOX2015 (NCT02758366)	II / 20	AE	Doxorubicin as add on to RT/TMZ	Italy
ADDIT-GLIO (NCT02649585)	I/II / 20	OS	DC as add on to TMZ after RT/TMZ	Belgium
CHLOROBRAIN	I / 13	MTD	Chloroquine as add on to RT/TMZ	Netherlands
AZD1390 (NCT03423628) Primary and relapse	I / 132	DLT	AZD1390 as add on to RT	England
GEINOGLAS (NCT03466450)	I/II / 75	MTD and OS	Glasdegib as add on to RT/TMZ	Spain
GEINO 1402 (NCT02270034)	I / 24	Safety	Crizotinib as add on to RT/TMZ	Spain
PAZOGLIO (NCT02331498)	I/II / 51	RP2D	Pazopanib as add on to TMZ after RT/TMZ	France

Table 4. A list of actively recruiting (targeted) trials in Europe in newly diagnosed adult patients with GB (non-surgical). Abbreviations: PFS: progression-free survival; DC: dendritic cell; IT: immune therapy; MTD: maximum tolerated dose; RP2D: recommended phase 2 dose; DLT: dose limiting toxicity; ORR: objective response rate; AE: adverse events; SOC: standard of care. *(Information gathered from www.clinicaltrials.gov). Assessed March 5th 2019)*

2.5 The molecular paradox

With the emerging technologies moving the next generation of genomic testing into WGS, proteomic, microbiomic etc, big data is being generated. We generate so much data that it can be difficult to translate it into the clinic and to the patients and truly demands international collaboration and focused research questions to be answered. It is a molecular paradox and what we know today is just the tip of the iceberg.

3

Materials and Methods

In the following, a short overview of material and methods is provided. Further details are described in the corresponding manuscripts (I-III.)

3.1 The Copenhagen Glioblastoma Cohort

The Copenhagen Glioblastoma Cohort included in this thesis, consists of newly diagnosed patients with GB treated at Rigshospitalet, University Hospital, Copenhagen in the period of February 2016 to August 2018. Study I-II included patients throughout the project period with a total of 108 patients. 35 patients underwent relapse surgery and signed a new informed consent with six patients having three surgeries in total. Study III included seven patients from the Copenhagen Glioblastoma Cohort and one patient that was not in the Copenhagen Glioblastoma Cohort. The inclusion period was from October 2017 to June 2018 with a total of eight patients. Inclusion criteria for study I-III were:

- ≥ 18 years
- Newly diagnosed GB
- No previous treatment for a secondary GB
- Surgical resection at Department of Neuro Surgery at Rigshospitalet, Copenhagen
- Signed informed consent

The project has been truly interdisciplinary with a fruitful cooperation between Department of Neuro Surgery, Center for Genomic Medicine, Danish Cancer Society, The Finsen Laboratory and Department of Oncology. Since 2013 the highly specialized Phase 1 unit at Rigshospitalet has performed NGS in a Genomic Profiling project on cancer patients with exhausted standard treatment options and a PS acceptable for experimental treatment. The program was planned for solid tumors but without GB. Until today > 1000 patients have been sequenced and 20% in a cohort of 500 patients, have been treated in experimental trials based upon matched treatment and genomic profiling [86]. From the beginning of the present PhD-project, we have built on this unique experience to include analyses for GB patients. 2016 was used for training, experience and adjusting the analyses to become GB-specific and all GB patients were included. Since January 2017, we included only patients upfront

eligible for RT/TMZ or 60Gy/30F as genomic profiling should have a therapeutic potential. If a patient progressed and was eligible for relapse surgery, we gathered a new informed consent and performed a new genomic report to investigate for tumor evolution and mechanisms of resistance. Tissue was collected in RNA-*later* whenever possible for optimal DNA and RNA purification. If tumor cells were insufficient or not enough material was available, we used formalin-fixed-paraffin-embedded (FFPE) tissue or snap frozen tissue. All three studies were carried out in accordance with the Declaration of Helsinki and with approval from the National Danish Ethics Committee (Journal number: H-3-2009-136 and 1707335 (study I-II) and H-17019401 (study III)) and Danish Data Protection Agency (Journal numbers: 2014-41-2857 and VD-2018-204, I-suite number: 6447 (study I-II) and RH-2017-269, I-Suite number: 05801 (study III)).

3.2 Patients and clinical information

Patients suspected of glioma signed an informed consent part A, at Department of Neuro Surgery and fresh tissue was collected and stored as described. If the patient was diagnosed with GB, a part B consent was collected when the patient came to Department of Oncology. The part B was more comprehensive and contained information regarding the molecular profiling, risk of secondary findings and level of information wanted. The consent was obtained during an interview with the patient and relatives for a more individualized and specified consultation. All patients but three accepted inclusion in study I and all patients identified and approached, accepted inclusion in study II and study III. If a patient had undergone relapse surgery, an interview was performed again to gather a new informed consent for the relapse tissue. For patients in study III, a study specific informed consent was collected prior to surgery. The following clinical information were gathered: symptoms prior to diagnosis, age at diagnosis, date of surgery and diagnosis, tumor location and extent of surgery, PS and corticosteroid dose prior to oncologic treatment, oncologic treatment, fulfilled planned treatment yes/no, relapse surgery yes/no, second line oncologic treatment, PFS and OS. Through 2016-2018, tissue was collected in collaboration with the Danish Cancer Society but since October 2018, we started a collaboration with the National Bio- and Genome Bank (RBGB) to which biological material from Danish patients has been collected since 2015. Now, tissue and blood from the GB patients are being stored at RBGB for optimal preservation and to secure the material for future research.

3.3 Pathological analyses

All samples underwent standard pathological examination according to the WHO diagnostic criteria [5] with IHC for GFA, map2, Olig2, *IDH*, p53, *ATRX* and Ki67 index. For patients < 55 years with normal *IDH*-status, sequencing was performed with Multiplex Ligation-dependent Probe Amplification (MLPA) of codon 132, 140 and 172. MGMT-status was assessed by polymerase chain reaction (PCR) with pyrosequencing (Qiagen) using a cut-off of 10%. When in doubt of diagnosis, 850K methylation with Infinium Methylation EPIC BeadChip array which targets >850.000 methylation positions in the human genome, was performed. In young patients and/or midline tumors and/or *IDH*-WT in combination with *ATRX*-loss, analysis for H3K27M with sequencing of H3F3A codon 28 to 35 with a sensitivity of 20% tumor cells was performed.

3.4 Genomic analyses

3.4.1 Whole exome sequencing

WES was performed using DNA from tissue and blood. DNA was extracted, isolated, purified and quantified and both tumor- and genomic DNA (200 ng) was fragmented to 300 bp. Paired-end sequencing (2x100 bp or 2x150 bp) was performed to gain an average coverage of 50-100x, using the HiSeq2500 or NextSeq500 platforms from Illumina and raw sequencing data were processed. Reads were aligned to the human reference genome (hg19/GRCh37) using CLC Biomedical Genomics Workbench (Qiagen), and variant calling was performed above 10% frequency in the tumor DNA. Somatic variants were identified by excluding variants found in blood WES data from the patient, and further analyzed using Ingenuity Variant Analysis (Qiagen). Based on data from COSMIC and TCGA, we designed a list of frequently mutated genes in GB and applied the list for filtration in Ingenuity. If the list was prolonged, every sample was rerun in Ingenuity for mutation calling of the added genes. Mutations were categorized based on the likelihood of being pathogenic [87]. An example of a genome browser view and examples of mutation calling is shown in *figure 6*.

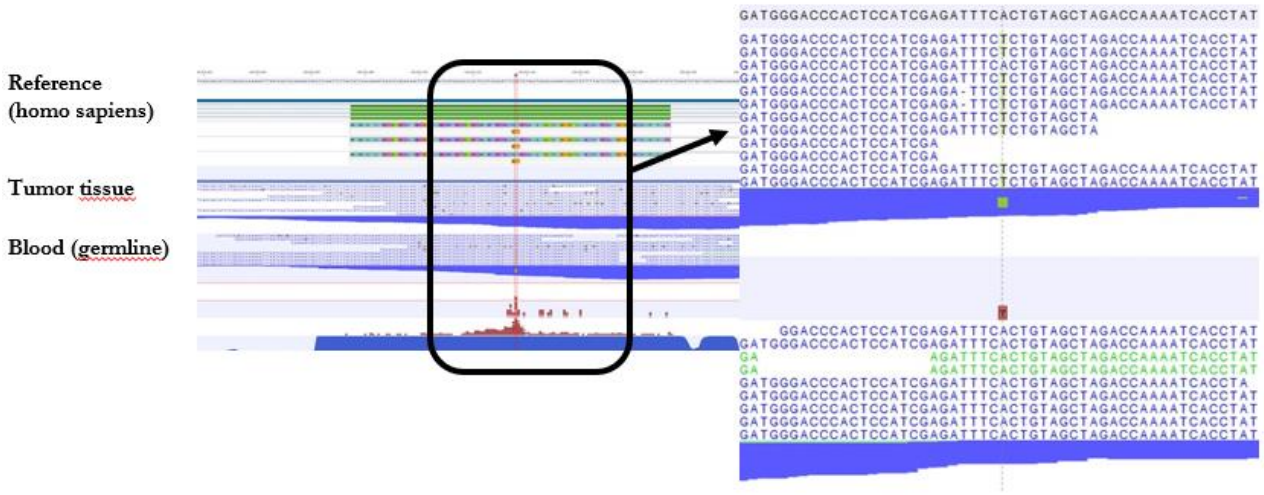

Chr	Position	Gene region	Gene symbol	Transcript variant	Protein variant	Translation impact
10	89692849	Exonic	PTEN	c.333G>A	p.W111*	Stop gain
17	29665752	Exonic	NF1	c.6789_6792delTTAC	p.Y2264fs*5	Frameshift
17	7578406	Exonic	TP53	c.128G>A	p.R136H	Missense
3	178947827	Exonic	PIK3CA	c.2702G>T	p.C901F	Missense
13	48934263	Exonic	RB1	c.718A>T	p.K240*	Stop gain
7	55241708	Exonic	EGFR	c.1997G>C	p.G666A	Missense

Figure 6. Top: Genome browser view with identification of a somatic *BRAF* variation from tumor/normal pair. The reference homo sapiens sequence, tumor and blood sample, respectively. An enlarged part of the genome browser view with visualization of the A>T mutation. The mutation is not present in the blood sample hence, it is a somatic mutation. Bottom: Examples of selected mutation callings from the patients in the Copenhagen Glioblastoma Cohort.

3.4.2 Analysis of somatic copy number alterations (study I-II)

CytoScan assay (Affymetrix, Santa Clara, USA) was performed on tumor samples and OncoScan assay (Affymetrix, Santa Clara, USA) for analysis of FFPE DNA material was performed. OSCHP files from OncoScan and .CEL files from the CytoScan assay were imported into NEXUS v8.0 (BioDiscovery) and used for the analysis and visualization of somatic copy number alterations (SCNA) and loss of heterozygosity (LOH). SCNAs (loss, gain, biallelic loss, or high amplification) and LOH calls for each sample were confirmed by visual inspection and followed by manual interpretation of whole-exome profiles (*figure 7*). Tumors were assessed for chromosomal instability (CI). The tumor was assigned as CI if it displayed in total more than 15 SCNA; i.e. segmental chromosomal aberrations (SCA) and/or numerical aberrations (NCA).

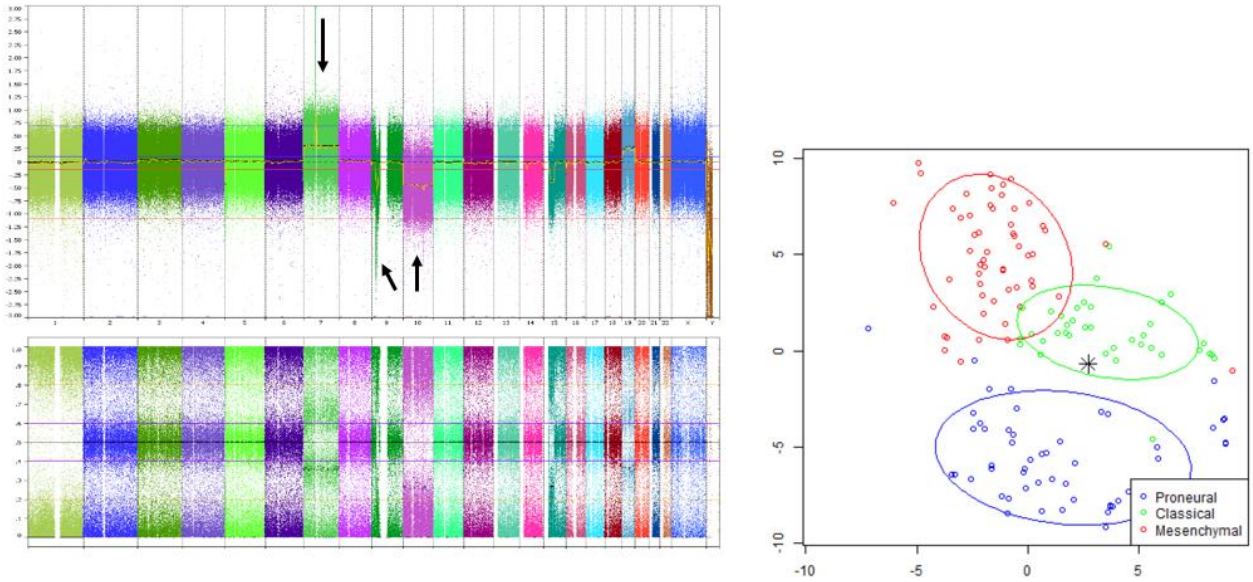

Figure 7. Left: SNP-array (CytoScan) from a patient in the Copenhagen Glioblastoma Cohort. Chromosomes 1-23. The patient had an amplification (amp) of chromosome (chr) 7 (*EGFR*), loss of chr 9 (*CDKN2A/B*) and chr 10 (*PTEN*). Right: Subclass analysis. Amp of chr 7/loss of chr 10 is typical for the classical subtype as was the case with this patient.

3.4.3 Gene expression analysis (Study I and II)

RNA was reverse-transcribed and used for cRNA synthesis, labelling and hybridization with GeneChip® Human Genome U133 Plus 2.0 Array (Affymetrix). Arrays were washed, stained and scanned in the Affymetrix GeneArray 3000 7G scanner to generate fluorescent images. Cell intensity files (.CEL files) were generated in the GeneChip Command Console Software (AGCC; Affymetrix).

3.4.4 Fusion analyses (Study I)

RNA-sequencing was done using TruSeq Stranded Total RNA Library Prep Kit and RNA was sequenced on a NextSeq500 (Illumina). Raw sequencing data from the Illumina sequencing platforms were processed with CASAVA-1.8.2. FusionMap bioinformatics tool (Array Suite) was used for screening of fusion transcripts as previously published (Ref: Ge H., Liu K., Juan T., et al: FusionMap: detecting fusion genes from next-generation sequencing data at base-pair resolution. Bioinformatics 2011; 27: pp. 1922-1928).

3.4.5 Tumor mutational burden (study I)

The following method was used for study I, performed at Center for Genomic Medicine, Rigshospitalet: Paired end sequencing reads with a length of 150 bp were aligned against the GRCh37.p13 reference genome using bwa mem 0.7.15. Somatic variants were called using Mutect2

according to the GATK best practices for somatic short variant discovery using GATK 4.0.10.1. Variants filtered by Mutect2 and variants annotated with an allele frequency > 5 % in gnomAD were excluded from the call set. The variants were further hard filtered by only including SN*Vs* and INDELs in coding regions. Finally, variants called at sites with a coverage of less than 10x and an allele depth of less than 5x were excluded. The tumor mutation burden was calculated as the number of non-filtered variants divided by the number of bases with a coverage of > 10x in all coding regions of the genome. Tumor mutational burden (TMB) estimates were reported as per megabase (Mb).

3.4.6 Tumor mutational burden (study II)

The following method was used for study II at The Finsen Laboratory, BRIC: For each surgical time-point, variant sites detected by MuTect were assessed in all matched patient samples using Samtools mpileup (v1.8). To ensure optimal sensitivity when comparing tumour mutation burden (TMB) between surgeries, any variant supported by two or more reads in a paired sample was considered present. To compensate for differences in sensitivity arising from tumour purity we computed a scaling factor between samples with differing purity. First a density distribution was computed for the variant allele frequencies (VAFs) of each sample using a gaussian kernel. The peak representing clonal heterozygous mutations was determined by selecting the peak at the greatest VAF (pkVAF) where the magnitude of the peak was at least one-third of the highest magnitude peak present. The difference in pkVAF values between paired samples was calculated and the value was subtracted from VAF of all variants in the sample with the greater pkVAF. Any variants with a negative VAF were considered to be below the artificial detection threshold and removed. A scaling factor was determined using the ratio of the raw TBM to the filtered TMB. The raw TMB of the sample with the lesser pkVAF was multiplied by the adjustment factor to obtain the adjusted TMB.

3.4.7 Signature analyses (Study II)

Linear combination decomposition analysis was performed using the YAPSA package (v1.8) (Huebschmann D, Gu Z, Schlesner M (2018). YAPSA: Yet Another Package for Signature Analysis. R package version 1.8.0. [https://rdrr.io/bioc/YAPSA/]) for the R statistical framework. Mutation contexts were determined based on the UCSC HG19 genome via the BSgenome (BSgenome.Hsapiens.UCSC.hg19) package for R. A signature cut-off of 1% was used to filter any signature that did not account for at least 1% of the mutations across the cohort.

3.4.8 TERT promotor status (Study I)

Telomerase Reverse Transcriptase promotor region (TERTp) mutation was determined using Sanger sequencing for the two most common mutations; c.-124C>T and c.-146C>T.

3.4.9 Subclass determination (Study I)

In house developed classifier based on the study data (E-GEOD-68850) [88] was used to assign the tumor into one of the three subtypes of interest (Classical, Mesenchymal and Proneural). The raw intensity .CEL files were preprocessed and gene summaries were extracted. The expression values of 4324 classifier genes were standardized across samples. A sample was considered to belong to a subtype when its corresponding Gaussian model gave the maximum probability density among the rest of the models and was greater than 0.001. Since subclass division was based upon expression analysis, tissue preserved in FFPE and hence RNA degradation, could not be divided into these and was noted N/A. *(Figure 7).*

3.4.10 cfDNA concentration and base pair detection (study III)

Peripheral blood was collected in cell-stabilizing Blood Collection Tubes (BCT; Streck Laboratories, Omaha, NE, USA). CfDNA was extracted from 4 ml plasma using the QIAsymphony Circulating DNA Kit (Qiagen, Hilden, Germany). Quantification of cfDNA was performed using the dsDNA HS Assay Kit on a Qubit Fluorometer (Thermo Fisher Scientific, Waltham, MA). CfDNA fragment distribution was assessed using the 4200 TapeStation System (Agilent). A distribution with fragment sizes and corresponding maximum peaks was generated. The peak of the curve with the highest % of fragments, was defined as the highest peak. *(Figure 8).*

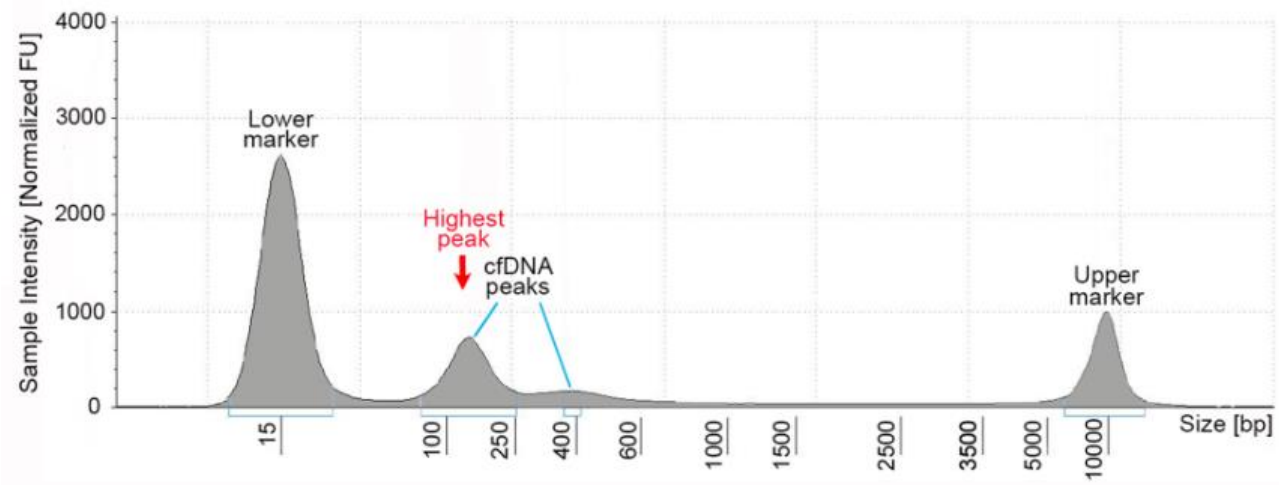

Figure 8. Fragment size distribution with a lower and higher ladder as reference, assessed using the Tape Station instrument. The peak of the curve with the highest amounts of fragments, was assigned as the base-pair peak.

3.5 Tumor size determination (study III)

A trained, senior neuro radiologist noted contrast enhanced (CE), measurable tumor of each MRI. We paired cfDNA concentration with tumor size if both were performed within 14 days of each other except for the MRI performed <48 hours after surgery which was paired with the cfDNA concentration one month after surgery without any treatment initiated.

3.6 Tumor board meeting (Study I and II)

A genomic report was generated for each included patient and results were discussed biweekly at a tumor board meeting with representation of experts from molecular oncology, bioinformatics, pathology, medical genetics and medical oncology. Each report was discussed regarding possible targetable alterations.

3.7. Statistical analyses

OS and PFS were estimated using the Kaplan-Meier method. Comparison of selected genes with SCNA´s (biallelic loss, amplification, LOH, deletion and LOH) and clinical characteristics, including comparison of selected genes with biallelic loss or amplification and completing RT/TMZ were calculated using the Fisher´s exact test. For univariate and multivariate analyses and OS, we used the Cox proportional hazards model. Results were presented as hazard ratios (HR) with 95% confidence interval (CI). P-values <0.05 were considered significant. Statistical analyses were done using SPSS (v.25.0) and RStudio (v.3.5.2).

4

Summary of results

An overview of the three included studies with patients, methods and main findings is listed in *table 5*.

Design	Patients and methods	Highlighted findings
	STUDY I	
Prospective	108 newly diagnosed patients from February 2016 to August 2018 (The CGC). Tissue in RNA-*later*, snap frozen or as FFPE was analyzed with WES, snp-array, RNAseq, expression analyses, Sanger- and hot spot sequencing	One *NTRK2* and three *FGFR3-TACC3* fusions were identified SCNA´s and mutations in genes previously described with new findings in *GRB2* and *SMYDA* TMB and CI predictive of outcome. Clinical trials are urgently needed as targetable alterations are already present
	STUDY II	
Prospective	35 paired samples from the CGC. Six patients had three sample from three surgeries. Samples underwent tumor purity adjustments (for TMB comparison), TMB- and signature analyses.	10 paired samples (28.6%) excluded for TMB comparison, mainly due to low tumor purity TMB/Mb increased with a factor 1.1 after treatment. No hypermutation nor TMZ-signature (AC11) was identified The age-related signature (1AC) was the most prevalent Strategies for optimizing tumor purity and for standardization of TMB is needed
	STUDY III	
Prospective	8 patients with 7 from the CGC. Plasma samples were analyzed for cfDNA concentrations (ng/ml) and fragment size (base pair peaks)	cfDNA increased in 3/4 patients with progression cfDNA did not increase in 3/4 patients without progression cfDNA could aid in 3/3 questionable cases of pseudo progression

Table 5. Overview of studies included in the thesis. Abbreviations: CGC: Copenhagen Glioblastoma Cohort; FFPE: formalin-fixed-paraffin-embedded; WES: whole exome sequencing; snp: single nucleotide polymorphism; SCNA: somatic copy number alteration; TMB: tumor mutational burden; CI: chromosomal instability.

4.1 STUDY I: Genomic profiling in patients with newly diagnosed glioblastoma – a prospective, translational study

The aims were to map the genomic composition in a cohort of newly diagnosed GB patients after the 2016 WHO classification of brain tumors and to investigate for predictive and prognostic factors. In study I we included 108 newly diagnosed patients in the Copenhagen Glioblastoma Cohort over a 2½ year period. All patients were diagnosed with GB according to the 2016 WHO classification for brain tumors and we performed WES, SNP-array, RNA-sequencing, expression analyses, Sanger sequencing, fusion- and subgroup analyses and determination of TMB and CI. In parallel, a blood sample was collected to retract for germline variants, relevant clinical information was gathered through patient interviews and PFS and OS were subsequently calculated. The included patients consisted of a standard population admitted to an oncologic department with 83 patients (76.9%) receiving RT/TMZ followed by adjuvant TMZ. At time of the inclusion period, our department participated in two international phase III trials, the CheckMate-498 and CheckMate-548 studies, and 10 patients (9.3%) were enrolled in these. Main findings included identification of a *NTRK2* fusion in a patient eligible for protocolled treatment with a TRK-inhibitor at progression. Other findings were confirmation of previously reported aberrated genes with new findings in *GRB2* and *SMYDA* that were prognostic of OS *(figure 9)*.

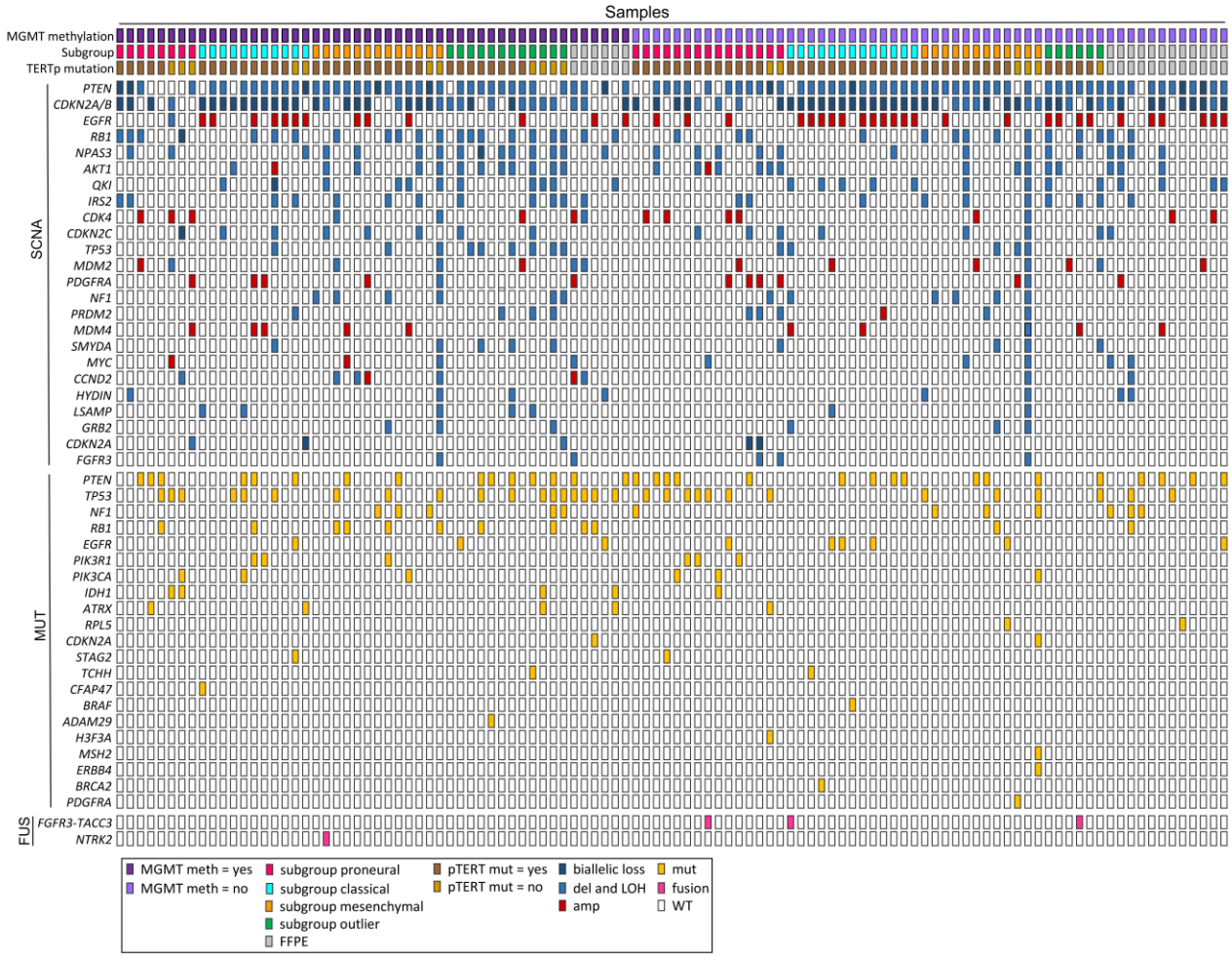

Figure 9. Landscape of somatic copy number variations (SCN*Vs*) in selected genes altered in ≥ 5 patients, glioblastoma specific mutations and fusions listed hierarchically. *N* = 108. Only mutations categorized as pathogenic are shown. The most aberrated genes were *PTEN, CDKN2A/B, EGFR, RB1 and NPAS3* and the most frequent mutations were in *PTEN, TP53, NF1, RB1* and *EGFR*. Abbreviations: mut: mutated; fus: fusions; FFPE: formalin-fixed-paraffin embedded; MGMT: O6-methyl-guanine-DNA-methyl-transferase; TERTp: Telomerase Reverse transcriptase promotor.

As others, we found MGMT-methylation and clinical factors like PS, age and corticosteroid dose as positive prognostic variables of OS and were incorporated in the OS analyses. Importantly, we found it feasible to have the genomic results ready at the time of first progression for possible protocolled treatment. The report of each patient was discussed at a tumor board meeting as described in section 3.6 and based upon the genomic profiling, we identified various targetable alterations in *EGFR, CDK4/6, NF1, FGFR3* and three patients were identified with a *FGFR3-TACC3* fusion. TMB and CI analyses revealed interesting prognostic results with a potential translational role for future GB patients. We found a better OS in TMB-low/median *vs.* TMB-high of 18.0 *vs* 10.0 months,

respectively; a better OS in CI low/high *vs.* CI-median of 18.7 *vs.* 14.8 months, respectively. Results were still significant when adjusting for MGMT status. When merging the two groups into a favorable *vs* non-favorable group (TMB median/low plus CI high/low *vs.* TMB-high and/or CI-median in any combination), there was a difference in OS of 20.9 *vs.* 14.8 months, respectively. *(Figure 10)*. We divided the patients into three subclasses; proneural, classical and mesenchymal and investigated for a predictive potential but this could not be verified in our cohort. We find that our results present with a translational value both concerning timely generated genomic reports for use in trial allocation and concerning TMB and CI that can be included for future stratification in clinical trials. Both warrant further investigation.

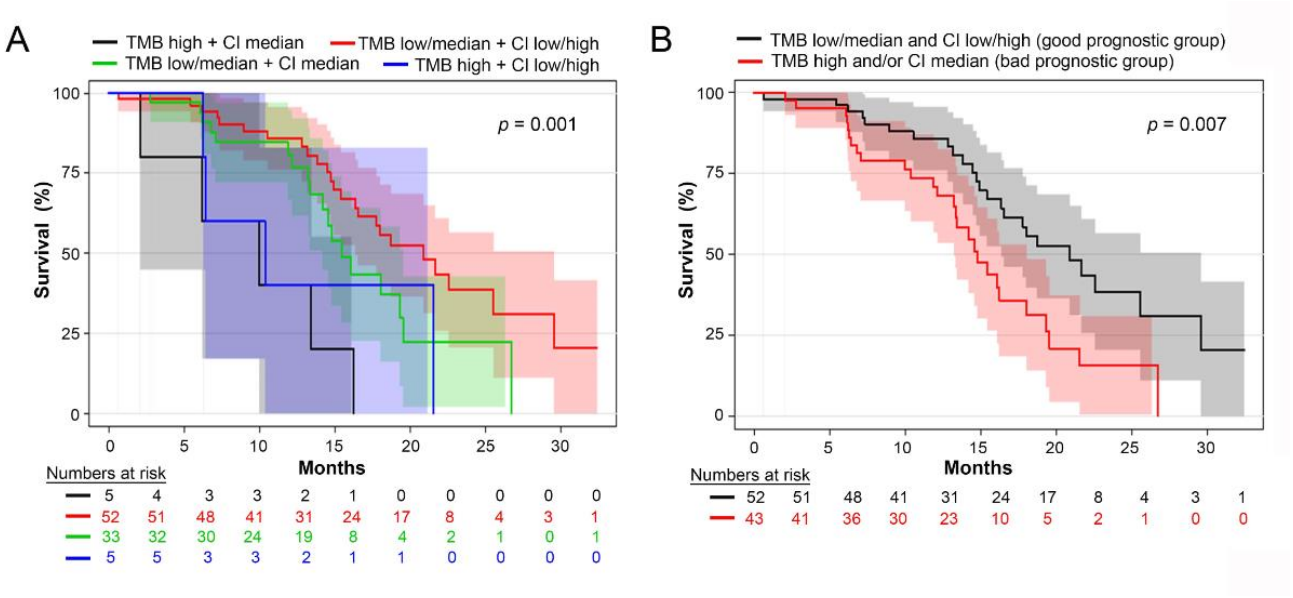

Figure 10.

Kaplan-Meier curves with numbers at risk for overall survival (OS) for (A) tumor mutational burden (TMB) and chromosomal instability (CI) in different combinations and (B) TMB and CI in a bad prognostic group and a good prognostic group, respectively. Figure includes patients having both analyses performed, *N*=95.
A: Patients were split into four groups based on previous found survival results: TMB-high plus CI-median (*N*=5), TMB-high plus CI-high/low (*N*=5), CI-median plus TMB-median/low (*N*=33) and TMB-median/low plus CI-high/low (*N*=52) with corresponding median OS of 10.0 (95% CI: 1.9-18.1), 10.4 (95% CI: 1.8-18.9), 15.4 (95% CI: 13.4-17.5) and 20.9 months (95% CI: 15.9-25.9), respectively (p=0.001).
B. The four groups were then segregated into a non-favorable (TMB-high and CI-median in any combination) *vs.* a favorable group (no TMB-high and/or CI-median in any combination) with a corresponding statistically significant difference in OS of 14.8 (95% CI: 12.4-17.1) *vs.* 20.9 months (95% CI: 15.9-25.9), respectively (p=0.007) and with a HR of 0.47 (95% CI: 0.26-0.82, p=0.008) in the good *vs.* bad prognostic group, respectively, calculated by a Cox proportional analysis.

4.2 STUDY II: Tumor mutational burden before and after treatment with Temozolomide in paired samples of glioblastoma

The aims were to investigate for treatment related changes with focus on TMB, clonal evolution (shared *vs.* private mutations) and signature analyses in patients with GB before and after first line treatment. Both RT and TMZ can alter the genomic composition in a tumor and knowledge about the present genomic structure at relapse can influence choice of treatment. TMB is particularly interesting as a predictive marker of response to IT, as has been shown in other cancers. If a patient from the Copenhagen Glioblastoma Cohort progressed and was eligible for relapse surgery, the patient was included in the paired samples cohort as described in section 3.2. We included a total of 35 patients with six patients having two relapse surgeries. We found that a remarkable high number of the relapse samples had a low tumor purity, making TMB comparison from a high tumor purity sample unreliable to a low tumor purity sample. Therefore, we developed a method to adjust for tumor purity and excluded a total of 10 (28.6%) samples for the TMB comparison part; three due to mutations < 5 and seven due to low tumor purity. Median TMB/Mb before and after treatment was 0.9 and 1.06 (range 0.4-1.5 and 0.4-2.4), respectively. Majority of mutations were shared between the primary and relapse sample and only few de novo mutations were developed at relapse. Patient RHGB003 had the highest increase after treatment from 1.5 to 2.4 mutations/Mb but still did not qualify as a hypermutated phenotype *(figure 11)*. Signature analyses revealed the highest prevalence of the age-related AC1 signature. AC6 and AC15, related to DNA MMR deficiency, was seen in nine (25.7%) and 18 (51.4%) patients, respectively. In line with lack of identification of hypermutation, we did not find evidence of signature AC11, the Temozolomide signature. When stratifying for treatment (RT/TMZ, *N*=29 *vs.* IT, *N*=3 *vs* RT, *N*=3), the highest increase was in the IT treated patients. However, numbers are small and should be evaluated in larger cohorts. This study underlines the need for development of better strategies to collect samples with high enough tumor purity to estimate TMB. This is particularly important in the relapse setting, where 7/32 samples (21.9%) in our study had to be excluded. A standardized assay to determine TMB is needed in order to compare TMB, both within the same cancer as well as across cancer types.

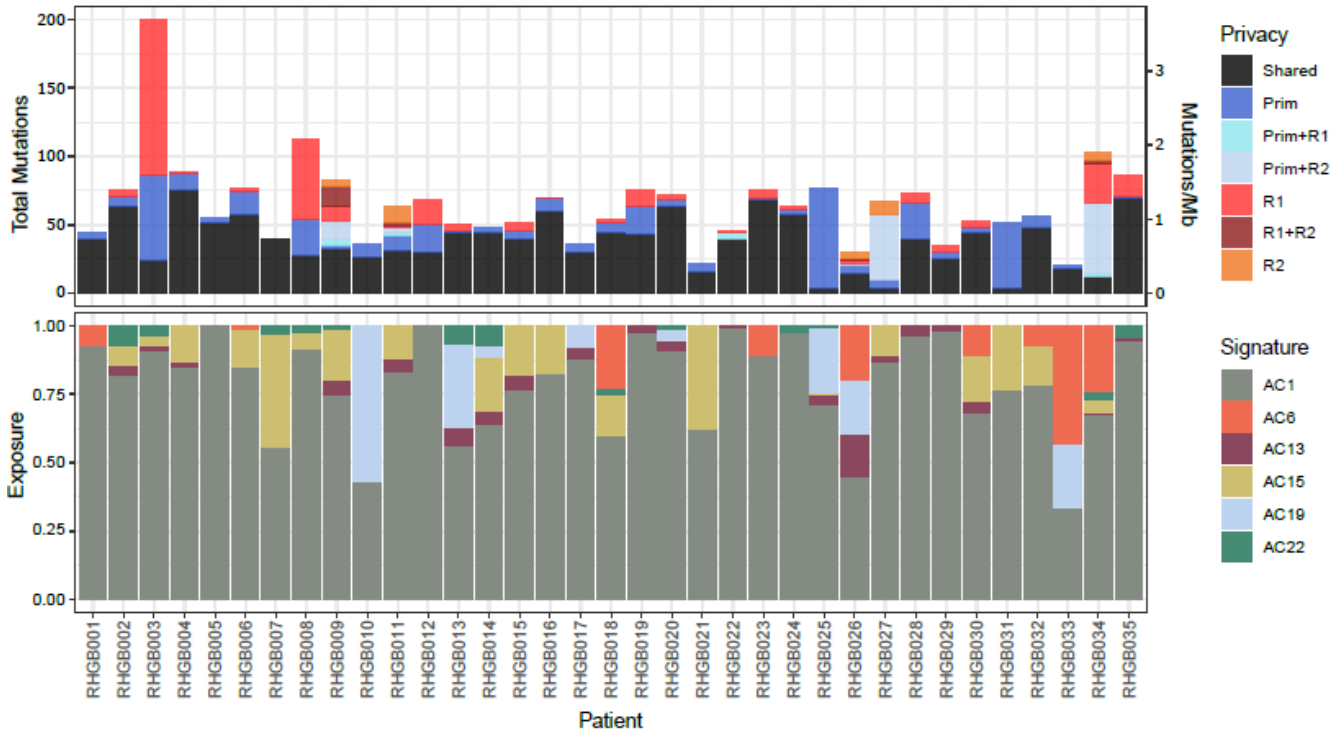

Figure 11. Top: Number of mutations, MGMT status and samples excluded for tumor mutational burde comparison across all specimens sequenced in each patient. Bar color indicates the privacy status of each category of variants depending on their presence in the primary (Prim), first relapse (R1), and second relapse (R2).

Bottom: Linear combination decomposition was used to detect the contribution of each of the thirty somatic mutation signatures found in the Catalogue Of Somatic Mutations In Cancer (COSMIC).

4.3 STUDY III: Cell-free DNA in newly diagnosed patients with glioblastoma – a clinical prospective feasibility study

Approximately 30 patients will undergo relapse surgery each year at our institution and histopathology from some surgeries will reveal only macrophages and fibrotic cells, hence not true progression. Therefore, the high-risk surgery can have been in vain and some patients experience complications to a degree that leaves them unfit for further treatment. For these reasons, new modalities for aiding in treatment evaluation is greatly needed. In study III, we included eight patients suspected of GB prior to diagnostic surgery with the first blood sample collected. If the diagnosis was confirmed by histopathology, blood sampling continued before and during oncologic treatment until progression. To increase the probability of measuring tumor derived DNA, we performed fragment size analyses with bp determination and defined a cut-off in bp peak ≤ 166 as having high probability of containing tumor derived DNA. We found that it was feasible to measure a cfDNA concentration and that all 80 collected samples but four had a bp-peak ≤ 166. In three out of four cases with progression, an increase in cfDNA was seen prior to or at progression and in three out of four patients without progression, no increase was seen in the last taken samples. In three out of three cases with suspected pseudo progression, cfDNA levels could aid in interpreting the clinical status of the patient (*figure 12).*

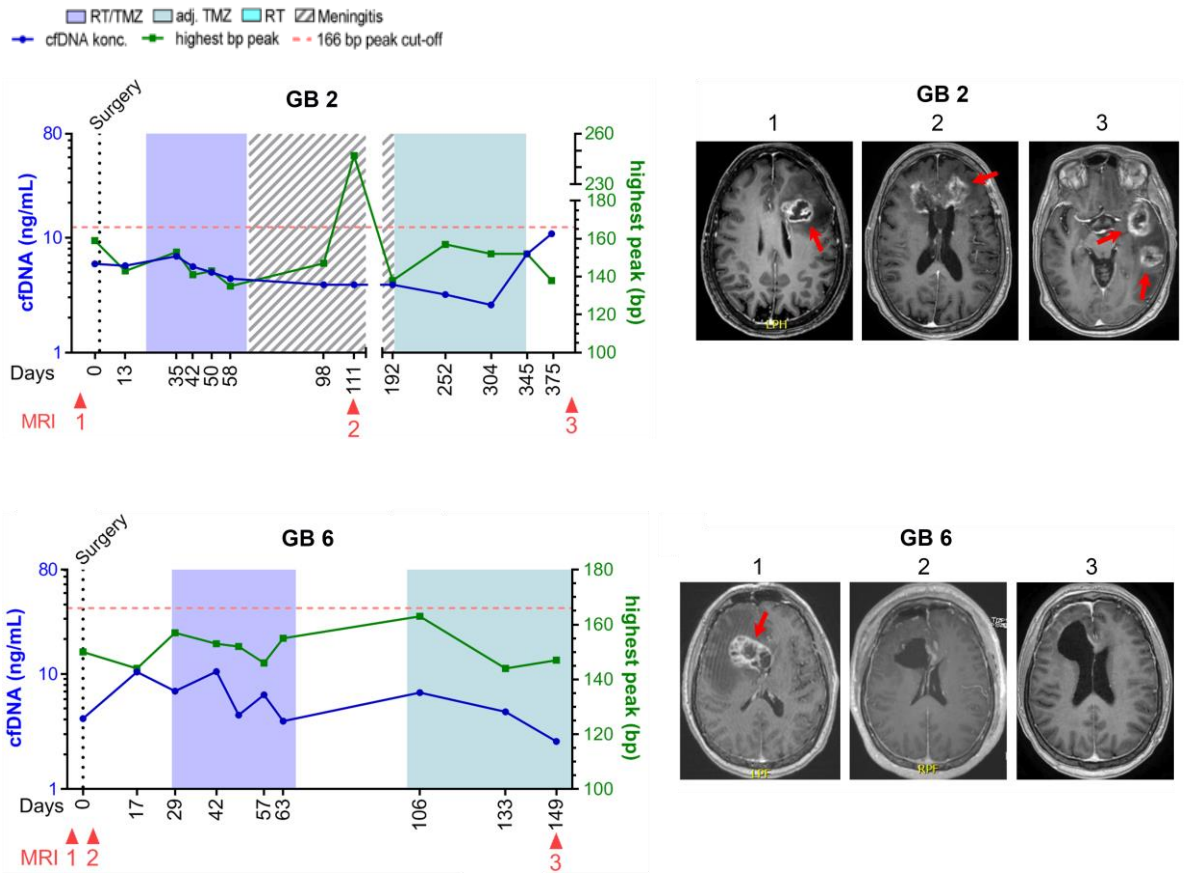

Figure 12. Left: Fluctuations in cell-free DNA (cfDNA) during study period at different treatment times with correlated basepar (bp) peaks. Right: Selected magnetic resonance imaging (MRI) during treatment period.
GB2 is a patient with progression: MR1: 32x23 mm CE tumor at diagnosis, MR2: During meningitis treatment showing growth of known CE tumor, including new lesions to a total of 2099 mm^3 CE tumor, MR3: Progression of all tumor lesions to a total 3863 mm^3. GB6 is a patient without progression. MR1: 46x29 mm CE tumor at diagnosis, MR2: <48 hours after surgery showing a small non-measurable CE lesion, MR3: stable disease with non-measurable CE lesion.

The four samples with bp-peaks > 166 were distributed in two patients: one before diagnosis with a large, partly necrotic tumor, one during RT, one during meningitis and one during an episode of intracerebral bleeding which illustrates that bp-distribution can be influenced by several factors. Overall, results from study III shows that it is clinically meaningful to investigate cfDNA in combination with fragment size distribution for future GB patients and we plan to investigate this in a large prospective study at our institution in grade II-IV gliomas.

5

Discussion

There is an undefined gap between basic science and clinical science that hinders many brilliant ideas to be tested in the clinic. With this translational PhD project, we sought to bridge between the two sections in neuro science. The main objective was to investigate the relevance of genomic testing in newly diagnosed patients with GB and again if an included patient had relapse surgery due to progression. Main research areas were predictive and prognostic factors in the newly diagnosed cohort with focus on TMB, CI and subgroups analyses and the main research foci in the paired samples cohort, were treatment related changes with tumor purity adjustment analyses and TMB measurements. Lastly, we investigated the clinical relevance of cfDNA as a marker of treatment response.

5.1 Genomic profiling gains access to trials

As stated continuously through this thesis, GB patients have a poor prognosis and limited treatment options. To alter these conditions, genomic testing might contribute but before a personalized treatment can be effectuated, clinical trials are needed. The golden standard is the double blinded randomized clinical trial (RCT) that gains solid and thoroughly tested results. However, an RCT normally needs hundreds of patients, is a slow and labor-intensive process and results might be outdated due to new knowledge gained from other studies. GB is no longer perceived as one disease but can be grouped into sub diagnoses and groups to be tested are getting smaller and smaller. Therefore, the inclusion period can be prolonged due to smaller number of eligible candidates for each group with the possibility that results from RCT´s can be even more time consuming. The consequence of this progress across cancers in the Phase 1 setting has been the development of umbrella and basket trials. However, most basket trials do not include brain cancer patients (or brain metastases) for several reasons, one being the BBB. Geographic accessibility to relevant trials can be challenging. Albeit Denmark has many factors in favor of participating in international trials with e.g. a well-run national Phase 1 unit, an East Danish Genome Center, a transparent infrastructure and excellent scientific conditions, Denmark is a small country that limits recruitment of trials. Therefore, patients may have to travel significant distances to enter a clinical trial. GB patients are fragile, due to the cancer and the morbidity that it causes. The expected life span is limited and should be evaluated

against spending the remaining time in a different country away from relatives and friends. Therefore, national trials are warranted. Allowing for smaller groups to be tested in a timely manner, a Bayesian adaptive design could be considered. The design includes dynamic arms that open or close as hypothesis are being accepted or dismissed or as new hypothesis are being generated. Another trial method is the umbrella trial with a fixed number of arms, testing different targeted treatments. A good example of this is the NCT Neuro Master Match (N^2M^2) trial (NCT03158389) for newly diagnosed GB patients with seven arms, six of which are targeted treatment arms.

5.2 Tumor mutational burden and chromosomal instability as prognostic markers

In study I we found some interesting results when investigating TMB, CI and OS that were all significant, showing that TMB-high and/or CI-median had the worst survival. This underlines the great potential of using TMB and CI as stratification for future studies by selecting the non-favorable group for experimental treatment upfront and be less aggressive with protocolled treatment for the favorable group and save this option for second line treatment. We find this strategy interesting, but results need further validation. Estimating TMB is not standardized and differs according the assays used and downstream analyses. For study I, we chose a method developed at Center for Genomic Medicine as described in section 3.4.5. With this method we had a median TMB of 21.9/Mb (range 1.9-71.0 with one extreme outlier having a TMB of 362.2/Mb). Bearing in mind that the patients in study I were all newly diagnosed, this is a high score as compared to the literature in which the general estimation of TMB is approximately 1-2 mutations/Mb in GB [34, 36]. Study II included 35 of the same patients as from study I. In this study, we found a median TMB/Mb in the primary, treatment unexposed, tissue of 0.9/Mb. The discrepancy illustrates different methods used and our specific TMB scores must be interpreted in relation to the specific study. For study II, we used a different method for TMB-score since these analyses were carried out at BRIC. For methods, see section 3.4.5. These different results truly illustrate the need for a unified estimation of TMB across cancers and highlights the difficulty in comparing TMB across studies.

5.3 Tumor heterogeneity and paired sampling (tumor purity)

To enter most molecular-based trials today, a fresh biopsy is needed since a tumor can alter the genetic composition quite significantly during time and/or treatment as discussed in section 2.2.4. Knowledge about tumor evolution with identification of genetic drivers, can be used for an individual treatment strategy depending on where in the disease progression the patient is. To pursue this in an intelligent way, genomic testing on multiple biopsies is gaining ground. In study II we collected paired samples

before and after treatment and investigated for genomic aberrations. We found that tumor purity constituted a major problem which was most evident in the precious relapse samples. Therefore, we found it necessary to develop a method to adjust for tumor purity and found that 10/35 samples (28.6%) had to excluded with 7/32 (21.9%) due to low tumor purity. Better methods are needed to optimize sampling. A consequence of study II is that we are in the process of implementing that every sample from a GB patient will be investigated by a neuro pathologist immediately after the sample arrives at Department of Pathology and before the sample is preserved in a biobank. The hope is that this procedure will increase the possibility of better tumor purity. Multisampling studies is another method of increasing knowledge of collecting representative samples.

5.4 Tumor mutational burden and immunotherapy for a selected group

As discussed in section 2.2.3, markers exist for prediction of response to IT with the most responsive tumors being exogenous-caused tumors with high TMB and/or high neoantigen load or biallelic MMR deficient tumors. TMB is an inclusion-criteria for an IT trial (NCT03668119) at our institution and to be included, a TMB > 10/Mb is required. In study II, we identified the highest TMB/Mb of 1.5. Even though we did not use the platform required for this specific study, it illustrates that only few patients with GB must be expected to respond to IT. However, it is important to identify the few potential candidates for IT and TMB should be further evaluated. To increase the potency of IT in immune depleted patients with GB, combination therapies might have a role. Several combination trials have been performed e.g. vaccination studies with adjuvants (*appendix 1*) and is performed, e.g. PD1i with RT/TMZ in different combinations and results are awaited. We did not investigate for PDL1-expression which would have provided another layer of how to understand the potential role for these patients.

5.5 Treatment monitoring using liquid biopsies

Evaluation with imaging is a central element in the treatment monitoring of GB patients. These modalities have some limitations which have been discussed in section 2.1.1. Therefore, we sought to investigate the role of cfDNA in study III. Interestingly, we found that cfDNA plus fragment size measurements indeed showed potential to contribute in evaluating the patients. Undeniable, ctDNA measurements would be preferable but this procedure is more expensive and demands both advanced machinery and special technical skills. CTC´s can provide more information but CTC´s are limited in GB and still needs further development before it can be implemented in clinical practice. Until these more comprehensive methods have been developed, we find that cfDNA is an applicable alternative

in the clinic. Including patients in the study before they had been diagnosed, raised both ethical and logistic issues and the pre-surgery sample did not provide additional information. We therefore suggest that the baseline sample should be the one before oncologic treatment, making recruitment to a larger study less complicated. For brain cancer patients, CSF also shows great potential, as discussed in section 2.3. However, CSF-sampling requires an invasive procedure with risk of complications and we do not find this strategy as compelling in routine diagnostics. A meaningful usage of CSF-monitoring could be in questionable cases of pseudo progression to select the right patients for relapse surgery.

5.6 Feasible and relevant in a daily clinical setting

During the study period we have performed WES on tumor tissue with a gene filter list based on common mutated genes in GB. The list has been evaluated throughout the study with application of new genes and reruns of the samples. During my research stay at Division of Molecular Genetics headed by Professor, Dr. Peter Lichter at the Deutsches Krebsforschungszentrum (DKFZ), we got acceptance from the Department of Pathology to use their neuro-gene panel list and we merged it to ours in March 2019. WES covers all protein coding regions in the genome in which location of majority of targetable aberrations must be expected. The field is now moving towards WGS with even more big data produced with the expense of increasing turnaround time, shallower sequencing and money. WGS is extremely important with research into e.g. introns and microRNA and will move neuro science in new directions. But for routine use we find WES acceptable and it is worth to consider a targeted approach with the above-mentioned panels since this can result in deeper and faster sequencing for known targetable aberrations. This is particularly important if we are to move genomic profiling to first line therapy. A supplement with methylation profiling will be useful since new entities seem to be discovered based on the analyses and facilitates an even more targeted treatment in a small group of patients.

6

Future perspectives and conclusion

The main reason to perform genomic profiles based on NGS techniques is to find targetable aberrations and to prolong OS. For genomic profiling to be applicable for daily clinical practice, the logistic setup must be stringent and precise, independent of work-schedule. This was the case for solid tumors at our institution when this PhD project was launched, and we have succeeded in implementing the same setup for GB patients. Today, a genomic report is ready for first or second relapse and if a patient has had relapse surgery, a genomic report will be accessible as well. To acknowledge the increasing need for tissue for research purposes, we initiated a collaboration with RBGB, Department of Pathology, -Neuro Surgery and Danish Cancer Society to establish a biobank with GB tissue for future research purposes. We succeeded with this project and tissue is now being collected and stored in a systematic and preservative manner according to current legislation. The clinical impact of the genomic profiling was not as high as hoped for as we treated only one patient in an experimental trial. The main reasons for this lack of treatment consequence were the limited number of clinical trials available at our institution and the clinical deterioration of patients necessitating a more aggressive approach to experimental treatment. We find that majority of GB patients should enter clinical trials and we should consider moving experimental treatment to first line, especially in the group of patients with the worst prognosis. In study I, we found this group to be patients with TMB-high and/or CI-median. Importantly, we identified a patient with a *NTRK2* fusion that illustrates the clinical potential of genomic profiling. New ways of designing trials are needed to increase visibility and access and to speed up the time to results, that being both negative and positive results. An example could be either the Bayesian adaptive model or umbrella/basket trials. Theoretically, umbrella trials would be preferred as brain cancer differs in many ways from other solid tumors but by including brain cancer patients in basket trials this would increase the eligible number of trials. Palliative trials testing when not to treat a GB patient is also warranted. Focus should here be on quality of life and palliation. Serial sampling of GB tissue is important for investigation in tumor heterogeneity and for clonal evolution analyses, and foci should be on tumor purity, especially in the relapse samples as concluded in study II, sampling bias and the role of the peritumoral tissue. For research purposes and to increase the amount of relapse tissue from GB patients, it is worth considering performing autopsy studies. In study III, we find that liquid biopsies with cfDNA/ctDNA

do have a future in GB and we find that cfDNA in combination with fragment size determination is a promising and easily accessible method that we wish to investigate further. The hope and strategy for future GB patients should be to find the few to cure, the majority to prolong life and the rest to palliate.

REFERENCES

1. Stupp, R., et al., *Radiotherapy plus concomitant and adjuvant temozolomide for glioblastoma.* N Engl J Med, 2005. **352**(10): p. 987-96.
2. Ostrom, Q.T., et al., *CBTRUS Statistical Report: Primary brain and other central nervous system tumors diagnosed in the United States in 2010-2014.* Neuro Oncol, 2017. **19**(suppl_5): p. v1-v88.
3. Hegi, M.E., et al., *MGMT gene silencing and benefit from temozolomide in glioblastoma.* N Engl J Med, 2005. **352**(10): p. 997-1003.
4. Verhaak, R.G., et al., *Integrated genomic analysis identifies clinically relevant subtypes of glioblastoma characterized by abnormalities in PDGFRA, IDH1, EGFR, and NF1.* Cancer Cell, 2010. **17**(1): p. 98-110.
5. Louis, D.N., et al., *The 2016 World Health Organization Classification of Tumors of the Central Nervous System: a summary.* Acta Neuropathol, 2016. **131**(6): p. 803-20.
6. Stoyanov, G.S. and D.L. Dzhenkov, *On the Concepts and History of Glioblastoma Multiforme - Morphology, Genetics and Epigenetics.* Folia Med (Plovdiv), 2018. **60**(1): p. 48-66.
7. Stupp, R., et al., *Effect of Tumor-Treating Fields Plus Maintenance Temozolomide vs Maintenance Temozolomide Alone on Survival in Patients With Glioblastoma: A Randomized Clinical Trial.* Jama, 2017. **318**(23): p. 2306-2316.
8. Sampson, J.H., et al., *Immunologic escape after prolonged progression-free survival with epidermal growth factor receptor variant III peptide vaccination in patients with newly diagnosed glioblastoma.* J Clin Oncol, 2010. **28**(31): p. 4722-9.
9. Sampson, J.H., et al., *Greater chemotherapy-induced lymphopenia enhances tumor-specific immune responses that eliminate EGFRvIII-expressing tumor cells in patients with glioblastoma.* Neuro Oncol, 2011. **13**(3): p. 324-33.
10. Schuster, J., et al., *A phase II, multicenter trial of rindopepimut (CDX-110) in newly diagnosed glioblastoma: the ACT III study.* Neuro Oncol, 2015. **17**(6): p. 854-61.
11. Weller, M., et al., *Rindopepimut with temozolomide for patients with newly diagnosed, EGFRvIII-expressing glioblastoma (ACT IV): a randomised, double-blind, international phase 3 trial.* Lancet Oncol, 2017. **18**(10): p. 1373-1385.
12. Malmstrom, A., et al., *Temozolomide versus standard 6-week radiotherapy versus hypofractionated radiotherapy in patients older than 60 years with glioblastoma: the Nordic randomised, phase 3 trial.* Lancet Oncol, 2012. **13**(9): p. 916-26.
13. Chinot, O.L., et al., *AVAglio: Phase 3 trial of bevacizumab plus temozolomide and radiotherapy in newly diagnosed glioblastoma multiforme.* Adv Ther, 2011. **28**(4): p. 334-40.
14. Gilbert, M.R., et al., *A randomized trial of bevacizumab for newly diagnosed glioblastoma.* N Engl J Med, 2014. **370**(8): p. 699-708.
15. Herrlinger, U., et al., *Bevacizumab Plus Irinotecan Versus Temozolomide in Newly Diagnosed O6-Methylguanine-DNA Methyltransferase Nonmethylated Glioblastoma: The Randomized GLARIUS Trial.* J Clin Oncol, 2016. **34**(14): p. 1611-9.
16. Malmstrom, A., et al., *Postoperative neoadjuvant temozolomide before radiotherapy versus standard radiotherapy in patients 60 years or younger with anaplastic astrocytoma or glioblastoma: a randomized trial.* Acta Oncol, 2017. **56**(12): p. 1776-1785.
17. Perry, J.R., et al., *Short-Course Radiation plus Temozolomide in Elderly Patients with Glioblastoma.* N Engl J Med, 2017. **376**(11): p. 1027-1037.
18. Hasselbalch, B., et al., *Cetuximab, bevacizumab, and irinotecan for patients with primary glioblastoma and progression after radiation therapy and temozolomide: a phase II trial.* Neuro Oncol, 2010. **12**(5): p. 508-16.
19. Macdonald, D.R., et al., *Response criteria for phase II studies of supratentorial malignant glioma.* J Clin Oncol, 1990. **8**(7): p. 1277-80.
20. Wen, P.Y., et al., *Updated response assessment criteria for high-grade gliomas: response assessment in neuro-oncology working group.* J Clin Oncol, 2010. **28**(11): p. 1963-72.
21. Wen, P.Y., et al., *Response Assessment in Neuro-Oncology Clinical Trials.* J Clin Oncol, 2017. **35**(21): p. 2439-2449.
22. Bailey, M.H., et al., *Comprehensive Characterization of Cancer Driver Genes and Mutations.* Cell, 2018. **173**(2): p. 371-385.e18.
23. Drilon, A., et al., *Efficacy of Larotrectinib in TRK Fusion-Positive Cancers in Adults and Children.* N Engl J Med, 2018. **378**(8): p. 731-739.

24. DuBois, S.G., et al., *The use of neoadjuvant larotrectinib in the management of children with locally advanced TRK fusion sarcomas.* Cancer, 2018. **124**(21): p. 4241-4247.
25. Shi, E., et al., *FGFR1 and NTRK3 actionable alterations in "Wild-Type" gastrointestinal stromal tumors.* J Transl Med, 2016. **14**(1): p. 339.
26. *Comprehensive genomic characterization defines human glioblastoma genes and core pathways.* Nature, 2008. **455**(7216): p. 1061-8.
27. Parsons, D.W., et al., *An integrated genomic analysis of human glioblastoma multiforme.* Science, 2008. **321**(5897): p. 1807-12.
28. Hartmann, C., et al., *Patients with IDH1 wild type anaplastic astrocytomas exhibit worse prognosis than IDH1-mutated glioblastomas, and IDH1 mutation status accounts for the unfavorable prognostic effect of higher age: implications for classification of gliomas.* Acta Neuropathol, 2010. **120**(6): p. 707-18.
29. Brennan, C.W., et al., *The somatic genomic landscape of glioblastoma.* Cell, 2013. **155**(2): p. 462-77.
30. Capper, D., et al., *DNA methylation-based classification of central nervous system tumours.* Nature, 2018. **555**(7697): p. 469-474.
31. Couzin-Frankel, J., *Breakthrough of the year 2013. Cancer immunotherapy.* Science, 2013. **342**(6165): p. 1432-3.
32. Rizvi, N.A., et al., *Cancer immunology. Mutational landscape determines sensitivity to PD-1 blockade in non-small cell lung cancer.* Science, 2015. **348**(6230): p. 124-8.
33. Snyder, A., et al., *Genetic basis for clinical response to CTLA-4 blockade in melanoma.* N Engl J Med, 2014. **371**(23): p. 2189-2199.
34. Alexandrov, L.B., et al., *Signatures of mutational processes in human cancer.* Nature, 2013. **500**(7463): p. 415-21.
35. Kandoth, C., et al., *Mutational landscape and significance across 12 major cancer types.* Nature, 2013. **502**(7471): p. 333-339.
36. Lawrence, M.S., et al., *Mutational heterogeneity in cancer and the search for new cancer-associated genes.* Nature, 2013. **499**(7457): p. 214-218.
37. Bouffet, E., et al., *Immune Checkpoint Inhibition for Hypermutant Glioblastoma Multiforme Resulting From Germline Biallelic Mismatch Repair Deficiency.* J Clin Oncol, 2016. **34**(19): p. 2206-11.
38. AlHarbi, M., et al., *Durable Response to Nivolumab in a Pediatric Patient with Refractory Glioblastoma and Constitutional Biallelic Mismatch Repair Deficiency.* Oncologist, 2018. **23**(12): p. 1401-1406.
39. Mansfield, A.S., et al., *Heterogeneity of Programmed Cell Death Ligand 1 Expression in Multifocal Lung Cancer.* Clin Cancer Res, 2016. **22**(9): p. 2177-82.
40. Hirsch, F.R., et al., *PD-L1 Immunohistochemistry Assays for Lung Cancer: Results from Phase 1 of the Blueprint PD-L1 IHC Assay Comparison Project.* J Thorac Oncol, 2017. **12**(2): p. 208-222.
41. Okada, H., et al., *Immunotherapy response assessment in neuro-oncology: a report of the RANO working group.* Lancet Oncol, 2015. **16**(15): p. e534-e542.
42. Desjardins, A., et al., *Recurrent Glioblastoma Treated with Recombinant Poliovirus.* N Engl J Med, 2018. **379**(2): p. 150-161.
43. Hilf, N., et al., *Actively personalized vaccination trial for newly diagnosed glioblastoma.* Nature, 2019. **565**(7738): p. 240-245.
44. Iwadate, Y., *Epithelial-mesenchymal transition in glioblastoma progression.* Oncol Lett, 2016. **11**(3): p. 1615-1620.
45. Tafani, M., et al., *Pro-inflammatory gene expression in solid glioblastoma microenvironment and in hypoxic stem cells from human glioblastoma.* J Neuroinflammation, 2011. **8**: p. 32.
46. Schou Noroxe, D., et al., *Extracranial metastases in glioblastoma-Two case stories.* Clin Case Rep, 2019. **7**(2): p. 289-294.
47. Lundemann, M., et al., *Feasibility of multi-parametric PET and MRI for prediction of tumour recurrence in patients with glioblastoma.* Eur J Nucl Med Mol Imaging, 2019. **46**(3): p. 603-613.
48. Minniti, G., et al., *Patterns of failure and comparison of different target volume delineations in patients with glioblastoma treated with conformal radiotherapy plus concomitant and adjuvant temozolomide.* Radiother Oncol, 2010. **97**(3): p. 377-81.
49. Joosse, S.A., et al., *Chromosomal Aberrations Associated with Sequential Steps of the Metastatic Cascade in Colorectal Cancer Patients.* Clin Chem, 2018. **64**(10): p. 1505-1512.
50. Indraccolo, S., et al., *Genetic, Epigenetic, and Immunologic Profiling of MMR-Deficient Relapsed Glioblastoma.* Clin Cancer Res, 2019. **25**(6): p. 1828-1837.

51. Abbosh, C., et al., *Phylogenetic ctDNA analysis depicts early-stage lung cancer evolution.* Nature, 2017. **545**(7655): p. 446-451.
52. Becerra, M.F., et al., *Comparative Genomic Profiling of Matched Primary and Metastatic Tumors in Renal Cell Carcinoma.* Eur Urol Focus, 2018. **4**(6): p. 986-994.
53. Schramm, A., et al., *Mutational dynamics between primary and relapse neuroblastomas.* Nat Genet, 2015. **47**(8): p. 872-7.
54. McShane, L.M., et al., *REporting recommendations for tumour MARKer prognostic studies (REMARK).* Br J Cancer, 2005. **93**(4): p. 387-91.
55. Martinez-Ricarte, F., et al., *Molecular Diagnosis of Diffuse Gliomas through Sequencing of Cell-Free Circulating Tumor DNA from Cerebrospinal Fluid.* Clin Cancer Res, 2018. **24**(12): p. 2812-2819.
56. De Mattos-Arruda, L., et al., *Cerebrospinal fluid-derived circulating tumour DNA better represents the genomic alterations of brain tumours than plasma.* Nat Commun, 2015. **6**: p. 8839.
57. Pentsova, E.I., et al., *Evaluating Cancer of the Central Nervous System Through Next-Generation Sequencing of Cerebrospinal Fluid.* J Clin Oncol, 2016. **34**(20): p. 2404-15.
58. Brat, D.J., et al., *Comprehensive, Integrative Genomic Analysis of Diffuse Lower-Grade Gliomas.* N Engl J Med, 2015. **372**(26): p. 2481-98.
59. Juratli, T.A., et al., *TERT Promoter Mutation Detection in Cell-Free Tumor-Derived DNA in Patients with IDH Wild-Type Glioblastomas: A Pilot Prospective Study.* Clin Cancer Res, 2018.
60. Figueroa, J.M., et al., *Detection of wild-type EGFR amplification and EGFRvIII mutation in CSF-derived extracellular vesicles of glioblastoma patients.* Neuro Oncol, 2017. **19**(11): p. 1494-1502.
61. Hagan, S., E. Martin, and A. Enriquez-de-Salamanca, *Tear fluid biomarkers in ocular and systemic disease: potential use for predictive, preventive and personalised medicine.* Epma j, 2016. **7**: p. 15.
62. Diaz, L.A., Jr. and A. Bardelli, *Liquid biopsies: genotyping circulating tumor DNA.* J Clin Oncol, 2014. **32**(6): p. 579-86.
63. Fassunke, J., et al., *EGFR T790M mutation testing of non-small cell lung cancer tissue and blood samples artificially spiked with circulating cell-free tumor DNA: results of a round robin trial.* Virchows Arch, 2017. **471**(4): p. 509-520.
64. Nilsson, R.J., et al., *Rearranged EML4-ALK fusion transcripts sequester in circulating blood platelets and enable blood-based crizotinib response monitoring in non-small-cell lung cancer.* Oncotarget, 2016. **7**(1): p. 1066-75.
65. Bottoni, P. and R. Scatena, *The Role of CA 125 as Tumor Marker: Biochemical and Clinical Aspects.* Adv Exp Med Biol, 2015. **867**: p. 229-44.
66. Das, V., J. Kalita, and M. Pal, *Predictive and prognostic biomarkers in colorectal cancer: A systematic review of recent advances and challenges.* Biomed Pharmacother, 2017. **87**: p. 8-19.
67. Pantel, K. and C. Alix-Panabieres, *Liquid biopsy and minimal residual disease - latest advances and implications for cure.* Nat Rev Clin Oncol, 2019.
68. Sullivan, J.P., et al., *Brain tumor cells in circulation are enriched for mesenchymal gene expression.* Cancer Discov, 2014. **4**(11): p. 1299-309.
69. Muller, C., et al., *Hematogenous dissemination of glioblastoma multiforme.* Sci Transl Med, 2014. **6**(247): p. 247ra101.
70. Beiter, T., et al., *Short-term treadmill running as a model for studying cell-free DNA kinetics in vivo.* Clin Chem, 2011. **57**(4): p. 633-6.
71. Tovbin, D., et al., *Circulating cell-free DNA in hemodialysis patients predicts mortality.* Nephrol Dial Transplant, 2012. **27**(10): p. 3929-35.
72. Destouni, A., et al., *Cell-free DNA levels in acute myocardial infarction patients during hospitalization.* Acta Cardiol, 2009. **64**(1): p. 51-7.
73. Ahlborn, L.B., et al., *Circulating tumor DNA as a marker of treatment response in BRAF V600E mutated non-melanoma solid tumors.* Oncotarget, 2018. **9**(66): p. 32570-32579.
74. El Messaoudi, S., et al., *Circulating DNA as a Strong Multimarker Prognostic Tool for Metastatic Colorectal Cancer Patient Management Care.* Clin Cancer Res, 2016. **22**(12): p. 3067-77.
75. Gray, E.S., et al., *Circulating tumor DNA to monitor treatment response and detect acquired resistance in patients with metastatic melanoma.* Oncotarget, 2015. **6**(39): p. 42008-18.
76. Zachariah, M.A., et al., *Blood-based biomarkers for the diagnosis and monitoring of gliomas.* Neuro Oncol, 2018. **20**(9): p. 1155-1161.
77. Boisselier, B., et al., *Detection of IDH1 mutation in the plasma of patients with glioma.* Neurology, 2012. **79**(16): p. 1693-8.

78. Majchrzak-Celinska, A., et al., *Detection of MGMT, RASSF1A, p15INK4B, and p14ARF promoter methylation in circulating tumor-derived DNA of central nervous system cancer patients.* J Appl Genet, 2013. **54**(3): p. 335-44.
79. Bettegowda, C., et al., *Detection of circulating tumor DNA in early- and late-stage human malignancies.* Sci Transl Med, 2014. **6**(224): p. 224ra24.
80. Underhill, H.R., et al., *Fragment Length of Circulating Tumor DNA.* PLoS Genet, 2016. **12**(7): p. e1006162.
81. Mouliere, F., et al., *High fragmentation characterizes tumour-derived circulating DNA.* PLoS One, 2011. **6**(9): p. e23418.
82. Thierry, A.R., et al., *Origin and quantification of circulating DNA in mice with human colorectal cancer xenografts.* Nucleic Acids Res, 2010. **38**(18): p. 6159-75.
83. Mouliere, F., et al., *Enhanced detection of circulating tumor DNA by fragment size analysis.* Sci Transl Med, 2018. **10**(466).
84. Jahr, S., et al., *DNA fragments in the blood plasma of cancer patients: quantitations and evidence for their origin from apoptotic and necrotic cells.* Cancer Res, 2001. **61**(4): p. 1659-65.
85. Schwarzenbach, H., D.S. Hoon, and K. Pantel, *Cell-free nucleic acids as biomarkers in cancer patients.* Nat Rev Cancer, 2011. **11**(6): p. 426-37.
86. Tuxen, I.V., et al., *Copenhagen Prospective Personalized Oncology (CoPPO)-Clinical Utility of Using Molecular Profiling to Select Patients to Phase I Trials.* Clin Cancer Res, 2019. **25**(4): p. 1239-1247.
87. Plon, S.E., et al., *Sequence variant classification and reporting: recommendations for improving the interpretation of cancer susceptibility genetic test results.* Hum Mutat, 2008. **29**(11): p. 1282-91.
88. Wang, Q., et al., *Tumor Evolution of Glioma-Intrinsic Gene Expression Subtypes Associates with Immunological Changes in the Microenvironment.* Cancer Cell, 2017. **32**(1): p. 42-56.e6.

FULL TEXT OF INCLUDED MANUSCRIPTS

STUDY I

Study I

Genomic profiling in newly diagnosed patients with glioblastoma – a prospective, translational study

Dorte Schou Nørøxe[†, ‡, *], Christina Westmose Yde[¶], Olga Østrup[¶], Signe Regner Michaelsen[†], Ane Yde Smith[¶], Savvas Kinalis[¶], Mathias Husted Torp[¶], Jane Skjøth-Rasmussen[¥], Jannick Brennum[¥], Petra Hamerlik[∞], Hans Skovgaard Poulsen[†, ‡], Finn Cilius Nielsen[¶], Ulrik Lassen[‡]

In preparation for resubmission

[†]Department of Radiation Biology, Rigshospitalet, Blegdamsvej 9, 2100 Copenhagen.
[‡]Department of Oncology, Rigshospitalet, Blegdamsvej 9, 2100 Copenhagen.
[¶]Center for Genomic Medicine, Rigshospitalet, Blegdamsvej 9, 2100 Copenhagen.
[¥]Department of Neuro Surgery, Rigshospitalet, Blegdamsvej 9, 2100 Copenhagen.
[∞]Danish Cancer Society, Strandboulevarden 49, 2100 Copenhagen.

*Corresponding author: anne.dorte.schou.noeroexe@regionh.dk

Importance of the study

Glioblastoma (GB) is incurable, difficult to treat and with unknown etiology. The omic-era has contributed with indispensable new knowledge and improved treatment strategies across different cancers. However, this has yet not translated into an increased survival in GB patients. Reasons can represent the heterogeneity of samples in international biobanks with both primary/relapsed GB, incomplete clinical information, unknown treatment exposure and demographic differences. To unify the sampling in our cohort, we performed a prospective collection of GB samples from 108 newly diagnosed patients before exposure to treatment and gathered relevant clinical information. We performed next generation sequencing to identify possible actionable targets and investigated the tumor mutational burden (TMB), chromosomal instability (CI) and subgroup division. We found significant prognostic value of TMB and CI and borderline significance in the classical subgroup. These prospective, translational results from the Copenhagen Glioblastoma Cohort can be integrated in the research community to contribute to future studies.

Abstract

Background: Glioblastoma (GB) is an incurable grade IV brain tumor and new treatment strategies are urgently needed. Next generation sequencing of GB has most often been performed on archival tissue from either diagnostic or relapse surgeries with limited knowledge of clinical information, including treatment given. Radiotherapy (RT) and Temozolomide (TMZ) can alter the genetic signature. We sought to investigate the genomic composition in treatment-naïve patients with GB, searched for possible targetable aberrations and investigated for prognostic and/or predictive factors.

Methods: A total of 108 newly diagnosed GB patients were prospectively included. Relevant clinical information was gathered, including progression-free survival (PFS) and overall survival (OS). Tissue was analyzed by whole-exome sequencing, SNP- and transcriptome-arrays, and RNA-sequencing, and assessed for mutations, fusions, tumor mutational burden (TMB), chromosomal instability (CI) and classified into GB subgroups. Each genomic report was discussed at a multidisciplinary tumor board meeting.

Results: Consecutive patients were asked and 97.3% accepted inclusion in this study. 86 patients (77%) were treated with RT/TMZ and adjuvant TMZ. One *NTRK2* and three *FGFR3-TACC3* fusions were identified. Copy number alterations in *GRB2* and *SMYD4* were significantly correlated with worse OS together with known clinical variables like age, performance status, steroid dose and O6-methyl-guanine-DNA-methyl-transferase (MGMT)-status. Patients with median CI or high TMB had significantly worse OS compared to CI-low/high or TMB low/median.

Conclusion: Performing genomic profiling at diagnosis ensures the availability of report at the first progression. Furthermore, high TMB or median CI had worse OS which can support the possibility to offering experimental treatment already at the first line.

Introduction

Glioblastoma (GB) is an incurable brain cancer with an incidence of 3.2/100.000 [1]. Biomarker-driven targeted therapy has proven effective in many cancer types and seems promising in GB based on case stories with specific aberrations [2-4]. This includes gene fusions that have resulted in approval of Tropomyosin Receptor Kinase (TRK)-inhibitors for TRK-fusion positive cancers, regardless of histology [5-7]. With the comprehensive genomic characterization of GB in 2008 [8] and the revised World Health Organization (WHO) classification of brain tumors in 2016 with integration of molecular analyses, the hope was that it would contribute to better treatment options in GB. Genomic testing is being used in the clinic today [9] but unfortunately has not yet translated into a better OS. Standard 1st line treatment remains concurrent radiotherapy (RT)/Temozolomide (TMZ) followed by adjuvant TMZ with a progression free survival (PFS) of 7 months and overall survival (OS) of 14-22 months, depending on prognostic and predictive markers like isocitrate dehydrogenase (*IDH*)-status and O6-methyl-guanine-DNA-methyl-transferase (MGMT) promotor-status [10-12]. Some explanations for lack of clinical impact into a better OS might be that majority of samples in international databases represent both primary and relapse samples, can have unknown *IDH*- and/or MGMT-status and limited information of treatment exposure. The latter can change the genetic composition with possible development of hypermutated phenotypes [13, 14] or higher chromosomal instability (CI) [15]. Also, overrepresentation from specific demographic areas can cause challenges as different ethnics groups can have a heterogenous genetic composition [16]. Lastly, at initiation of international databases, molecular diagnostics was not incorporated to the same extent as today and work with methylation profiling on cases from the databases has shown that 12% of samples with discrepancies could have a new diagnosis assigned [17]. To face some of these challenges, we have performed a prospective study with inclusion in the Copenhagen Glioblastoma Cohort (CGC) to determine the genomic profile in newly diagnosed patients with GB, with the purpose to investigate whether a genomic profile could lead to an altered treatment strategy and to investigate prognostic/predictive relevance of genomic variants. To our knowledge, this is the first study performed after the 2016 WHO-classification with prospective translational results, including clinical, pathological and genomic data on all included patients.

Materials and methods

Collection of tissue

Over a 2½ year period from February 2016 to August 2018 we included 108 patients with newly diagnosed GB at Rigshospitalet, Copenhagen. The diagnosis was based on the WHO-classification from 2016 with histopathology and molecular examination for *IDH*-and MGMT-status [11]. Patients who had previously received treatment for a lower grade glioma with transformation into a grade IV GB, were not included. In the first year, we included all newly diagnosed patients, but shifted to include only patients suitable for RT/TMZ. This decision was based on that a genomic profile should have a potential clinical impact on future treatment of included patient. All patients gave informed, signed consent 24 hours prior to surgery. Whenever possible, 5-ALA was used during surgery [18, 19]. Three representative tissue chunks from diagnostic surgery was immediately preserved in RNA-*later* for optimal DNA and RNA purification. In case of insufficient amount of tumor material, we used formalin-fixed-paraffin-embedded (FFPE) tissue or snap frozen tissue. Patients further delivered a blood sample (10 ml) for germline retraction. (*Figure 1).* The project was carried out in accordance with the Declaration of Helsinki and with approval from the National Danish Ethics Committee (Journal number: H-3-2009-136 and 1707335) and Danish Data Protection Agency (Journal numbers: 2014-41-2857 and VD-2018-204 with I-suite number: 6447).

Clinical data

Clinical data was noted from patient interviews and medical records, including age at diagnosis, location of the tumor, extent of surgery, performance status (PS) and corticosteroid dose before oncologic treatment, treatment given, number of cycles of adjuvant TMZ completed, completed full planned treatment yes/no, relapse surgery yes/no, PFS and OS. Date of datalock was 10.01.2019.

Pathological examination

Every sample underwent standard pathological examination with immunohistochemistry (IHC) for GFA, map2, Olig2, *IDH*, p53, *ATRX* and Ki67 index. For patients < 55 years with normal *IDH*-status, sequencing of codon 132, 140 and 172 was done. Polymerase chain reaction (PCR) with pyrosequencing (Qiagen) was performed for *MGMT*-status with a cut-off of 10%. When in doubt of diagnosis, 850K methylation with Infinium Methylation EPIC BeadChip array which targets >850.000 methylation positions in the human genome, was performed. In young patients and/or midline tumors and/or *IDH* WT in combination with *ATRX* loss, an analysis for H3K27M was added with sequencing of *H3F3A* codon 28 to 35 with a sensitivity of 20% tumor cells.

WES

Whole exome sequencing (WES) was performed using DNA from tissue and blood. DNA from tumor samples (tDNA) was extracted using the AllPrep DNA/RNA purification kit and the QIACube workstation (Qiagen) according to manufacturer's instructions. Genomic DNA from whole blood samples (gDNA) was isolated using the liquid handling automated station (Tecan). Purified DNA was quantified using the Qubit instrument (Life Technologies). Both tDNA and gDNA (200 ng) were fragmented to approximately 300 bp using Covaris S2 (Agilent) and adaptor ligation was performed using KAPA HTP Library Preparation Kit (Roche). Exomes were enriched with SureSelectXT Clinical Research Exome kit (Agilent). Paired-end sequencing (2x100 bp or 2x150 bp) was performed to gain an average coverage of 50-100x, using the HiSeq2500 or NextSeq500 platforms from Illumina. Raw sequencing data were processed using CASAVA-1.8.2. Reads were aligned to the human reference genome (hg19/GRCh37) using CLC Biomedical Genomics Workbench (Qiagen), and variant calling was performed above 10% frequency in the tumor DNA. Somatic variants were identified by excluding variants found in blood WES data from the patient, and further analyzed using Ingenuity Variant Analysis (Qiagen). A gene list based upon frequent mutated genes in GB, was used to filtrate for mutation calling in Ingenuity (*table S1)* and mutations were categorized based on the likelihood of being pathogenic [20].

Tumor mutational burden

Paired end sequencing reads with a length of 150 bp were aligned against the GRCh37.p13 reference genome using bwa mem 0.7.15. Somatic variants were called using Mutect2 according to the GATK best practices for somatic short variant discovery using GATK 4.0.10.1. Variants filtered by Mutect2 and variants annotated with an allele frequency > 5 % in gnomAD were excluded from the call set. The variants were further hard filtered by only including SNVs and INDELs in coding regions. Finally, variants called at sites with a coverage of less than 10x and an allele depth of less than 5x were excluded. The tumor mutation burden was calculated as the number of non-filtered variants divided by the number of bases with a coverage of > 10x in all coding regions of the genome. Tumor mutational burden (TMB) estimates were reported as mutations per megabase (Mb).

Analysis of somatic copy-number alterations

CytoScan assay (Affymetrix, Santa Clara, USA) was performed on tumor samples according to the manufacturer´s instructions. OncoScan assay (Affymetrix, Santa Clara, USA) for analysis of FFPE DNA material was performed according to the manufacturer´s instructions. OSCHP files from OncoScan and .CEL files from the CytoScan assay were imported into NEXUS v8.0 (BioDiscovery) and used for the analysis and visualization of somatic copy number alterations (SCNA)s and loss of heterozygosity (LOH). SCNAs (loss, gain, biallelic loss, or high amplification) and LOH calls for each sample were confirmed by visual inspection and followed by manual interpretation of whole-exome profiles. Tumors were assessed for chromosomal instability (CI). The tumor was assigned as CI if it displayed in total more than 15 SCNA; i.e. segmental chromosomal aberrations (SCA) and/or numerical aberrations (NCA).

Gene expression analysis

RNA was reverse-transcribed and used for cRNA synthesis, labelling and hybridization with GeneChip® Human Genome U133 Plus 2.0 Array (Affymetrix) according to the manufacturer's protocol. The arrays were washed and stained with phycoerytrin conjugated streptavidin using the Affymetrix Fluidics Station 450, and the arrays were scanned in the Affymetrix GeneArray 3000 7G scanner to generate fluorescent images. Cell intensity files (.CEL files) were generated in the GeneChip Command Console Software (AGCC; Affymetrix).

Fusion analysis

RNA-sequencing was done using TruSeq Stranded Total RNA Library Prep Kit and RNA was sequenced on a NextSeq500 (Illumina). Raw sequencing data from the Illumina sequencing platforms were processed with CASAVA-1.8.2. FusionMap bioinformatics tool (Array Suite) was used for screening of fusion transcripts as previously published (Ref: Ge H., Liu K., Juan T., et al: FusionMap: detecting fusion genes from next-generation sequencing data at base-pair resolution. Bioinformatics 2011; 27: pp. 1922-1928).

Determining of TERTp

Telomerase Reverse Transcriptase promotor region (TERTp) mutation was determined using Sanger sequencing for the two most common mutations; c.-124C>T and c.-146C>T. In brief, primers were designed to produce PCR products covering the sites. The purified PCR products were sequenced by Sanger sequencing using an ABI 3730 DNA Analyzer according to the manufacturer's instructions (Applied Biosystems).

Subclass analysis

In house developed classifier based on the study data (E-GEOD-68850) [21] was used to assign the tumor into one of the three subtypes of interest (Classical, Mesenchymal and Proneural). Briefly, the raw intensity .CEL files were preprocessed by quantile normalization and gene summaries were extracted via robust multi-array average (RMA). The expression values of 4324 classifier genes were standardized across samples. The 2-dimensional t-distributed stochastic neighbor embedding (t-SNE) algorithm was applied to a fraction of the dataset multiple times. A sample was considered to belong to a subtype when its corresponding Gaussian model gave the maximum probability density among the rest of the models and that probability was greater than 0.001. Since subclass division was based upon expression analysis, tissue preserved in FFPE and hence RNA degradation, could not be divided into these and was noted N/A.

Statistics

OS and PFS were estimated using the Kaplan-Meier method. Comparison of selected genes with SCNA´s (biallelic loss, amplification, LOH, deletion and LOH) and clinical characteristics, including comparison of selected genes with biallelic loss or amplification and completing RT/TMZ were calculated using the Fisher´s exact test. For univariate and multivariate analyses and OS, we used the Cox proportional hazards model and results were presented as hazard ratios (HR) with 95% confidence interval (CI). P-values <0.05 were considered significant. Statistical analyses were done using SPSS (v.25.0) and RStudio (v.3.5.2).

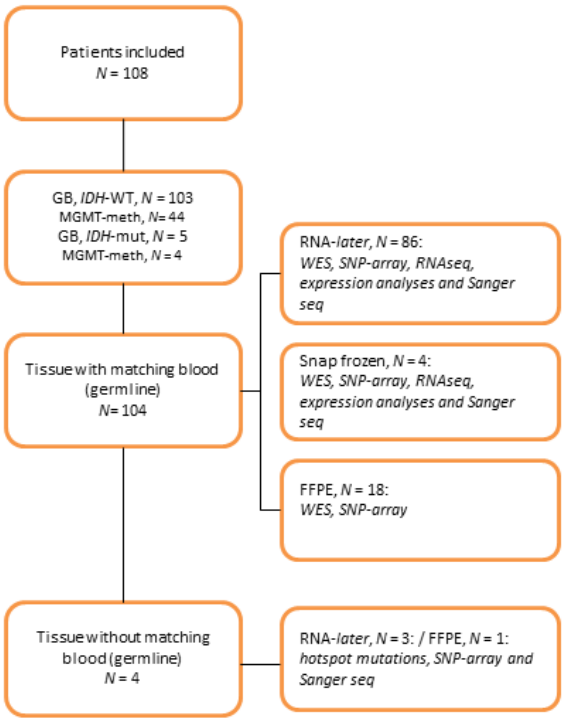

Figure 1. CONSORT diagram. The inclusion criterias were: Newly diagnosed glioblastoma (GB), no previous treatment from a lower grade glioma, signed informed consent. Diagnosis based upon WHO classification for brain cancers 2016. DNA was used to perform WES, SNP-array and Sanger seq and RNA was used to perform RNAseq, expression- and fusion analyses. Only tissue preserved in RNA-*later* or as snap frozen could be used to determine Telomerase Reverse Transcriptase promotor (TERTp)-status and subtype division. Abbreviations: IDH: isocitrate dehydrogenase; WT: wildtype; meth; methylated; mut: mutated; MGMT: O-6-methyl-guanine-DNA-methyl-transferase; FFPE: formalin-fixed-paraffin-embedded; WES: whole exome sequencing; RNAseq: RNA sequencing; SNP: single nucleotide polymorphism.

Results

Patient characteristics

A total of 108 patients were included (*table 1).* The patients resembled a standard clinical setting with patients eligible for RT/TMZ. *ATRX* mutation was found in five patients (4.6%), four of these (3.7%) were under the age of 45 and three (2.8%) had an *IDH*-mutation. One of the patients with the combined *ATRX* and *IDH*-mutation had a *H3K27M* mutation, causing a highly aggressive tumor. Median PFS and OS was 7.8 months and 16.3 months, respectively.

Number of patients	**108**
Sex	
- **Female (%)**	44 (41)
- **Male (%)**	64 (59)
Age at diagnosis, median (range)	62 (18-89)
Performance status, median (%)	0 (0-4)
- **0**	59 (55)
- **1**	34 (32)
- **2**	13 (12)
- **3**	1 (1)
- **4**	1 (1)
MGMT methylated (%)	48 (44.4)
***IDH* wild-type (%)**	103 (95)
***ATRX* mutated (%)**	5 (4.6)
Corticosteroid dose, mg (median, min-max)	15 (0-75)
Treatment (%)	
- **RT/TMZ and adj TMZ**	83 (77)
- **RT/TMZ plus IT or placebo (trial)**	6 (6)
- **IT/RT and adj IT (trial)**	4 (4)
- **TMZ monotherapy**	2 (2)
- **60Gy/30F**	5 (5)
- **34 Gy/10F**	7 (7)
- **None**	1 (1)
RT/TMZ and adj TMZ completed (%)	31 (37)
- **Median number of cycles (range)**	5 (0-11)
Still on-treatment at datalock (%)	6 (7)
Relapse surgery (%)	
- **Yes**	43 (40)
- **No**	41 (38)
- **Not yet progressed**	24 (22)
Tumor location (%) / complete resection (%)	
- **frontal**	33 (31) / (76)
- **parietal**	22 (20) / (91)
- **temporal**	30 (28) / (60)
- **occipital**	8 (7) / (100)
- **brainstem**	1 (9) / (0)
- **other**[a]	14 (13) / (64)
PFS, median (months)	7.8
- **MGMT-WT**	6.7
- **MGMT-methylated**	13.7
OS, median (months)	16.3
- **MGMT-WT**	14.7
- **MGMT methylated**	Not reached

Table 1. Patient characteristics. Performance status (PS) and corticosteroid dose was noted approximately one month after surgery when the patient was seen at Department of Oncology, before start on oncologic treatment. [a]: tumor overlapping two lobes. Abbreviations: TMZ: Temozolomide; adj: adjuvant; RT: radiotherapy; IT: immuno therapy, PFS: progression-free survival; MGMT: O6-methyl-guanine-DNA-methyl-transferase; OS: overall survival.

The genomic landscape, TERT promotor status and fusion analyses

SNP-array was successfully performed in all samples and WES in 104 (96.3%) patients, where both tumor and blood samples were available. *Figure 2* presents the genomic landscape of SCNAs present in at least 5 patients, all GB related mutations with pathological significance and fusions. The top five most aberrated genes were *PTEN, CDKN2A/B, EGFR, RB1* and *NPAS3.* The most frequent mutations were in *PTEN, TP53, NF1, RB1* and *EGFR.* A list of all identified mutations is shown in *Table S2*. TERTp was mutated in 74 (68.5%) of the samples with 51 (68.9%) having the c.124 C>T mutation and 23 (21.3%) having the c.146 C>T mutation, respectively. In the 17 patients with FFPE material, TERTp status was not assigned. Mutations in TERTp did not relate to worse OS (data not shown). We investigated all patients for fusions with *FGFR, NTRK* and *MET* and identified *NTRK2* in one patient (0.9%) with a MGMT-methylated tumor and *FGFR3-TACC3* in 3 patients (2.8%) all of which were in MGMT-WT tumors.

Subtype division

Subtype division was possible in 91 patients (84.3%) and was equally distributed with 23 patients (25.8%) having proneural, 24 patients (27.0%) classical and 25 patients (28.1%) mesenchymal subtype. 17 patients (19.1%) were outliers. We did not find subgroup division to be predictive. After adjusting for MGMT-status, the classical subgroup and the outliers had a borderline significant difference in OS. (*Figure S1 and S2A-D).*

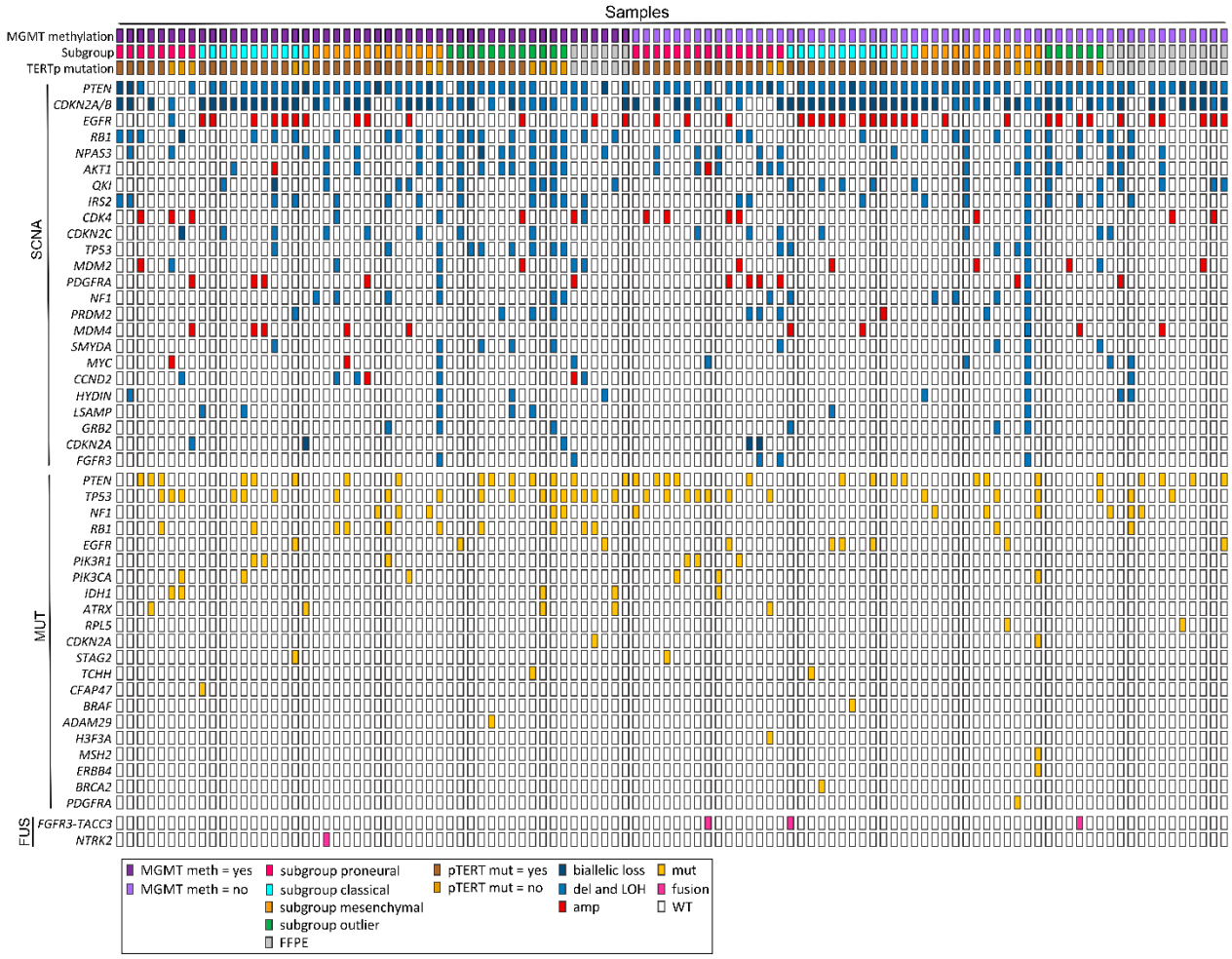

Figure 2. Landscape of somatic copy number alterations (SCNA) in selected genes altered in ≥ 5 patients, glioblastoma specific mutations and fusions listed hierarchically. *N* = 108. Only mutations categorized as pathogenic are shown. The most aberrated genes were *PTEN, CDKN2A/B, EGFR, RB1 and NPAS3* and the most frequent mutations were in *PTEN, TP53, NF1, RB1* and *EGFR.* Abbreviations: mut: mutated; fus: fusions; FFPE: formalin-fixed-paraffin embedded; MGMT: O6-methyl-guanine-DNA-methyl-transferase; TERTp: Telomerase Reverse transcriptase promotor.

Individualized treatment

Each genomic report was discussed at bi-weekly tumor board meetings with specialists from molecular biology, clinical genetics, bioinformatics, pathology and medical oncology. It was feasible to have the results ready for time of the first progression. In the study period, we found one patient with *NTRK2* fusion and patients with *IDH*-mutation eligible for experimental treatment based on the on-site available trials. One patient with *H3F3A*-mutation was included in the international ONC-201 protocol (*NCT03295396*). Other potential targets were mutations in *EGFR, CDK4/6, NF1, FGFR3*, as well as *FGFR3-TACC3* fusions.

Genomic changes and OS

We further investigated genomic alterations and OS. First, we tested clinical and genetic variables in a univariate analysis and found age < 70 years, PS 0-1 and corticosteroid dose < 10 mg once daily to be statistically correlated with better survival. MGMT-status and genes with SCNAs in ≥ 5 patients were tested in a univariate analysis. MGMT-WT, growth factor receptor bound (*GRB2)*- and SET and MYND4 (*SMYD4)* were significantly correlated to worse survival. (*Table S3).*

Testing for genomic variations with correlation to treatment completion

A total of 83 (76.9%) patients were eligible for and received RT/TMZ. 31 patients (37.4%) completed the planned treatment and 46 patients (55.4%) did not. Six patients (7.2%) were still on-treatment at time of data-lock why they were excluded in the following analysis. The main reason for not completing the planned treatment was progression. Patients completing the planned treatment, had a statistically significant survival benefit of 25.6 months *vs.* 14.6 months for patients not completing the treatment (p < 0.000) even though all the patients were eligible for concurrent treatment upfront and hence should be comparable at start of treatment. After adjusting for the three clinical (age, PS and corticosteroid dose) and genetic variables (MGMT, *GRB2* and *SMYDA*), the result was still significant, showing that completion of therapy was not alone dependent of belonging to a good prognostic group (data not shown). Next, we investigated the predictive potential for completing the treatment by testing genes with amplification and/or biallelic loss and the three clinical variables but could not identify any besides the known MGMT-status with p=0.02. *(Table S4 and figure S3).*

Tumor mutational burden

The evaluation of tumor mutational burden (TMB) was feasible in 99 patients (91.7%). Median TMB before diagnosis was 21.9/megabase (Mb) with a range of 1.9-71.0 and an extreme outlier of 362.2. When dividing TMB into low (0-15, *N*=23), median (16-30, *N*=66) and high (>30, *N*=10) we found a worse survival of 10.0 months in the TMB-high patients *vs.* 16.5 and 20.9 months in the TMB-median and TMB-low, respectively (p=0.001). We then merged TMB-median and low and compared them to TMB-high tumors, still yielding statistically significant results in OS with 18.0 months in the combined group (p=0.0005) and with a HR of 0.29 (95% CI: 0.14-0.61) in TMB-median/low *vs.* TMB-high, respectively (p=0.001). (Figure 3A-B). After testing in a multivariate analysis with adjustment for the above identified three clinical variables (age, PS and corticosteroid dose) and MGMT-status, the results remained significant with p=0.004, HR: 0.27 (95% CI: 0.11-0.65). (Data not shown).

Chromosomal instability

Next, we explored whether CI could prognosticate OS based on number of SCNAs and/or aneuploid background. Evaluation of CI was possible in 104 patients (96.3%). CI was divided into low (0-7 SCA, N=35), median (8-15 SCA, N=42) and high (>15 SCA or aneuploid background, N=27). CI-median had the worst OS of 14.8 months *vs.* CI-high and CI-low with OS of 16.5 and 20.9 months, respectively, with borderline statistically significance (p=0.094). Again, we merged the two groups with the best survival in comparison to CI-median and found a median OS of 18.7 months in the combined group (p=0.034) with a HR of 0.56 (95% CI: 0.33-0.97) in CI-high/low *vs.* CI-median, respectively (p=0.037). (Figure 3C-D). When adjusting for MGMT-status and the three clinical variables (i.e. age, PS and corticosteroid dose), the difference was still borderline significant with p=0.13, HR: 0.66 (95% CI: 0.39-1.13). (Data not shown).

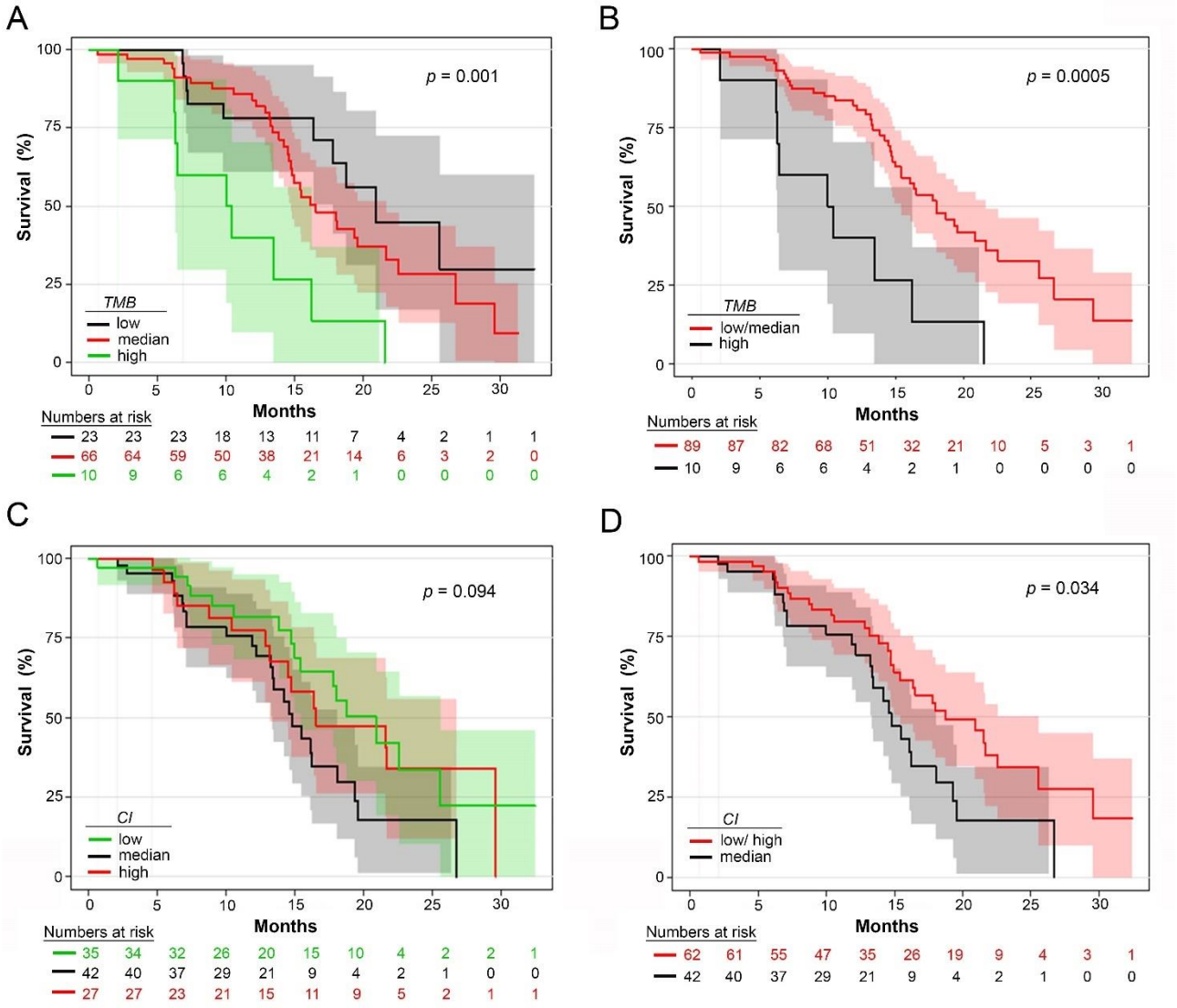

Figure 3A-D.
Kaplan-Meier curves with numbers at risk for overall survival (OS) for (A) tumor mutational burden (TMB)-high, TMB-median and TMB-low, (B) TMB-high and TMB median/low, (C) chromosomal instability (CI)-high, CI-median and CI-low and (D) CI-median and CI-high/low.
A-B: TMB was defined as number of mutations/megabase (Mb) into low (0-15, *N*=23), median (16-30, *N*=66), and high (> 30, *N*=10). Total *N*=99.
A: TMB-high *vs.* TMB-median and low had a significantly worse OS of 10.0 months (95% CI: 3.8-16.1) *vs.* 16.5 months (95% CI: 13.5-19.6) and 20.9 months (95% CI: 15.5-26.3), respectively (p=0.001).
B: Groups were segregated into TMB-high (*N*=10) *vs.* TMB-low/median (*N*=89). A statistically significant difference remained with median OS of 18.0 months (95% CI: 14.8-21.2) in the combined group (p=0.0005) and with a hazard ratio (HR) calculated using a Cox regression analyses of 0.29 (95% CI: 0.14-0.61, p=0.001) in TMB-median/low *vs.* TMB-high, respectively.
C-D: CI was split into low (0-7 segmental chromosomal aberrations (SCA), *N*=35), median (8-15 SCA, *N*=42) and high (>15 SCA or aneuploid background, *N*=27). Total *N*=104.
C: CI-median *vs.* CI-high and CI-low had a worse median OS of 14.8 months (95% CI: 21.5-17.1) *vs.* 16.5 months (95% CI: 8.1-24.9) and 20.9 months (95% CI: 16.0-25.8), respectively. Results were borderline significant (p=0.094).
D: Groups were then segregated into CI-median *vs.* CI-high/low with a median OS of 18.7 months in the combined group (95% CI: 13.8-23.7) (p=0.034) and with a HR of 0.56 (95% CI: 0.33-0.97, p=0.037) in CI-high/low *vs.* CI-median, respectively.

Combined tumor mutational load and chromosomal instability

Next, we used the results to segregate patients with a combined TMB and CI analysis (*N*=95, 88.0%) into four groups starting with the less favorable to the most favorable group; TMB-high plus CI-median (*N*=5), TMB-high plus CI high/low (*N*=5), CI-median plus TMB median/low (*N*=33) and TMB-median/low plus CI-high/low (*N*=52) with corresponding median OS of 10.0, 10.4, 15.4 and 20.9 months, respectively (p=0.001). (Figure 4). Translating this into a non-favorable (TMB-high and CI-median in any combination) *vs*. a favorable group (no TMB-high and/or CI-median in any combination), the results were still significant with a median OS of 14.8 *vs.* 20.9 months, respectively (p=0.004) and a HR of 0.47 (95% CI: 0.26-0.82) in the favorable *vs.* non-favorable prognostic group, respectively (p=0.008).

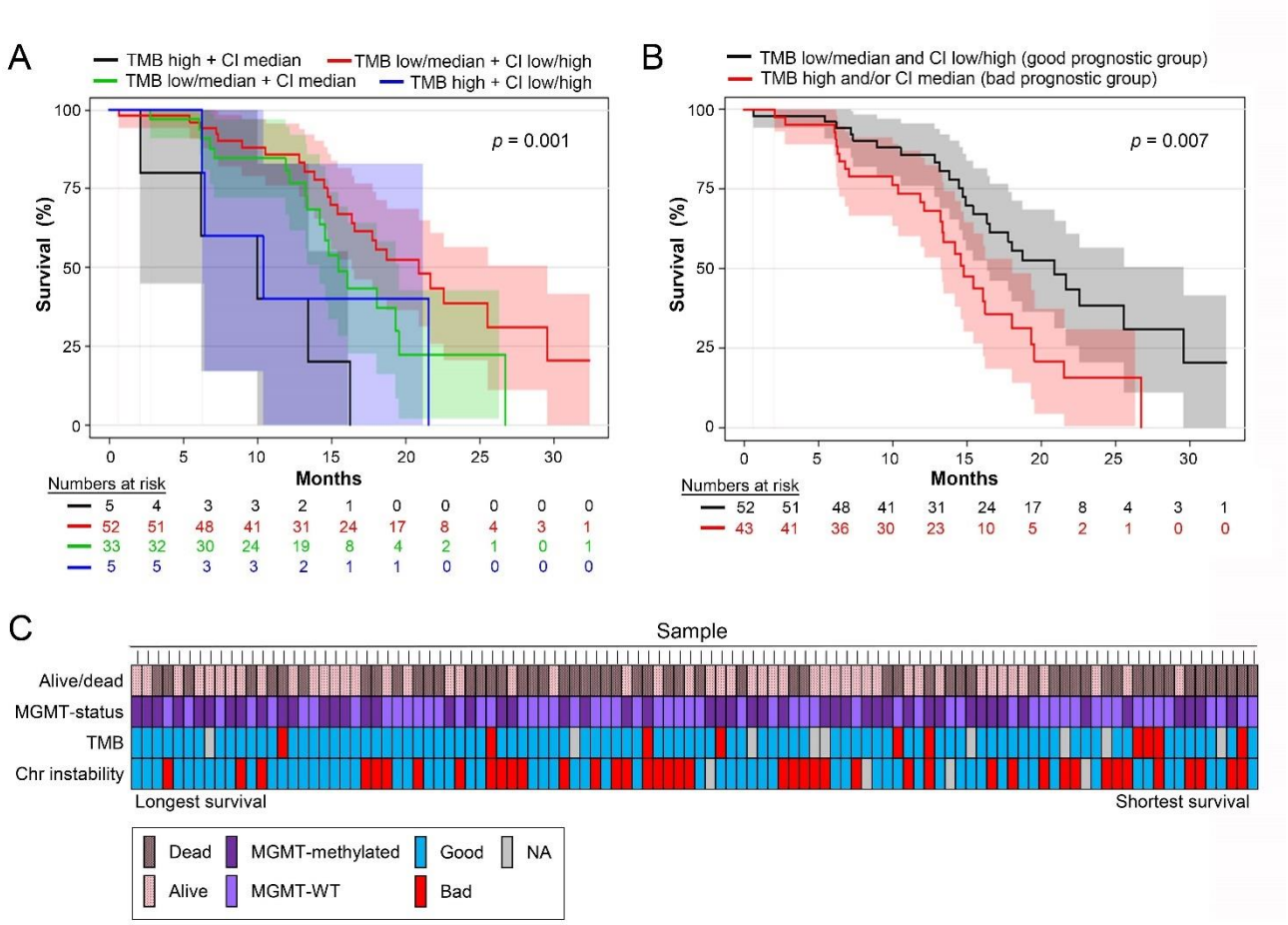

Figure 4A-B.

Kaplan-Meier curves with numbers at risk for overall survival (OS) for (A) tumor mutational burden (TMB) and chromosomal instability (CI) in different combinations and (B) TMB and CI in a bad prognostic group and a good prognostic group, respectively. Figure includes patients having both analyses performed, *N*=95.

A: Patients were split into four groups based on survival results from figure 3: TMB-high plus CI-median (*N*=5), TMB-high plus CI-high/low (*N*=5), CI-median plus TMB-median/low (*N*=33) and TMB-median/low plus CI-high/low (*N*=52) with corresponding median OS of 10.0 (95% CI: 1.9-18.1), 10.4 (95% CI: 1.8-18.9), 15.4 (95% CI: 13.4-17.5) and 20.9 months (95% CI: 15.9-25.9), respectively (p=0.001).

B. The four groups were then segregated into a non-favorable (TMB-high and CI-median in any combination) *vs*. a favorable group (no TMB-high and/or CI-median in any combination) with a corresponding statistically significant difference in OS of 14.8 (95% CI: 12.4-17.1) *vs.* 20.9 months (95% CI: 15.9-25.9), respectively (p=0.007) and with a HR of 0.47 (95% CI: 0.26-0.82, p=0.008) in the

good *vs.* bad prognostic group, respectively, calculated by a Cox proportional analysis.
C. All patients and TMB, CI- and MGMT-status, ranged with highest survival first.

Discussion

Here, we report a prospective study using the Copenhagen Glioblastoma Cohort with treatment naïve GB-patients. Findings represented known SCNAs, mutations and clinical variables and new findings were identification of *GRB2* and *SMYD4* correlating to a worse survival. All samples but two had a SCNA in either *PTEN* and/or *CDKN2A/B*, essential for development of GB. The obvious targeted treatment would be a tyrosine kinase inhibitor. However, they show a high toxicity and lower than expected efficiency [22]. In our study, sequencing depth was sufficient to find possible drivers, but sampling bias can pose another challenge due to intratumor heterogeneity where undetectable, targetable sub clones can be present at diagnosis [23] and in some cases it might be worth considering a deeper sequencing for selected targetable oncogenic drivers like *BRAF* in histologic subtypes [24, 25] or NTRK-fusions in *IDH*-WT patients [26].

Subclass division did not predict outcome

To investigate another approach of predictive value, we divided our cohort into the three subclasses: i) proneural; ii) classical, and iii) mesenchymal according to Verhaak et al [27]. However, we failed to validate their predictive value in our cohort. Recent work from TCGA showed that the predictive advantage to TMZ in the classical subtype and the prognostic value in the proneural subtype was attributed to MGMT-methylation [28], why we investigated each subclass stratified for MGMT-status. The known predictive advantage of MGMT-methylation was confirmed and a borderline significant difference in OS was found in the classical subgroup and the outliers. However, numbers are small and should be interpreted accordingly. This lack of coherence was also found in a study by the German Glioma Network [29].

Treatment completion and genetic composition

Not surprisingly, we found a statistical survival benefit in the group of patients able to complete the planned concurrent treatment, even after stratifying for the three clinical and genetic variables. Indisputable, it would be extremely valuable if we could predict who would benefit from RT/TMZ to select future patients for 1st line standard treatment or 1st line experimental treatment. Unfortunately, we could not find a predictive genetic composition for completing RT/TMZ and conclude that more research is needed in this important question. It is worth noticing that only a small subset of the intended/scheduled treatment was completed in 31 (40.3%) out of 77 evaluable patients with a median number of five cycles completed (range 0-11). A full course with RT/TMZ and adjuvant TMZ includes > eight months of treatment and with a median PFS of 7.8 months, a large percentage of patients will not be able to complete the full treatment.

TMB and CI predicts outcome

The median TMB was 21.9 mutations/Mb with one extreme outlier of 362.2. Patients with TMB-high had a significantly worse survival as compared to both median and low TMB, respectively. TMB has proved to be a useful clinical marker for IT [30, 31]. As shown in our results, TMB holds a great potential for a group of GB-patients and might have a role in future treatment stratification. In addition, TMB combined with CI shows even stronger biomarker potential. CI is a shared feature across 60-80% of cancer histologies [32] and can cause inflammation, activation of the innate immune system, universal hypomethylation with general activation of genes and a deficient mismatch repair (MMR) system [33-35]. High and low CI can both show low aggressiveness; high due to the enormous DNA instability and low due to the low growth potential [36]. However, optimal CI can create equilibrium between genomic chaos and cell survival and was defined as median CI in our cohort. Median CI lead to significantly worse survival compared to high and low group.

When we combined the less favorable group (TMB high and/or CI-median) *vs.* the favorable group (TMB-median/low plus CI-high/low), the two clustered groups showed significant difference in OS, indicating the great potential of clinical application of TMB and CI. When comparing to other studies, the median TMB of 21.9/Mb is higher and should be evaluated in the context of the methods used in our study. An agreement of how to report TMB is greatly needed [37].

Impact of molecular profiling on GB treatment

The hopes of extensive molecular profiling are in finding the targeted, efficient treatment. We identified potentially targetable aberrations including gene fusions in *NTRK2* and *FGFR3-TACC3*, mutations and/or SCNA´s in *H3F3A, EGFR, CDK4/6, IDH, NF1* and *FGFR3*. *NTRK* fusions are rare and have only been detected in 0.3% of cancers with a higher prevalence in GB of 1.4% [38]. Given the degree of positive results with TRK-inhibitors, *TRK* fusions are important to identify [5-7]. At study onset, our institution participated in basket trials with rare gene fusions, as well as *BRAF*- and *IDH*-mutation. Specifically, we have an open phase two basket trial with Larotrectinib (LOXO-101) (EudraCT: 2015-003582-28) in which the patient with the *NTRK2* fusion is a candidate at time of progression. The patients with *IDH*-mutation were candidates for experimental treatment but at the time of progression, the trial had closed for inclusion. One patient was included in an early clinical trial based upon a *H3F3A* mutation. This lack of therapeutic consequence from the genomic profiling was due to the limited number of open trials for patients with GB at our institution and the rare incidence of the gene fusions. However, identification of the *NTRK*-fusion has great clinical importance. Trial availability is a dynamic process and recently a new trial opened at our institution with TMB as inclusion criteria (NCT03668119). International umbrella- and basket trials for alterations found in our cohort do exist and are open for inclusion but this is complicated for these fragile patients. However, our study shows that it is possible to have genomic results ready at time of first progression and that GB indeed does harbor alterations for targeted therapy. Whenever possible, a relapse sample for a new genomic profile should be performed due to clonal evolution during treatment. Furthermore, the study underlines the necessity to set up international trials with adaptive designs to account for rare aberrations and for better cooperation, speed and visibility. Majority of patients with GB should enter clinical trials but a huge obstacle is the clinical deterioration that hinders participation in such. We should consider moving experimental treatment to 1st line as is elegantly done in the N^{2}M^2 trial umbrella trial (NCT03158389) or in the CheckMate trials 209-498/548 (NCT02617589 and NCT02667587). What is equally important is not to treat patients with significantly known unfavorable markers and focus on quality of life.

Conclusion

Our study shows feasibility of genomic profiling in GB for therapeutic purposes. Noticeably, we identified one *NTRK2* fusion and found high TMB or median CI to be significantly correlated with worse survival. Based on the lack of patient inclusion into targeted therapy trials, we propose a marker-based approach in experimental adaptive trials already for the 1st line treatment. We further aim on improving the clinical utility and application of the results. The molecular knowledge and technology are ahead of the clinical trials offered in GB and we foresee that future studies have a greater translational focus to make benefit of all the tremendous research already performed in this field.

Strengths and limitations

Our study has the strength of being a prospective study with only newly diagnosed, treatment naïve GB-patients included, diagnosed after the 2016 WHO classification of brain tumors and with full clinical data. We had a multidisciplinary translational collaboration with all the specialties involved in GB; surgeons, pathologists, radiologists, clinicians, Center for Genomic Medicine and the Danish Cancer Society. Limitations were the limited number of open trials for GB-patients at our institution and hence a minimal clinical utility of the results.

Author contributions

DSN, UL and HSP concepted the study. DSN included the patients, designed the clinical database and wrote the manuscript, JSR and JB applied the specimens, PH headed the preparation of tissue in RNA-*later*, CWY, OØ and AYS headed the genomic analyses and wrote the reports, SK performed subgroup analyses, MHT performed the TMB analyses, UL, HSP, SRM, CWY and OØ performed critical review of the manuscript and all authors have read and approved of the manuscript.

Acknowledgements

The authors wish to thank Monica Marie Blomstrøm and Christopher Meulengracht for helpful preparation and delivery of samples. Julie Buur Fisker, Maria Guschina, Aseeba Ayub, Miriam Yan Juk Guo and Heidi Ugleholdt for friendly and professional collaboration with the laboratory work. The authors send a special thanks to all participating patients.

Funding

Danish Cancer Society (R124-A7681 Rp12037)

1. Ostrom, Q.T., et al., *CBTRUS Statistical Report: Primary brain and other central nervous system tumors diagnosed in the United States in 2010-2014.* Neuro Oncol, 2017. **19**(suppl_5): p. v1-v88.
2. Kaley, T., et al., *BRAF Inhibition in BRAF(V600)-Mutant Gliomas: Results From the VE-BASKET Study.* J Clin Oncol, 2018: p. Jco2018789990.
3. Pusch, S., et al., *Pan-mutant IDH1 inhibitor BAY 1436032 for effective treatment of IDH1 mutant astrocytoma in vivo.* Acta Neuropathol, 2017. **133**(4): p. 629-644.
4. Ralff, M.D., et al., *ONC201: a new treatment option being tested clinically for recurrent glioblastoma.* Transl Cancer Res, 2017. **6**(Suppl 7): p. S1239-s1243.
5. Drilon, A., et al., *Efficacy of Larotrectinib in TRK Fusion-Positive Cancers in Adults and Children.* N Engl J Med, 2018. **378**(8): p. 731-739.
6. DuBois, S.G., et al., *The use of neoadjuvant larotrectinib in the management of children with locally advanced TRK fusion sarcomas.* Cancer, 2018. **124**(21): p. 4241-4247.
7. Shi, E., et al., *FGFR1 and NTRK3 actionable alterations in "Wild-Type" gastrointestinal stromal tumors.* J Transl Med, 2016. **14**(1): p. 339.
8. *Comprehensive genomic characterization defines human glioblastoma genes and core pathways.* Nature, 2008. **455**(7216): p. 1061-8.
9. Synhaeve, N.E., et al., *Clinical evaluation of a dedicated next generation sequencing panel for routine glioma diagnostics.* Acta Neuropathol Commun, 2018. **6**(1): p. 126.

10. Stupp, R., et al., *Radiotherapy plus concomitant and adjuvant temozolomide for glioblastoma.* N Engl J Med, 2005. **352**(10): p. 987-96.
11. Louis, D.N., et al., *The 2016 World Health Organization Classification of Tumors of the Central Nervous System: a summary.* Acta Neuropathol, 2016. **131**(6): p. 803-20.
12. Mansouri, A., et al., *MGMT promoter methylation status testing to guide therapy for glioblastoma: refining the approach based on emerging evidence and current challenges.* Neuro Oncol, 2018.
13. Johnson, B.E., et al., *Mutational analysis reveals the origin and therapy-driven evolution of recurrent glioma.* Science, 2014. **343**(6167): p. 189-193.
14. Muscat, A.M., et al., *The evolutionary pattern of mutations in glioblastoma reveals therapy-mediated selection.* Oncotarget, 2018. **9**(8): p. 7844-7858.
15. Bakhoum, S.F., et al., *Numerical chromosomal instability mediates susceptibility to radiation treatment.* Nat Commun, 2015. **6**: p. 5990.
16. Asimit, J.L., et al., *Trans-ethnic study design approaches for fine-mapping.* Eur J Hum Genet, 2016. **24**(9): p. 1330-6.
17. Capper, D., et al., *DNA methylation-based classification of central nervous system tumours.* Nature, 2018. **555**(7697): p. 469-474.
18. Roessler, K., et al., *Intraoperative tissue fluorescence using 5-aminolevolinic acid (5-ALA) is more sensitive than contrast MRI or amino acid positron emission tomography ((18)F-FET PET) in glioblastoma surgery.* Neurol Res, 2012. **34**(3): p. 314-7.
19. Stummer, W., et al., *Predicting the "usefulness" of 5-ALA-derived tumor fluorescence for fluorescence-guided resections in pediatric brain tumors: a European survey.* Acta Neurochir (Wien), 2014. **156**(12): p. 2315-24.
20. Plon, S.E., et al., *Sequence variant classification and reporting: recommendations for improving the interpretation of cancer susceptibility genetic test results.* Hum Mutat, 2008. **29**(11): p. 1282-91.
21. Wang, Q., et al., *Tumor Evolution of Glioma-Intrinsic Gene Expression Subtypes Associates with Immunological Changes in the Microenvironment.* Cancer Cell, 2017. **32**(1): p. 42-56.e6.
22. Dasanu, C.A., et al., *Cardiovascular toxicity associated with small molecule tyrosine kinase inhibitors currently in clinical use.* Expert Opin Drug Saf, 2012. **11**(3): p. 445-57.
23. Schramm, A., et al., *Mutational dynamics between primary and relapse neuroblastomas.* Nat Genet, 2015. **47**(8): p. 872-7.
24. Dahiya, S., et al., *BRAF-V600E mutation in pediatric and adult glioblastoma.* Neuro Oncol, 2014. **16**(2): p. 318-9.
25. Schindler, G., et al., *Analysis of BRAF V600E mutation in 1,320 nervous system tumors reveals high mutation frequencies in pleomorphic xanthoastrocytoma, ganglioglioma and extra-cerebellar pilocytic astrocytoma.* Acta Neuropathol, 2011. **121**(3): p. 397-405.
26. Ferguson, S.D., et al., *Targetable Gene Fusions Associate With the IDH Wild-Type Astrocytic Lineage in Adult Gliomas.* J Neuropathol Exp Neurol, 2018. **77**(6): p. 437-442.
27. Verhaak, R.G., et al., *Integrated genomic analysis identifies clinically relevant subtypes of glioblastoma characterized by abnormalities in PDGFRA, IDH1, EGFR, and NF1.* Cancer Cell, 2010. **17**(1): p. 98-110.
28. Brennan, C.W., et al., *The somatic genomic landscape of glioblastoma.* Cell, 2013. **155**(2): p. 462-77.
29. Reifenberger, G., et al., *Molecular characterization of long-term survivors of glioblastoma using genome- and transcriptome-wide profiling.* Int J Cancer, 2014. **135**(8): p. 1822-31.
30. Goodman, A.M., et al., *Tumor Mutational Burden as an Independent Predictor of Response to Immunotherapy in Diverse Cancers.* Mol Cancer Ther, 2017. **16**(11): p. 2598-2608.
31. Samstein, R.M., et al., *Tumor mutational load predicts survival after immunotherapy across multiple cancer types.* Nat Genet, 2019. **51**(2): p. 202-206.
32. Carter, S.L., et al., *A signature of chromosomal instability inferred from gene expression profiles predicts clinical outcome in multiple human cancers.* Nat Genet, 2006. **38**(9): p. 1043-8.

33. Bakhoum, S.F. and L.C. Cantley, *The Multifaceted Role of Chromosomal Instability in Cancer and Its Microenvironment.* Cell, 2018. **174**(6): p. 1347-1360.
34. Kawano, H., et al., *Chromosomal instability associated with global DNA hypomethylation is associated with the initiation and progression of esophageal squamous cell carcinoma.* Ann Surg Oncol, 2014. **21 Suppl 4**: p. S696-702.
35. McClelland, S.E., *Role of chromosomal instability in cancer progression.* Endocr Relat Cancer, 2017. **24**(9): p. T23-t31.
36. Andor, N., et al., *Pan-cancer analysis of the extent and consequences of intratumor heterogeneity.* Nat Med, 2016. **22**(1): p. 105-13.
37. Buttner, R., et al., *Implementing TMB measurement in clinical practice: considerations on assay requirements.* ESMO Open, 2019. **4**(1): p. e000442.
38. Gatalica, Z., et al., *Molecular characterization of cancers with NTRK gene fusions.* Mod Pathol, 2019. **32**(1): p. 147-153.

SUPPLEMENTARY

ABCB1	CDX4	HEATR7B2	PIK3CA	SULT1B1
ABCC9	CHEK2	IDH1	PIK3RI	TCHH
ADAM29	COL1A2	IDH2	PLCH2	TERT
AFM	CFAP47	IL18RAP	PODNL1	TMEM147
ALK	DCAF12L2	KEL	POT1	TP53
ANKRD36	DRD5	KMT2C	PTEN	TPTE2
ATRX	DYNC1I1	KRTAP20-2	QKI	TRPV6
BCOR	EGFR	LCE4A	RB1	UGT2a3
BRAF	ERBB1	LRRC55	RFX6	VEGFA
BRCA1	ERBB2	LUM	RPL5	WNT2
BRCA2	ERBB3	LZTR1	SCN9A	ZNF844
GCSAML	ERBB4	MET	SEMA3C	ZNF99
CALCR	FGA	MMP13	SEMA3E	ATM
CARD6	FOXR2	NF1	SEMG1	MLH1
CD3EAP	FRMD7	NLRP5	SIGLEC8	MSH2
CDH18	GABRA1	NOTCH	SLC26A3	MSH6
CDH9	GABRA6	ODF4	SPRYD5	PMS2
CDHR3	GPX5	PARD6B	SPTA1	POLE
CDKN2A	H3F3A	PDGFRA	STAG2	H3F3B

Table S1. Filter list for 95 genes used for mutation calling.

Gene	Variant	Variant	Variant
ABCB1	c.3262G>A; p.D1088N	c.1738C>T; p.R580W	
ABCC9	c.2599G>A; p.V867I		
ADAM29	**c.1043G>A; p.R348H**	c.731T>C; p.L244S	
ATRX	c.6332G>A; p.R2111Q	**c.3967G>T; p.E1323***	**c.6895_6896delCC; p.P2299fs*22**
	c.5408G>A; p.R1803H	**c.4269_4272delGAAA; p.K1424fs*65**	**c.1507C>T; p.Q503***
	c.6889_6890delTT; p.L2297fs*24	**c.4809G>T; p.Q1603H**	
AFM	c.433G>A; p.E145K	c.1954delG; p.D652fs*8	c.4049G>T; p.G1350V
BCOR	c.3874G>T; p.E1292*	c.3800_3801dupCA; p.G1268fs*68	
BRCA2	c.3847_3848delGT; p.V1283fs*2		
BRAF	**c.1786G>C; p.G596R**		
CFAP47	**c1660C>T; p.R554C**		
CALCR	c.265G>T; p.V89L		
CDH9	c.2307C>A; p.D769E	c.2307C>A; p.D769E	
CDKN2A	**c.250G>A; p.D84N**	**c.193G>A; p.G65S**	
CDH18	c.1890_1892delGGT; p.V631del		
CDX4	c.625A>C; p.N209H		
CFAP47	c.7400T>A; p.L2467Q	c.3827A>G; p.Y1276C	
COL1A2	c.1558G>T; p.G520C	c.3103G>A; p.A1035T	
EGFR	c.865G>A; p.A289T	**c.787A>G; p.T263P**	c.664C>T; p.R222C
	c.866C>T; p.A289V (x3)	**c.2156G>C; p.G719A**	**c.1793G>T; p.G598V**
	c.1793G>T; p.G598V	c.1934C>G; p.S645C	**c.754C>T; p.R252C**
	c.2006G>A; p.R669Q	**c.664C>T; p.R222C**	
ERBB4	**c.2777C>T; p.T926M**		
GABRA6	c.198T>A; p.S66R	c.1223C>T; p.S408L	
GABRB2	c.442G>T; p.V148F		
H3F3A	**c.83A>T; p.K28M**		
IDH1	**c.395G>A; p. R132H (x5)**		
IL18RAP	c.475G>A; p. A159T	c.1234G>A; p.V412I	
KEL	c.1283G>A; p.R428H		
KMT2C	c.1555C>G; p.H519D	c.2015A>G; p.E672G	
LZTR1	c.727T>C; p.F243L	c.467A>G; p.K156R	
MET	c.2533C>A; p.L845I	c.1579A>C; p.S527R	
MMP13	c.120+1G>T	c.998G>A; p.R333H	
MSH2	**c.1735A>T; p.K579***		
NF1	**c.3479delG; p.G1160fs*6**	**c.479+2T>G (splice site)**	**c.5565_5567delTCT; p.L1856del**
	C.3739_3742delTTTG; p.F1247fs*18	**c.4108C>T; p.Q1370***	**c.1318C>T; p.R440***
	c.4169T>G; p.L1390R	**c.3861_3862delCT; p.F1287fs*26**	c.4157delA; p.K1386fs*20
	c.5902C>T; p.R1968*	**c.7996_7997delAG; p.S2666fs*5**	**c.1888delG; p.V630***
	c.7348C>T; p.R2450*	**c.3916C>T; p.R1306***	**c.1746CA>; p.C582***
	c.1527+1_1527+4delGTAA; p.Y2264fs*5	**c.6789_6792delTTAC; p.Y2285fs*5**	**c.3089C>A; p.S1030***
	c.7996_7997delAG; p.S2666fs*5		
NLRP5	c.509G>A; p.G170E	c.1552C>T; p.R518C	
NOTCH1	c.2380G>C; p.E794Q	c.3317A>T; p.Q1106L	
PDGFRA	c.862T>A; p.Y288N	c.1607T>A; p.V536E	**c.868T>C; p.C290R**
PIK3CA	c.1638G>T; p.Q546H	**c.1030G>A; p.V344M**	**c.263G>A; p.R88Q**
	c.1634A>G; p.E545G	c.1134T>G; p.C378W	**c.353G>A; p.G118D**
	c.3139C>T; p.H1074Y	**c.277C>T; p.R93W**	
PIK3R1	**c.584delG; p.R195fs*15**	c.918-920delGAG; p.R307del	**c. 880A>G; p.N294D**
	c.827_829delCGA; p.T276del	c.1691A>G; p.N564S	**c.483dupA; p.R162fs*5**
	c.1690A>G; p.N564D	c.918_920delGAG; p.R307del	c.869A>G; p.D290G
	c.316G>A; p.g106R	c.543_545delATA; p.E181_Y182delinsD	c.937T>C; p.W313R

	c.918_920delGAG; p.R307del		
PLCH2	c.3571C>T; p.R1191C	c.1622T>C; p.V541A	
PTEN	**c.388C>G; p.R130G**	**c.301dupA; p.I101fs*6**	**c.1133_1136delGATA: p.R378fs**
	c.517C>T; p.R173C	**c.302T>C; p.I101T**	**c.377C>G; p.A126G**
	c.492+1G>T (splice site)	**c.170delT; p.L57fs*42**	**c.1113delC; p.D371fs**
	c.209+1G>A (splice site)	**c.385G>T; p.G129***	**c.72C>G; p.D24E**
	c.517C>T; p.R173C	**c.989_990delAA; p.K330fs*12**	c.737C>T; p.P246L
	c.479C>A; p.T160N	**c.139A>G; p.R47G**	**C800delA; p.K267fs*9**
	c.388C>G; p.R130G (x2)	**c.820delT; p.W274fs*2**	**c.728+1_728+4delGTAA (splice site)**
	c.567dupA; p.P190fs*12	c.209+1_209+4delGTAA	**c.333G>A; p.W111***
	c.955_958delACTT; p.T319*	c.166T>G; p.F56V	c.518G>A; p.R173H
	c.373A>G; p.K125E	**c.955_958delACTT; p.T319***	**c.87T>G; p.Y29***
	c.610C>A; p.P204T	**c.209+1209+4delGTAA**	**c.987_990delTAAA; p.N329fs*14**
	c.945T>A; p.Y315*	c.466G>A; p.G156R	c.98T>C; p.I33T
	c.907delA; p.I303fs*4	**c.1007dupA; p.Y336***	**c.212G>A; p.C71Y**
	c.389G>A; p.R130Q	**c.697C>T; p.R233***	
RB1	**c.368dupA; p.N123fs*8**	**c.446C>G; p.S149***	**c.1422-1G>C (splice site)**
	c.1494T>G; p.Y498*	**c.763C>T; p.R255***	**c.718A>T; p.K240***
	c.2520+1G>A	**c.1422-1G>C (splice site)**	**c.264+1G>C (splice site)**
	c.2663G>A; p.S888N	**c.1575delC; p.F526fs*6**	**c.277C>T; p.Q93***
	c.1499-1G>A (splice site)		
RPL5	**c.125delA; p.N42fs*10**	**c.3+1G>A (splice site)**	
SCN9A	c.1901G>A; p.R634H	c.326T>C; p.L109P	c.3541A>G; p.S1181G
	c.1502C>T; p.S501L		
SEMA3C	c.328-1G>A		
SLC26A3	c.1697G>A; p.R566Q		
STAG2	**c.2285_2289delAGAAA; p.K762fs*21**	**c.913C>T; p.R305***	
SULT1B1	c.824A>T; p.E275V		
TCHH	c.4322G>A; p.R1441H	c.2533C>T; p.R845C	c.513G>C; p.E1713Q
	c.2318C>T; p.A773V	**c.682C>T; p.Q228***	**c.4873G>A; p.E1625K**
TERT	c.3116C>T; p.T1039M		
TP53	c.422G>A; p.C141Y	**c.292C>T; p.P98S**	**c.1024C>T; p.R342***
	c.733G>A; p.G245S	**c.646G>A; p.V216M**	**c.817C>T; p.R273C**
	c.451C>T; p.P151S	**c.916C>T; p.R306***	**c.749C>T; p.P250L**
	c.713G>A; p.C238Y	**c.427G>A; p.V143M**	**c.649delG; p.V217fs*30**
	c.445dupT; p.S149fs*32	**c.818G>A; p.R273H**	**c.725G>T; p.C242F**
	c.844C>T; p.R282W	**c.473G>A; p.R158H**	**c.814G>A; p.V272M**
	c.963dupA; p.322fs*15	**c.517G>C; p.V173L**	**c.772G>T; p.E258***
	c.746G>T; p.R249M	**c.853G>A; p.E285K**	**c.1023_1024delCC; p.F341fs*5**
	c.434T>G; p.L145R	**c.817C>T; p.R273C**	**c.587G>C; p.R169P**
	c.200delC; p.P67fs*56	**c.527G>A; p.C176Y**	**c.1024C>T; p.R342***
	c.592G>T; p.E198*	**c.712T>A; p.C238S**	**c.770T>A; p.L257Q**
	c.934_935dupAC; p.S313fs*33	**c.653_654delTG; p.V218fs*3**	**c.524G>A; p.R175H**
	c.818G>A; p.R273H	**c.832C>A; p.P278T**	**c.712T>A; p.C238S**
	c.653_654delTG; p.V218fs*3	**c.814G>A; p.R175H**	
TRPV6	c.536G>A; p.R179H		
UGT2A3	c.350T>C; p.I117T		
WNT2	c.89T>A; p.M30K		

Table S2. A list of all tumor specific mutations called. Mutations in **bold** were defined as pathological. For definition, see Material and Method section.

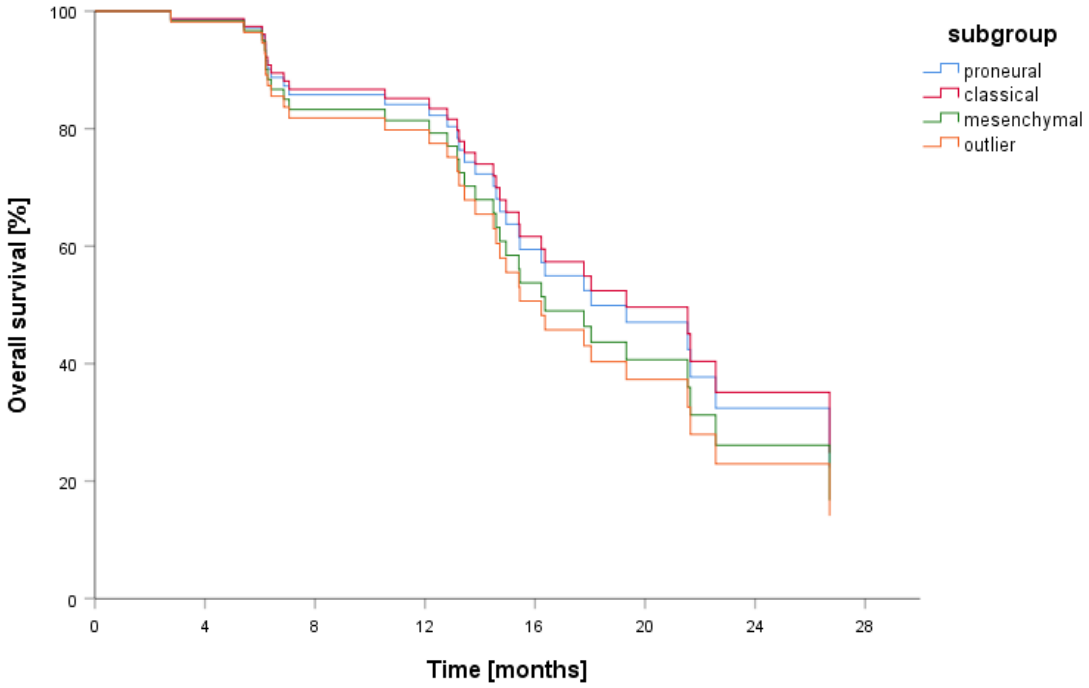

Figure S1. Cox regression analysis. Patients receiving radiotherapy/Temozolomide and had a subgroup done. N = 66. No difference in overall survival and subgroup distribution. P = 0.91.

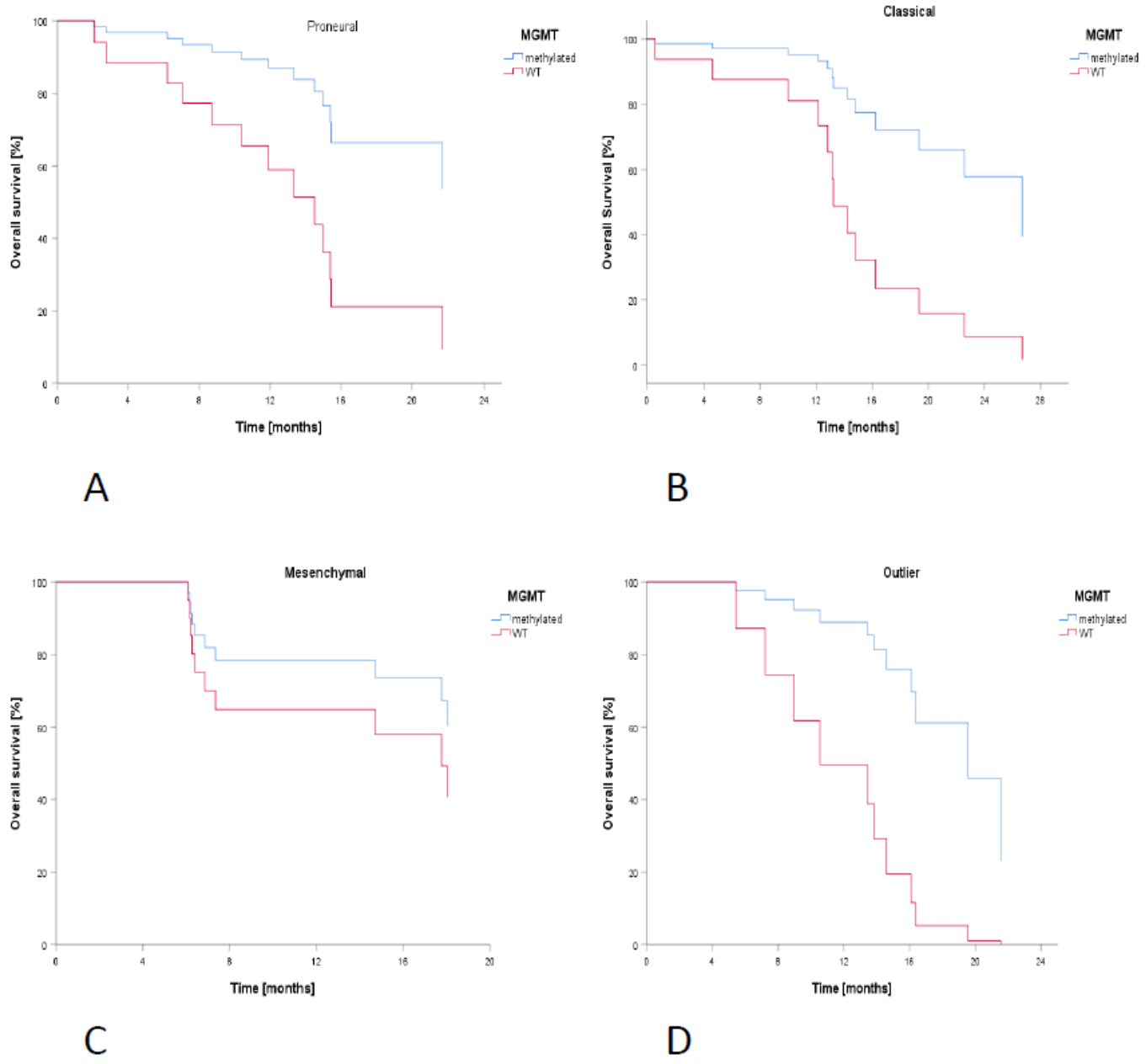

Figure S2A-D. Cox regression analyses with MGMT-status and overall survival in each subgroup.
A: Proneural. N = 23 (MGMT-meth, N=8 / MGMT-WT, N =15). P = 0.092, HR: 0.26, (95% CI: 0.06-1.24).
B: Classical. N = 24 (MGMT-meth, N=10 / MGMT-WT, N=14). P = 0.054, HR: 0.23, (95% CI: 0.05-1.02).
C: Mesenchymal. N = 25 (MGMT-meth, N=12 / MGMT-WT, N=13). P = 0.400, HR: 0.56, (95% CI: 0.14-2.17).
D: Outlier. N = 17 (MGMT-meth, N=11 / MGMT-WT, N=6). P = 0.013, HR: 0.17, (95% CI: 0.04-0.69).

Covariate	HR (95 % CI)	*P*-value
Genes (2-fold change)		
TERT promotor region	1.62 (0.68-3.85)	0.275
PTEN	0.71 (0.30-1.67)	0.438
CDKN2A/B	1.00 (0.50-1.20)	0.996
EGFR	0.94 (0.55-1.62)	0.831
MGMT-WT	0.31 (0.17-0.58)	0.0002*
RB1	0.64 (0.36-1.14)	0.127
NPAS3	0.64 (0.34-1.22)	0.175
AKT1	0.69 (0.36-1.30)	0.248
IRS2	0.67 (0.36-1.28)	0.228
QKI	1.06 (0.58-1.94)	0.860
TP53	0.58 (0.28-1.19)	0.136
CDK4	0.66 (0.33-1.31)	0.232
CDKN2C	0.73 (0.33-1.60)	0.426
SMYDA	0.32 (0.12-0.89)	0.029*
MDM2	0.56 (0.25-1.23)	0.147
NF1	0.81 (0.35-1.89)	0.621
PDGFRA	0.58 (0.21-1.62)	0.300
PRDM2	0.55 (0.17-1.77)	0.314
MYC	0.53 (0.23-1.25)	0.148
MDM4	0.56 (0.20-1.55)	0.265
GRB2	0.23 (0.06-0.94)	0.040*
CCND2	0.37 (0.12-1.19)	0.097
HYDIN	0.84 (0.26-2.32)	0.734
LSAMP	0.72 (0.26-2.02)	0.535
CDKN2A	1.89 (0.44-8.16)	0.392
FGFR3	0.23 (0.03-1.70)	0.150
AKT3	0.26 (0.04-1.90)	0.184
ATRX	1.00 (0.31-3.21)	0.995
CCNE1	1.07 (0.26-4.41)	0.928
IDH1	0.24 (0.03-1.76)	0.161
Clinical variables		
Age at diagnosis (≥70 years *vs.* < 70 years)	0.39 (0.22-0.70)	0.001*

Corticosteroid use (yes *vs.* no)	0.56 (0.32-0.98)	0.04*
WHO performance status (≥ 2 *vs.* 0-1)	0.40 (0.20-0.81)	0.01*
Completes aggressive treatment (yes *vs.* no)	2.32 (1.33-4.04)	0.003*

Table S3: Univariate analyses modelling the probability of selected genes and clinical variables as compared to OS. Fishers exact test.

Covariate	***P*-value**
Genes (2-fold change)	
TERT promotor region	0.88
MGMT-WT	0.02*
CDKN2A/B	0.36
EGFR	0.47
CDK4	0.71
PDGFRA	1.00
MDM4	0.68
PTEN	1.00
MDM2	0.30
IDH1	0.15
CDKN2A	1.00
MET	1.00
MYC	1.00
RB1	0.40
CCND2	0.40
CDKN2C	1.00
AKT1	1.00
AKT3	0.40
FGFR2	0.40
NPAS3	0.40
PRDM2	1.00
QKI	1.00
Clinical variables	
Age at diagnosis (≥70 years *vs.* < 70 years)	0.51
Corticosteroid use (yes *vs.* no)	0.09
WHO performance status (≥ 2 *vs.* 0-1)	0.08

Table S4. Fishers exact test for modelling the probability of completing the planned treatment. *N* = 77 whereof 31 has completed radiotherapy/Temozolomide and adjuvant Temozolomide and 46 has not. Only genes with biallelic losses or amplifications are shown.

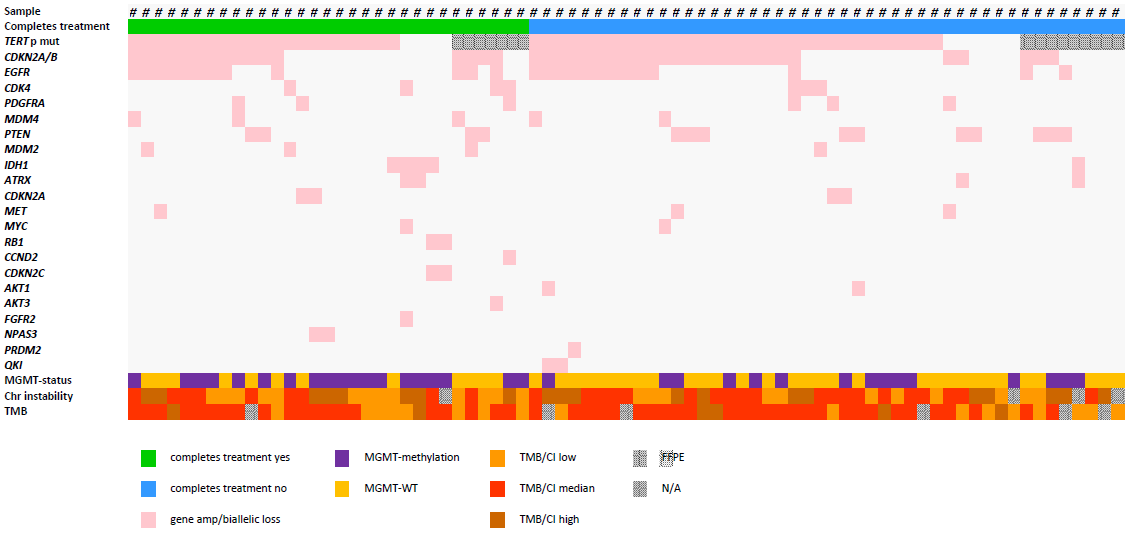

Figure S3. Landmap of patients completing treatment yes/no and genes with amplification and/or biallelic loss. Tumor mutational burden (TMB) and chromosomal (chr) instability are included.

STUDY II

Tumor mutational burden before and after treatment with Temozolomide in paired samples of glioblastoma

Dorte Schou Nørøxe[†, ‡, *], Aidan Flynn[£], Christina Westmose Yde[¶], Olga Østrup[¶], Finn Cilius Nielsen[¶], Jane Skjøth-Rasmussen[¥], Jannick Brennum[¥], Petra Hamerlik[∞], Joachim Weischenfeldt[£], Hans Skovgaard Poulsen[†, ‡], Ulrik Lassen[‡]

DSN and AF shared first authorship

Manuscript in preparation

Study II

[†]Department of Radiation Biology, Rigshospitalet, Blegdamsvej 9, 2100 Copenhagen.

[‡]Department of Oncology, Rigshospitalet, Blegdamsvej 9, 2100 Copenhagen.

[£]Biotech Research and Innovation Centre (BRIC), University of Copenhagen, Ole Maaløes Vej 5, 2200 Copenhagen

[¶]Center for Genomic Medicine, Rigshospitalet, Blegdamsvej 9, 2100 Copenhagen.

[¥]Department of neuro surgery, Rigshospitalet, Blegdamsvej 9, 2100 Copenhagen.

[∞]Danish Cancer Society, Strandboulevarden 49, 2100 Copenhagen.

*Corresponding author: anne.dorte.schou.noeroexe@regionh.dk

Abstract

Background: Treatment of the incurable glioblastoma (GB) remains a challenging task with limited treatment options. Immunotherapy (IT) has proven effective across different cancers with remarkable response rates. Tumor mutational burden (TMB) is a marker of response, but the role of TMB in GB remains undiscovered.
Materials and Methods: A prospective collection of paired samples from 35 patients with newly diagnosed GB before and after treatment with radio therapy and Temozolomide. Six patients had two relapse surgeries and tissue from all three was collected. Tumor purity in the relapse samples constituted a problem when comparing TMB. Hence, we developed a model to adjust for tumor purity. Signature analyses were performed in all 35 patients.
Results: After tumor purity adjustment, we found TMB comparison reliable in 25/35 patients (71.4%). TMB increased with a factor 1.1 from 0.9/Megabase (Mb) to 1.1/Mb before and after treatment, respectively. Signature AC1 was the most prominent signature, associated with cellular ageing.
Conclusion: Comparison of TMB was possible in 25 patients. No significant increase was identified. We did not find a signature AC11, associated with TMZ exposure, nor did we find hypermutation after treatment.

Introduction

Tumor mutational burden (TMB) is a promising new marker of response to immunotherapy (IT). TMB is the number of nonsynonymous somatic mutations in a tumor sample and is associated with genome instability, a hallmark of cancer [1]. A high TMB can cause an increased number of neoantigens that serves as a marker of recruiting the adaptive immune system which makes the TMB-high tumor susceptible to IT. Good clinical response rates have been shown in TMB-high tumors like melanoma, non-small-cell lung cancer (NSCLC), renal cell carcinoma and mismatch repair (MMR) deficient colon cancer [2-5]. Mutations in these tumor types are mainly caused by exogenous mutagenesis and have a TMB-average of 3-400/Megabase (Mb) (range to more than 1000) [6]. This is opposite of glioblastoma (GB), where the majority of somatic mutations have an unknown etiology with increasing incidence with age [7] making the ratio between new/memory T-cells lower, causing a less effective immunologic response which includes aggravated DNA-repair mechanisms. Despite a huge unmet medical need, the clinical role of TMB in GB has yet to be explored. GB is incurable with a progression free survival (PFS) of 7-8 months and a median overall survival (OS) of 16-22 months depending on prognostic and predictive markers [8-11]. Standard treatment includes the alkylating drug Temozolomide (TMZ) [12] that can cause hypermutated phenotypes [13, 14] Response to IT in GB has been shown in case stories based upon mutations in MMR genes [15-17] making TMB clinically interesting as a marker for response to IT. Studies of TMB across different brain cancers have included both high grade glioma (HHG), low grade glioma (LGG) and pediatric gliomas with inclusion of both primary and relapse samples with limited data on prior treatment, unknown tumor purity estimation, whole genome sequencing (WGS) *vs.* whole exome sequencing (WES) *vs.* targeted sequencing, different data processing analyses and lack of validated assays [3, 4, 7, 16, 18-24]. These factors challenge the estimation of TMB in GB but has been estimated to approximately 1-2 mutations/Megabase (Mb) [6, 25]. Tumors with high TMB are more prevalent in TMZ-exposed HGG with a prevalence of 3.5% to 17% [13, 18-20]. This clonal evolution during TMZ exposure may make the resistant tumor more susceptible to IT. However, a study in recurrent GB with Bevacizumab (BEV) *vs.* the Programmed Death1 inhibitor (PD1i), Nivolumab showed no difference in OS [26]. The study did not stratify for TMB, but TMB is being analyzed retrospectively and is being incorporated in future studies as an endpoint (NCT02667587). Whether or not TMB is predictive in GB is now being tested [18, 26]. In the present study, we sought to investigate TMB before and after exposure to first line treatment in paired samples from 35 patients with newly diagnosed GB, isocitrate dehydrogenase (*IDH*)-WT. We examined the influence of tumor purity on TMB estimates and applied a simple method to perform tumor purity adjustment. This enabled a comparable analysis between tumor samples with vastly different tumor purities, which is especially pertinent in relapse samples. They are normally less enriched with tumor cells, e.g. due to infiltration of inflammatory cells following exposure to radiotherapy (RT) and TMZ.

Materials and Methods

Patients

A total of 35 patients were included from February 2016 to August 2018 at Rigshospitalet, Copenhagen. All patients had newly diagnosed GB based on the 2016 WHO-classification [1] and had a second surgical procedure performed due to progression. All patients had provided an informed, signed consent. Clinical data was noted through patient interviews and medical records, including age at diagnosis, gender, date and extent of surgery as assessed by the neuro-surgeon, treatment given at Department of Oncology, PFS and OS. Date of datalock was 10.03.2019. The project was carried out in accordance with the Declaration of Helsinki and with approval from the Danish National Ethics Committee (Journal number: H-3-2009-136 and 1707335) and Danish Data Protection Agency (Journal numbers: 2014-41-2857 and VD-2018-204 with I-suite number: 6447).

Collection of tissue

Tissue from surgery was immediately preserved in RNA-later for optimal DNA and RNA purification. In case of insufficient amount of tissue, we used supplement tissue that was either snap frozen or formalin-fixed-paraffin-embedded (FFPE). Patients further delivered a blood sample for germline retraction.

WES

WES was performed using DNA from tissue and blood. DNA from tumor samples (tDNA) was extracted using the AllPrep DNA/RNA purification kit and the QIACube workstation (Qiagen) according to manufacturer's instructions. Genomic DNA from whole blood samples (gDNA) was isolated using the liquid handling automated station (Tecan). Purified DNA was quantified using the Qubit instrument (Life Technologies). Genomic DNA (200 ng) was fragmented to 300 bp using on Covaris S2 (Agilent) and adaptor ligation was performed using KAPA HTP Library Preparation Kit (Roche). Exomes were enriched with SureSelectXT Clinical Research Exome kit (Agilent). Paired-end sequencing (2x100 bp or 2x150 bp) was performed to gain an average coverage of 50-100x, using the HiSeq2500 or NextSeq500 platforms from Illumina. Raw sequencing data were processed using CASAVA-1.8.2. Reads were aligned to the human reference genome (hg19/GRCh37) using BWA-mem (v0.7.10). Somatic variant calling was performed using MuTect (v1.1.7) [27]; a high-confidence call set was established by removing frequently miscalled sites and variants with an allele frequency below 10% in the tumor DNA. Somatic variants were identified by excluding variants found in blood WES data from the patient, and further analyzed using Ingenuity Variant Analysis (Qiagen).

Tumor mutational burden

For each surgical time-point, variant sites detected by MuTect were assessed in all matched patient samples using Samtools mpileup (v1.8) [28]. To ensure optimal sensitivity when comparing TMB between surgeries, any variant supported by two or more reads in a paired sample was considered present. To compensate for differences in sensitivity arising from tumor purity we computed a scaling factor between samples with differing purity. First a density distribution was computed for the variant allele frequencies (VAFs) of each sample using a gaussian kernel. The peak representing clonal heterozygous mutations was determined by selecting the peak at the greatest VAF (pkVAF) where the magnitude of the peak was at least one-third of the highest magnitude peak present. The difference in pkVAF values between paired samples was calculated and the value was subtracted from VAF of all variants in the sample with the greater pkVAF. Any variants with a negative VAF were considered to be below the artificial detection threshold and removed. A scaling factor was determined using the ratio of the raw TBM to the filtered TMB. The raw TMB of the sample with the lesser pkVAF was multiplied by the adjustment factor to obtain the adjusted TMB.

Signature analyses

Linear combination decomposition analysis was performed using the YAPSA package (v1.8) (Huebschmann D, Gu Z, Schlesner M (2018). YAPSA: Yet Another Package for Signature Analysis. R package version 1.8.0. [https://rdrr.io/bioc/YAPSA/]) for the R statistical framework. Mutation contexts were determined based on the UCSC HG19 genome via the BSgenome (BSgenome.Hsapiens.UCSC.hg19) package for R. A signature cut-off of 1% was used to filter any signature that did not account for at least 1% of the mutations across the cohort.

Results

Clinical data

A total of 35 patients were included *(table 1)*. Paired tissue samples were collected from the diagnostic and relapse surgery, respectively. Six patients had three surgical procedures due to relapse twice and tissue from all three surgeries has been included in this study.

Number of patients	35
Gender	
- Female (%)	10 (28.6)
- Male (%)	25 (71.4)
Age at diagnosis, median (range)	61 (40-80)
PS after diagnostic surgery (%)	
- 0	20 (57.1)
- 1	13 (37.1)
- 2	2 (5.7)
PS after relapse surgery (%)	
- 0	11 (31.4)
- 1	12 (34.3)
- 2	12 (34.3)
MGMT-status (%)	
- Methylated	7 (20.0)
- WT	28 (80.0)
IDH-WT (%)	35 (100)
Treatment	
- STUPP[a]	28 (80.0)
- IT (trial)[b]	4 (11.4)
- Other[c]	3 (8.6)
Sample preservation, diagnostic surgery (%)	
- RNA-*later*	25 (71.4)
- FFPE	8 (22.9)
- Snap frozen	2 (5.7)
Sample preservation, relapse surgery (%)	
- RNA-*later*	19 (54.3)
- FFPE	16 (45.7)
- Snap frozen	0 (0)
PFS diagnostic surgery, median (months)	7.5
PFS relapse surgery, median (months)	5.5
OS, diagnostic surgery, median (months)	16.2
OS relapse surgery, median (months)	8.9

Table 1: Patient characteristics.

[a]Radio therapy (RT) with 60 Gy/30F concomitant with Temozolomide (TMZ) followed by adjuvant TMZ. [b]RT/TMZ plus a Programmed Death1 inhibitor (PD1i) in a trial. One patient received RT/TMZ plus PD1i or placebo. [c]30Gy/10F or 60 Gy/30F.

Pseudo progression

Three patients had ≤ 3 mutations in the relapse sample and did not have true progression. This was supported by the histopathological examination without identification of vital tumor cells and by the clinical decision. One patient continued the adjuvant TMZ after the relapse surgery and two patients continued in a follow-up program with one patient having progression approximately three months after relapse surgery and the other having no evidence of relapse at time of datalock, living +22 months from diagnosis.

Tumor mutational burden and signature analyses before and after treatment

A shown in the CONSORT diagram, a total of 32 paired samples were included. An unadjusted TMB score was estimated in 32/32 samples (100%). When adjusting for tumor purity, TMB comparison was possible in 25/32 samples (78%). A total of 7/32 samples (22%) were excluded due to low tumor content ≤15% and represented all relapse samples *(figure 1)*. An unadjusted median TMB/Mb before and after treatment was stable at 0.91 (range: 0.3-1.5) vs. 0.85 (range: 0.3-2.4), respectively. When adjusting for tumor purity, the median TMB/Mb before and after treatment was 0.91 (range: 0.4-1.5) vs. 1.06 (range: 0.4-2.4), respectively. We segregated the adjusted TMB by the median and defined TMB-high as ≥ 0.91 mutations/Mb and TMB-low as <0.91 mutations/Mb.

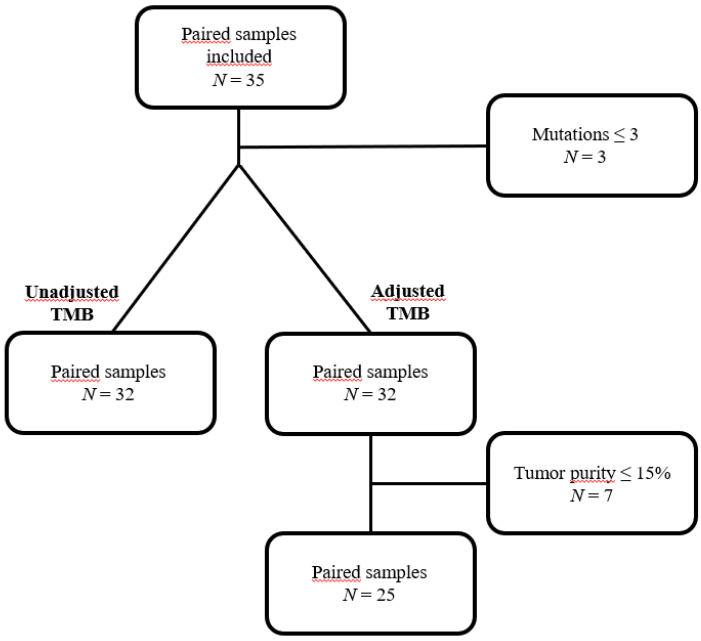

Figure 1. Consort diagram of included patients. *N(patients)* = 35. Three samples were excluded upfront due to a mutation count ≤ 3. For the adjusted TMB-scores, seven samples were excluded due to a tumor purity ≤ 15%.

We next performed a comparative analysis of the TMB between the paired samples to identify the number of shared and private mutations in each patient (Figure 2, top panel). The majority of mutations were shared between the primary and relapse sample and most of the relapse samples presented with de novo mutations. The patients with three surgical procedures presented with de novo mutations private for the second relapse. Patient RHGB003 had the highest increase in TMB after treatment. Even so, the increase could not qualify for development of a hypermutated phenotype. Mutational signature analysis has been used across a wide range of cancers to explore underlying mutational processes driving tumor evolution. We applied linear combination decomposition (LCD) using a curated set of thirty mutation signatures made available by the Catalogue of Somatic Mutations in Cancer (COSMIC). Signature 1 (AC1), which is associated with spontaneous deamination of 5-methylcytosine and generally considered a consequence of cellular ageing, was the most prevalent signature across the cohort. Signature AC19, a signature with unknown etiology previously seen in pilocytic astrocytoma, was found in eight cases. The DNA mismatch repair (MMR) deficiency signatures AC6 and AC15, were found in nine and 18 cases, respectively. Approximately half of the patients (16/35) had at least 10 % of the mutational signatures attributable to MMR, suggesting that MMR was a prominent mutational process in these GB tumors, although none of these cases exhibited significantly greater mutational burden as might be expected in repair deficient tumors. We found a small number of cases with signature AC13, associated with stranded G-to-C transversions and APOBEC enzyme activity. We note that the low number of overall mutations may decrease the sensitivity to less frequent mutational signatures. We did not find evidence of AC11, associated with TMZ exposure, however, we also did not see evidence of TMZ induced hyper-mutation profiles. A table of filtered genes present in the primary vs. first and second relapse is shown in *supp table ST2* and *supp table ST3.*

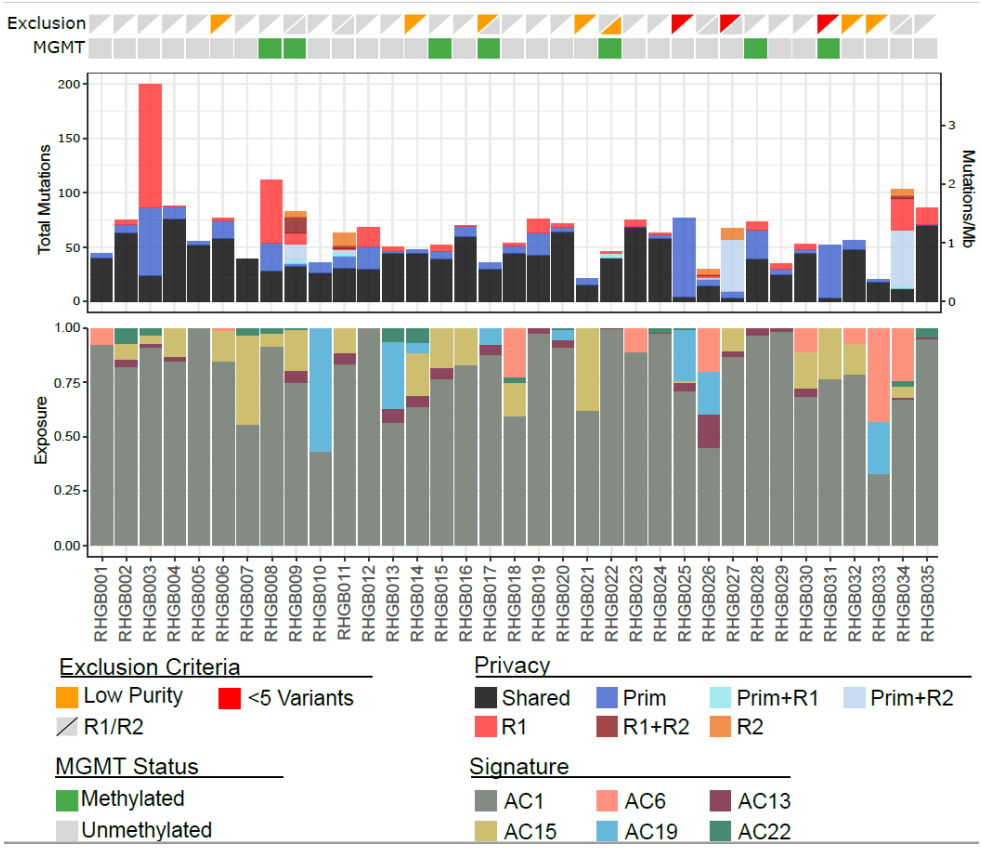

Figure 2.

Top: Number of mutations, MGMT status and samples excluded for tumor mutational burde comparison across all specimens sequenced in each patient. Bar color indicates the privacy status of each category of variants depending on their presence in the primary (Prim), first relapse (R1), and second relapse (R2).

Bottom: Linear combination decomposition was used to detect the contribution of each of the thirty somatic mutation signatures found in the Catalogue Of Somatic Mutations In Cancer (COSMIC).

Study II

Purity adjustment and influence on TMB

The digital nature of next-generation sequencing technologies provides excellent sensitivity for detecting mutations in mixed populations of cells. Despite this, these technologies are still vulnerable to the effects of sample purity and excessive contamination with normal tissue will adversely affect the sensitivity of variant calling algorithms. To facilitate TMB comparisons between samples of varying purity we attempted to model the loss of sensitivity in less pure samples. Initially, the density distribution of VAFs was used to estimate tumor purity. Samples with a peak density less than 0.075 (representing 15% tumor) were deemed to be unreliable for TMB-score *(figure 3)*. Using this definition, we excluded 7/32 samples (22%) and all excluded samples were from relapse surgery *(supp figure S1-S2 and ST3)*.

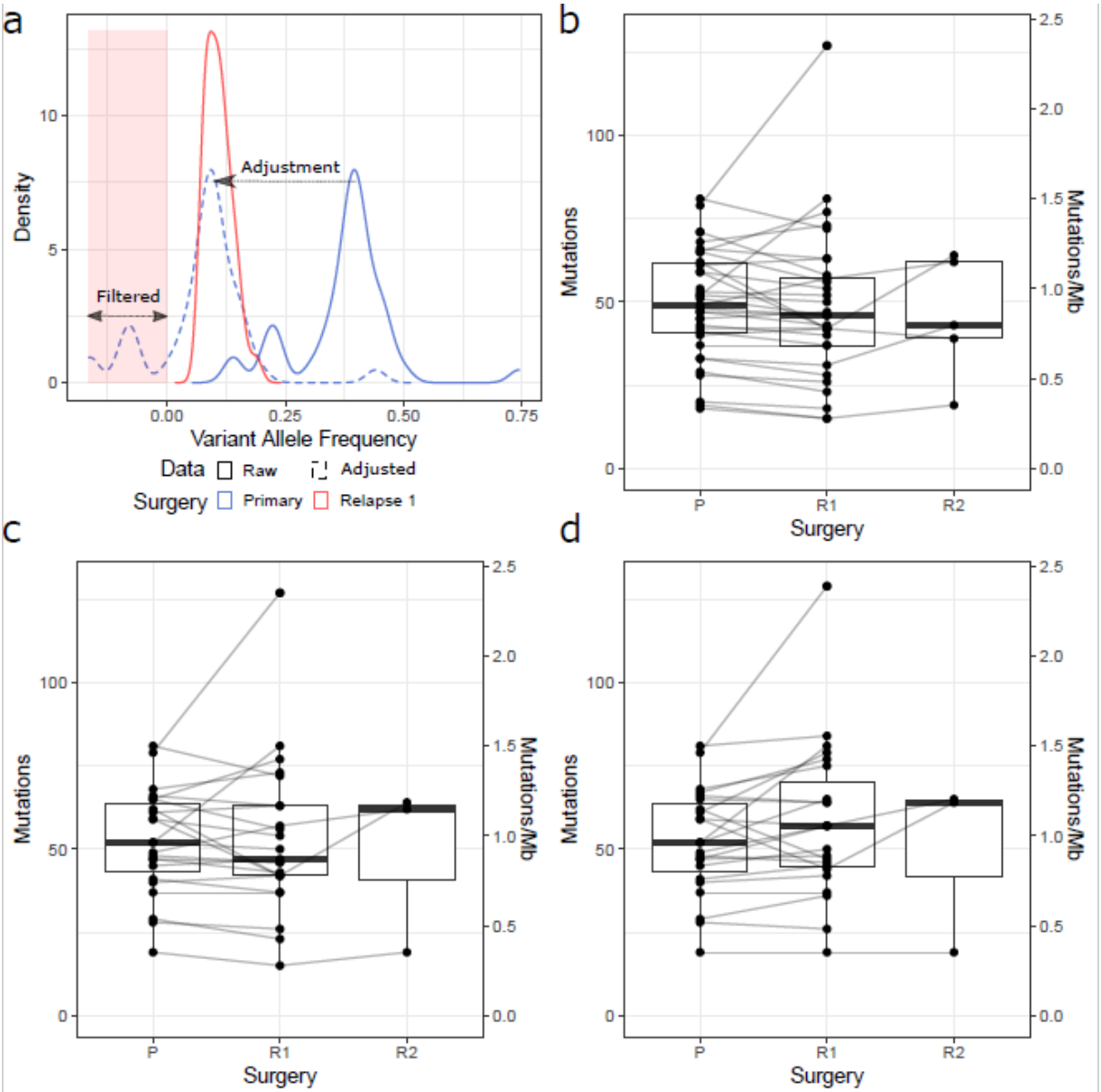

Figure 3
(a) Schematic illustrating the method for purity normalisation. A density distribution was derived for the variant allele frequencies in each sample (solid red and blue lines). The peaks of each distribution were found and the distribution of the more pure sample was adjusted to match the less pure (dashed blue line). The adjustment value was subtracted from all variants in more pure sample, and variant that subsequently had a frequency less than zero was removed. The ratio of the raw tumour mutation burden (TMB) to the filtered variant count was used to calculate a correction factor for the less pure specimen. (b) Raw unadjusted TMB for all cases. (c) Raw unadjusted TMB for all cases considered to be of reliable purity (d) Adjusted tumour mutation burden for cases of reliable purity

TMB and MGMT-status

MGMT-methylated tumors (*N*=3) were all concentrated in the TMB-high group whereas the MGMT-WT tumors (*N*=22) were distributed with nine and 13 in the TMB-high and TMB-low, respectively. The difference was significant using a paired T-test (p=0.001).

TMZ did not induce hypermutation

In the TMZ-exposed patients (*N*=19), the median TMB changed from 0.96 to 1.01 (range 0.4-1.5 to 0.4-2.4), representing an increase with a factor 1.1. Three patients received IT in a trial with a change in median TMB from 0.76 to 0.93 (range 0.6-0.8 to 0.8-1.2), representing a factor 1.2. The remaining three patients received RT only with a change in median TMB from 1.15 to 0.87 (range 0.7-1.2 to 0.7-1.4), representing a factor 0.8 *(figure 4).*

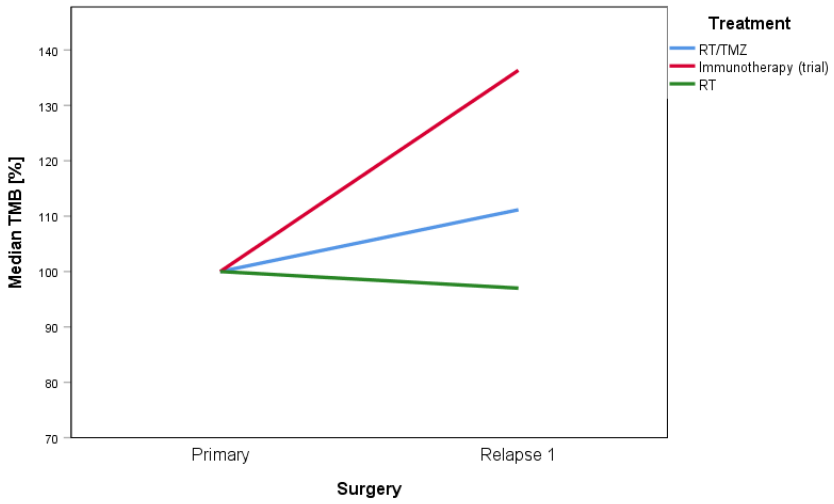

Figure 4. Tumor mutational burden/Megabase (TMB/Mb), normalized, before (Primary) and after treatment (Relapse 1). Categorized after treatment in first line. Radio therapy (RT)/Temozolomide (TMZ) *N* = 29 (82.9%). Immunotherapy *N* = 3 (8.6%). RT *N* = 3 (8.6%).

Discussion

Here we present a prospective study with results based on paired samples from a vulnerable patient cohort where tissue is extremely difficult to obtain due to the invasive procedure of brain surgery. Newly diagnosed patients with GB were included and again at relapse surgery. The inclusion period extended over 2½ year and median PFS was 7.5 months; accordingly, the actual inclusion period for the relapse sampling was < 2 years. At our institution, we perform relapse surgery on approximately 30 patients/year and this study represents an inclusion of 60-70% of eligible patients. Previous studies on paired samples in GB have been with sample sizes of < 40 and, to our knowledge, have been on archival tissue. This illustrates the complexity in obtaining paired samples in GB patients. To increase availability of datasets from paired samples, the international GLASS consortium has been initiated with the aim of generating longitudinal genomic and molecular data in *IDH*-WT, *IDH*-mutant and 1p/19q co-deleted tumors [29].

Exclusion of samples for paired TMB comparison

Upfront, we had to exclude three samples from patients not having true progression and hence limited mutations in the samples. They illustrate the dilemma between performing surgery or not when in doubt of progression and the consequences that follow with either a preliminary shift from an effective treatment or a continuation of a non-effective treatment. Majority of the relapse samples had low tumor purity, which can affect TMB estimates and can cause comparison unreliable. Therefore, we developed a method to adjust for tumor purity by adjusting the density distribution of the variant allele frequencies in the more pure sample to match that of the less pure sample. Our assumption was that in normalizing the densities we could simulate the rate at which information was lost from the less pure sample through normal contamination and use the ratio of the original counts in the pure sample to the "post-normalization" counts to produce a scaling factor. We then obtained an approximation of what the counts might have been in the less pure sample if it had higher tumor content by multiplying by the scaling factor. We found that the purity-based correction became unstable at tumor purities below 15% and therefore decided that further 7 samples had to be excluded, leaving 25 paired samples for the paired TMB analyses.

TMB and signature analysis

We estimated a median TMB of 0.9/Mb in treatment naïve samples that was comparable with previous findings [6, 25]. We then investigated the effect of first line treatment and development in TMB and found that TMZ did not induce a hypermutation There was a small difference in TMB increase after treatment in the TMZ-exposed vs. IT treated vs. RT only exposed tumors with a factor 1.1, 1.2 and 0.8, respectively. It was unexpected that TMZ did not cause a greater increase in TMB, since other reports have shown that TMZ treatment can result in development of hypermutation and has been found in up to 17% of TMZ-exposed relapse samples [13, 30]. The IT treated patients had the highest increase, but numbers are small and should

be validated in larger cohorts, e.g. within the GLASS consortium. In line with those results, and opposite to what we expected, signature analysis did not reveal a development of the TMZ-signature AC13. However, it is well-established that the sensitivity of mutational signature analyses is highly dependent on larger sample cohorts.

MGMT-methylated tumors all had TMB-high

All seven MGMT-methylated tumors were significantly pooled in the TMB-high group. The use of TMB-high as prognostic to a worse OS has been replicated in a larger cohort that included the patients from the present study, using TMB estimate without purity-adjustment (paper submitted). To our knowledge, the relationship between MGMT-status and TMB has not been previously investigated and warrants further investigation in the context of future treatment stratification in trials.

Comparison of TMB between cancers

When comparing to other cancer types, our study-specific definition of TMB-high (> 0.91/Mb) is lower than a TMB-high definition for other cancer types. It is difficult to compare TMB across cancers due to different etiologies and possible exogenous exposure causing an increased mutational burden by itself. Therefore, inclusion criteria to experimental trials based on TMB-score alone, can make inclusion of GB patients difficult and TMB scoring should preferably be compared to the same disease entity. Even when doing so, there are many technical biases that can hamper comparison between studies and the clinical use of TMB, e.g. bioinformatics, data processing, preservation and age of tumor specimens, sequencing technology and depth, filtering of false positive and false negative variants, treatment naïve vs. pretreated tissue and the unit used and a standardization is needed [21, 24, 31, 32]. Whether or not hypermutation caused by somatic- or germline mutations or by TMZ is comparable, is unclear and results from relapse studies cannot be directly translated to newly diagnosed patients due to biases of treatment and clonal evolution.

TMB as a predictive marker to IT in GB

The use of TMB as a predictive marker of response to IT has a great potential. However, it will be relevant for only a minority of GB patients as illustrated by the results in our study; none had a TMB score allowing for IT according to present approved inclusion criteria and none developed a hypermutation after treatment. Since hypermutation is greater in relapsed TMZ-exposed patients as compared to newly diagnosed patients, it would be expected that IT could have an important role for relapse patients. The CheckMate 209-143 investigated the PD1i Nivolumab vs. BEV in relapse GB. Preliminary results did not show superiority to Nivolumab. However, it was found that the duration of response was longer in the Nivolumab-treated group, suggesting that IT is relevant for a small subgroup [33, 34]. There are ongoing studies with Nivolumab in newly diagnosed GB patients where TMB is an endpoint and results are awaited. The predictive role of TMB

cannot stand alone though, since response to IT has also been shown in melanoma, GB and NSCLC tumors with low TMB [3, 4, 35]. Other factors for response to IT is age, tumor infiltrating lymphocytes (TILs), PD-L1 expression, mutations and expression of DNA-repair-genes [36, 37]. Furthermore, IT has been investigated in other tumors like prostate and pancreatic cancer with no effect, which may be explained in part by the low TMB in these tumors [7].

Conclusion

TMB estimation was possible in all paired samples from 35 patients included. However, the relapse samples presented with a low degree of tumor purity, making inter-sampling comparison of TMB unreliable. Therefore, we developed a method to adjust for tumor purity and ended up with 25 paired samples for TMB comparison. No significant increase in TMB was seen after first line treatment with majority of patients receiving RT/TMZ. Signature AC1 was the most prominent signature, associated with cellular ageing. We did not find a signature AC11, associated with TMZ exposure, nor did we find hypermutation after treatment. MGMT-methylated tumors had TMB-high.

Acknowledgements

The authors wish to thank Monica Marie Blomstrøm and Christopher Meulengracht for helpful preparation and delivery of samples. Julie Buur Fisker, Maria Guschina, Aseeba Ayub, Miriam Yan Juk Guo and Heidi Ugleholdt for friendly and professional collaboration with the laboratory work. The authors send a special thanks to all participating patients.

Reference List

1. Hanahan, D. and R.A. Weinberg, *Hallmarks of cancer: the next generation.* Cell, 2011. **144**(5): p. 646-674.
2. Pavel, A.B. and K.S. Korolev, *Genetic load makes cancer cells more sensitive to common drugs: evidence from Cancer Cell Line Encyclopedia.* Sci. Rep, 2017. **7**(1): p. 1938.
3. Rizvi, N.A., et al., *Cancer immunology. Mutational landscape determines sensitivity to PD-1 blockade in non-small cell lung cancer.* Science, 2015. **348**(6230): p. 124-128.
4. Snyder, A., et al., *Genetic basis for clinical response to CTLA-4 blockade in melanoma.* N. Engl. J. Med, 2014. **371**(23): p. 2189-2199.
5. Yarchoan, M., et al., *Targeting neoantigens to augment antitumour immunity.* Nat. Rev. Cancer, 2017. **17**(4): p. 209-222.
6. Lawrence, M.S., et al., *Mutational heterogeneity in cancer and the search for new cancer-associated genes.* Nature, 2013. **499**(7457): p. 214-218.
7. Alexandrov, L.B., et al., *Signatures of mutational processes in human cancer.* Nature, 2013. **500**(7463): p. 415-421.
8. Louis, D.N., et al., *The 2016 World Health Organization Classification of Tumors of the Central Nervous System: a summary.* Acta Neuropathol, 2016. **131**(6): p. 803-20.
9. Thon, N., et al., *Outcome in unresectable glioblastoma: MGMT promoter methylation makes the difference.* J Neurol, 2017. **264**(2): p. 350-358.
10. Michaelsen, S.R., et al., *Clinical variables serve as prognostic factors in a model for survival from glioblastoma multiforme: an observational study of a cohort of consecutive non-selected patients from a single institution.* BMC. Cancer, 2013. **13**: p. 402.
11. Stupp, R., et al., *Effects of radiotherapy with concomitant and adjuvant temozolomide versus radiotherapy alone on survival in glioblastoma in a randomised phase III study: 5-year analysis of the EORTC-NCIC trial.* Lancet Oncol, 2009. **10**(5): p. 459-466.
12. Stupp, R., et al., *Radiotherapy plus concomitant and adjuvant temozolomide for glioblastoma.* N Engl J Med, 2005. **352**(10): p. 987-96.
13. Wang, J., et al., *Clonal evolution of glioblastoma under therapy.* Nat Genet, 2016. **48**(7): p. 768-76.
14. van Thuijl, H.F., et al., *Evolution of DNA repair defects during malignant progression of low-grade gliomas after temozolomide treatment.* Acta Neuropathol, 2015. **129**(4): p. 597-607.
15. Snyder, A. and J.D. Wolchok, *Successful Treatment of a Patient with Glioblastoma and a Germline POLE Mutation: Where Next?* Cancer Discov, 2016. **6**(11): p. 1210-1211.

16. Bouffet, E., et al., *Immune Checkpoint Inhibition for Hypermutant Glioblastoma Multiforme Resulting From Germline Biallelic Mismatch Repair Deficiency.* J Clin Oncol, 2016. **34**(19): p. 2206-11.
17. AlHarbi, M., et al., *Durable Response to Nivolumab in a Pediatric Patient with Refractory Glioblastoma and Constitutional Biallelic Mismatch Repair Deficiency.* Oncologist, 2018. **23**(12): p. 1401-1406.
18. Hodges, T.R., et al., *Mutational burden, immune checkpoint expression, and mismatch repair in glioma: implications for immune checkpoint immunotherapy.* Neuro. Oncol, 2017.
19. Johnson, A., et al., *Comprehensive Genomic Profiling of 282 Pediatric Low- and High-Grade Gliomas Reveals Genomic Drivers, Tumor Mutational Burden, and Hypermutation Signatures.* Oncologist, 2017. **22**(12): p. 1478-1490.
20. Draaisma, K., et al., *PI3 kinase mutations and mutational load as poor prognostic markers in diffuse glioma patients.* Acta Neuropathol. Commun, 2015. **3**: p. 88.
21. Kandoth, C., et al., *Mutational landscape and significance across 12 major cancer types.* Nature, 2013. **502**(7471): p. 333-339.
22. McGranahan, N., et al., *Clonal neoantigens elicit T cell immunoreactivity and sensitivity to immune checkpoint blockade.* Science, 2016. **351**(6280): p. 1463-9.
23. Van Allen, E.M., et al., *Genomic correlates of response to CTLA-4 blockade in metastatic melanoma.* Science, 2015. **350**(6257): p. 207-211.
24. Buttner, R., et al., *Implementing TMB measurement in clinical practice: considerations on assay requirements.* ESMO Open, 2019. **4**(1): p. e000442.
25. Alexandrov, L.B., et al., *Signatures of mutational processes in human cancer.* Nature, 2013. **500**(7463): p. 415-21.
26. Filley, A.C., M. Henriquez, and M. Dey, *Recurrent glioma clinical trial, CheckMate-143: the game is not over yet.* Oncotarget, 2017. **8**(53): p. 91779-91794.
27. Cibulskis, K., et al., *Sensitive detection of somatic point mutations in impure and heterogeneous cancer samples.* Nat Biotechnol, 2013. **31**(3): p. 213-9.
28. Li, H., et al., *The Sequence Alignment/Map format and SAMtools.* Bioinformatics, 2009. **25**(16): p. 2078-9.
29. *Glioma through the looking GLASS: molecular evolution of diffuse gliomas and the Glioma Longitudinal Analysis Consortium.* Neuro Oncol, 2018. **20**(7): p. 873-884.
30. Choi, S., et al., *Temozolomide-associated hypermutation in gliomas.* Neuro Oncol, 2018. **20**(10): p. 1300-1309.

31. Berger, M.F., et al., *Melanoma genome sequencing reveals frequent PREX2 mutations.* Nature, 2012. **485**(7399): p. 502-506.
32. Stenzinger, A., et al., *Tumor mutational burden (TMB) standardization initiatives: Recommendations for consistent TMB assessment in clinical samples to guide immunotherapy treatment decisions.* Genes Chromosomes Cancer, 2019.
33. Omuro, A., et al., *Nivolumab with or without ipilimumab in patients with recurrent glioblastoma: results from exploratory phase I cohorts of CheckMate 143.* Neuro Oncol, 2018. **20**(5): p. 674-686.
34. Reardon, D.A., et al., *OS10.3 Randomized Phase 3 Study Evaluating the Efficacy and Safety of Nivolumab vs Bevacizumab in Patients With Recurrent Glioblastoma: CheckMate 143.* Neuro-Oncology, 2017. **19**(suppl_3): p. iii21-iii21.
35. Zhao, J., et al., *Immune and genomic correlates of response to anti-PD-1 immunotherapy in glioblastoma.* Nat Med, 2019. **25**(3): p. 462-469.
36. Subrahmanyam, P.B., et al., *Distinct predictive biomarker candidates for response to anti-CTLA-4 and anti-PD-1 immunotherapy in melanoma patients.* J Immunother Cancer, 2018. **6**(1): p. 18.
37. Ji, R.R., et al., *An immune-active tumor microenvironment favors clinical response to ipilimumab.* Cancer Immunol Immunother, 2012. **61**(7): p. 1019-31.

Supplementary

Paired sample	Primary	First relapse	Second relapse
RHGB026P01/ RHGB026R01/ RHGB026R02	ND	ND	ND
RHGB023P01/ RHGB023R01	*TCHH, ABCC9, SCN9A*	*TCHH, ABCC9, SCN9A*	ND
RHGB032P01/ RHGB032R01	*CDKN2C, ATR*	*CDKN2C, ATR*	ND
RHGB024P01/ RHGB024R01	*TP53*	*TP53*	ND
RHGB003P01/ RHGB003R01	*PIK3CA*	*TSC2, PIK3R1, EGFR*	ND
RHGB028P01/ RHGB028R01	*SPTA1, PTEN, ACVR1, FGFR1*	*SPTA1*	ND
RHGB014P01/ RHGB014R01	*TRPV6*	*TRPV6*	ND
RHGB016P01/ RHGB016R01	*PIK3CA*	*PIK3CA*	ND
RHGB006P01/ RHGB006R01	*TP53, PIK3R1, GNAS*	*NF1, PIK3R1, GNAS*	ND
RHGB027P01/ RHGB027R01/ RHGB027R02	*SPTA1*	ND	*SPTA1*
RHGB005P01/ RHGB005R01	*APC*	*APC*	ND
RHGB002P01/ RHGB002R01	*TCHH, PIK3C2G, TP53, CIC, MSH6, ACVR1, KIT*	*TCHH, PIK3C2G, TP53 (1, 2), CIC, MSH6, ACVR1, KIT*	ND
RHGB013P01/ RHGB013R01	*PDGFRA, JAK2 (1, 2, 3), KDM6A*	*PDGFRA, JAK2 (1, 2, 3), KDM6A*	ND
RHGB025P01/ RHGB025R01	*PTEN*	ND	ND
RHGB035P01/ RHGB035R01	*ZNF99, PIK3R1*	*ZNF99, PIK3R1*	ND
RHGB020P01/ RHGB020R01	*TP53, CALCR, MET*	*TP53, CALCR, MET*	ND
RHGB010P01/ RHGB010R01	*TP53, ADAM29, BCOR*	*TP53, ADAM29, BCOR*	ND
RHGB008P01/ RHGB008R01	*AFM, GNAS*	*AFM*	ND
RHGB033P01/ RHGB033R01	*NF1, MYCN*	*NF1, MYCN*	ND
RHGB009P01/ RHGB009R01/ RHGB009R02	*BRAF*	*PTPN11*	*PTPN11, BRAF*
RHGB017P01/ RHGB017R01	*PTEN, RB1*	*PTEN*	ND
RHGB030P01/ RHGB030R01	*SETD2*	*SETD2, EGFR*	ND
RHGB015P01/ RHGB015R01	*PTEN, ATR*	*ATR*	ND
RHGB011P01/RHGB011R01/ RHGB011R02	*TP53*	*TP53*	*TP53*
RHGB001P01/ RHGB001R01	*PIK3R1*	*PIK3R1*	ND
RHGB007P01/ RHGB007R01	*PTEN, TP53*	*PTEN, TP53*	ND
RHGB004P01/ RHGB004R01	*CTNNB1*	*CTNNB1*	ND
RHGB034P01/ RHGB034R01/ RHGB034R02	ND	*PTEN, ABCC9, DICER1*	ND
RHGB031P01/ RHGB031R01	*SPTA1, PDGFRA*	ND	ND
RHGB018P01/ RHGB018R01	ND	*FGA, EGFR*	ND
RHGB012P01/ RHGB012R01	*AKT3*	*AKT3, ABCB1*	ND
RHGB022P01/ RHGB022R01/ RHGB022R02	*EGFR*	*EGFR*	*EGFR*

Supplementary table ST1. Genes present in primary and relapse samples(s), respectively. Gene filter list applied (The Heidelberg Brain Tumor Panel and the Glioblastoma anel from Rigshospitalet).

ABCB1	CDH9	FGFR3	KLF4	NRAS	SMAD4
ABCC9	CDHR3	FGFR4	KLK1	NTRK2	SMARCA2
ABL1	CDK4	FLT3	KMT2C	ODF4	SMARCA4
ACVR1	CDK6	FOXO3	KRAS	PARD6B	SMARCB1
ADAM29	CDKN2A	FOXR2	KRTAP20-2	PCDH8	SMARCD1
AFM	CDKN2B	FRMD7	LCE4A	PDGFRA	SMARCD2
AKT1	CDKN2C	FUBP1	LDB1	PIK3CA	SMARCE1
AKT2	CDX4	GABRA1	LRRC55	PIK3C2G	SMO
AKT3	CHEK2	GABRA6	LUM	PIK3R1	SPRYD5
ALK	CIC	GABRB2	LZTR1	PLCH2	TRIM51
ANKRD36	COL1A2	GNA11	MDM2	PMS2	SPTA1
APC	CREBBP	GNAQ	MDM4	PODNL1	STAG2
ARID1A	CSF1R	GNAS	MET	POLE	SUFU
ARID1B	CTNNB1	GPX5	MGMT	POT1	SULT1B1
ARID2	CFAP47	H2AFX	MLH1	PPM1D	TBR1
ATM	CXorf22	H3F3A	MSH2	PRKAR1A	TCF4
ATR	D2HGDH	HDAC2	MLL2	PTCH1	TCHH
ATRX	DAXX	HEATR7B2	MMP13	PTCH2	TERT
BCOR	DCAF12L2	MROH2B	MPL	PTEN	TMEM147
BRAF	DDX3X	HIST1H3B	MRE11A	PTPN11	TP53
BRCA1	DICER1	HIST1H3C	MSH2	QKI	TPTE2
BRCA2	DRD5	HNF1A	MSH6	Rad50	TRAF7
BRPF1	DYNC1I1	HRAS	MYB	RAF1	TRPV6
BRPF3	EGFR	IDH1	MYBL1	RB1	TSC1
GCSAML	ERBB1	IDH2	MYC	RET	TSC2
C1orf150	ERBB2	IL18RAP	MYCN	RFX6	UGT2A3
C11ORF95	ERBB3	IDO2	MYL1	RPL5	VEGF
CALCR	ERBB4	JAK2	NBN	SCN9A	VHL
CARD6	EGFR	JAK3	NDRG2	SEMA3C	WNT2
CCND1	EZH2	KDM6A	NF1	SEMA3E	ZNF844
CCND2	FBXW7	KDR	NF2	SEMG1	ZNF99
CD3EAP	FGA	KEL	NLRP5	SETD2	
CDH1	FGFR1	KIAA0182	NOTCH	SIGLEC8	
CDH18	FGFR2	KIT	NOTCH2	SLC26A3	

Supplementary table ST2. Gene list used for filtration for mutation calling. Merged from The Heidelberg Brain Tumor Panel and the Glioblastoma Panel from Rigshospitalet.

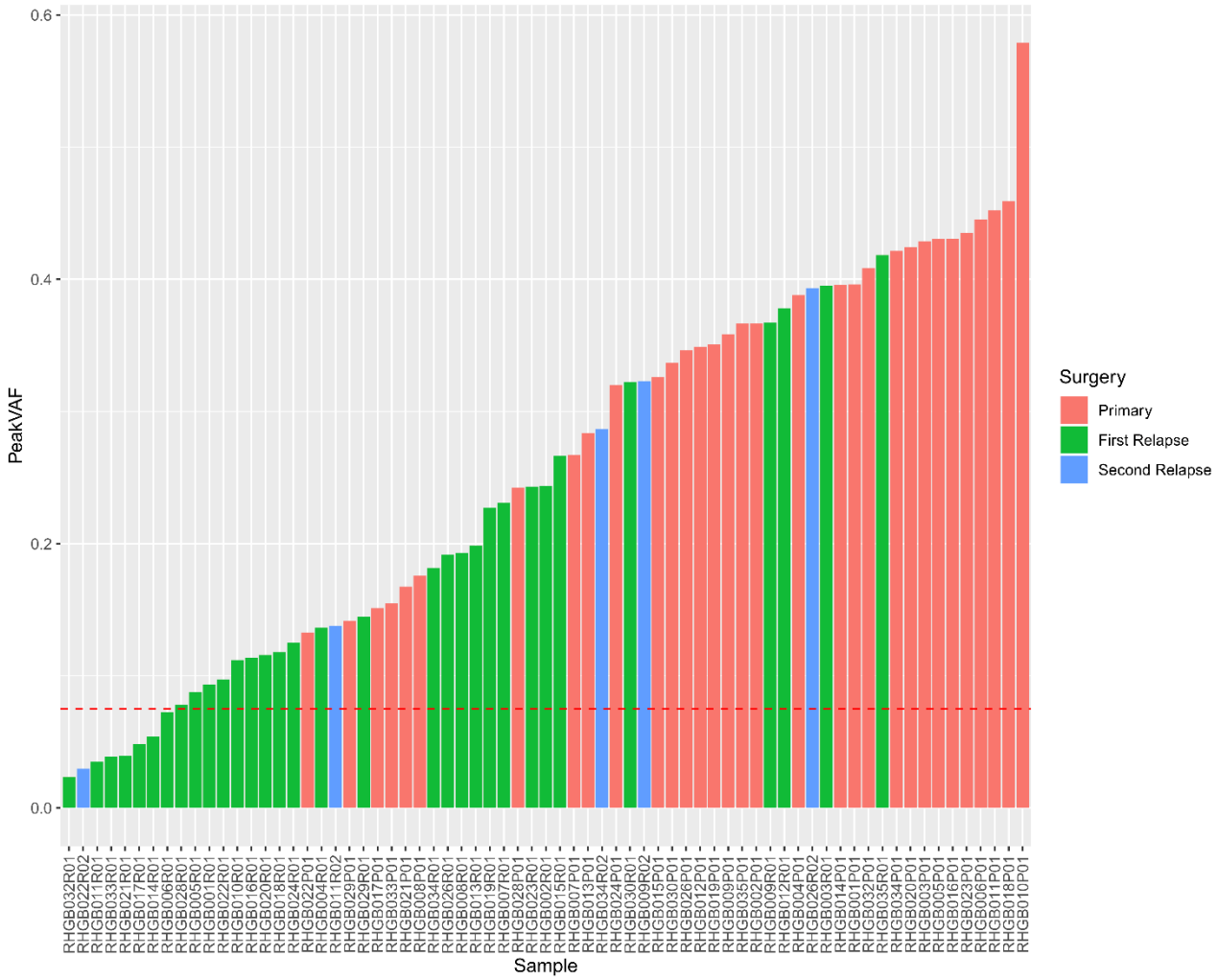

Supplementary figure S1. Density analysis of the variant allele frequencies of each tumor was used to determine the allele frequency representing clonal variants within each sample. This value was used as a surrogate for tumor purity and a threshold (0.075, red line) was used to exclude samples that were considered unreliable.

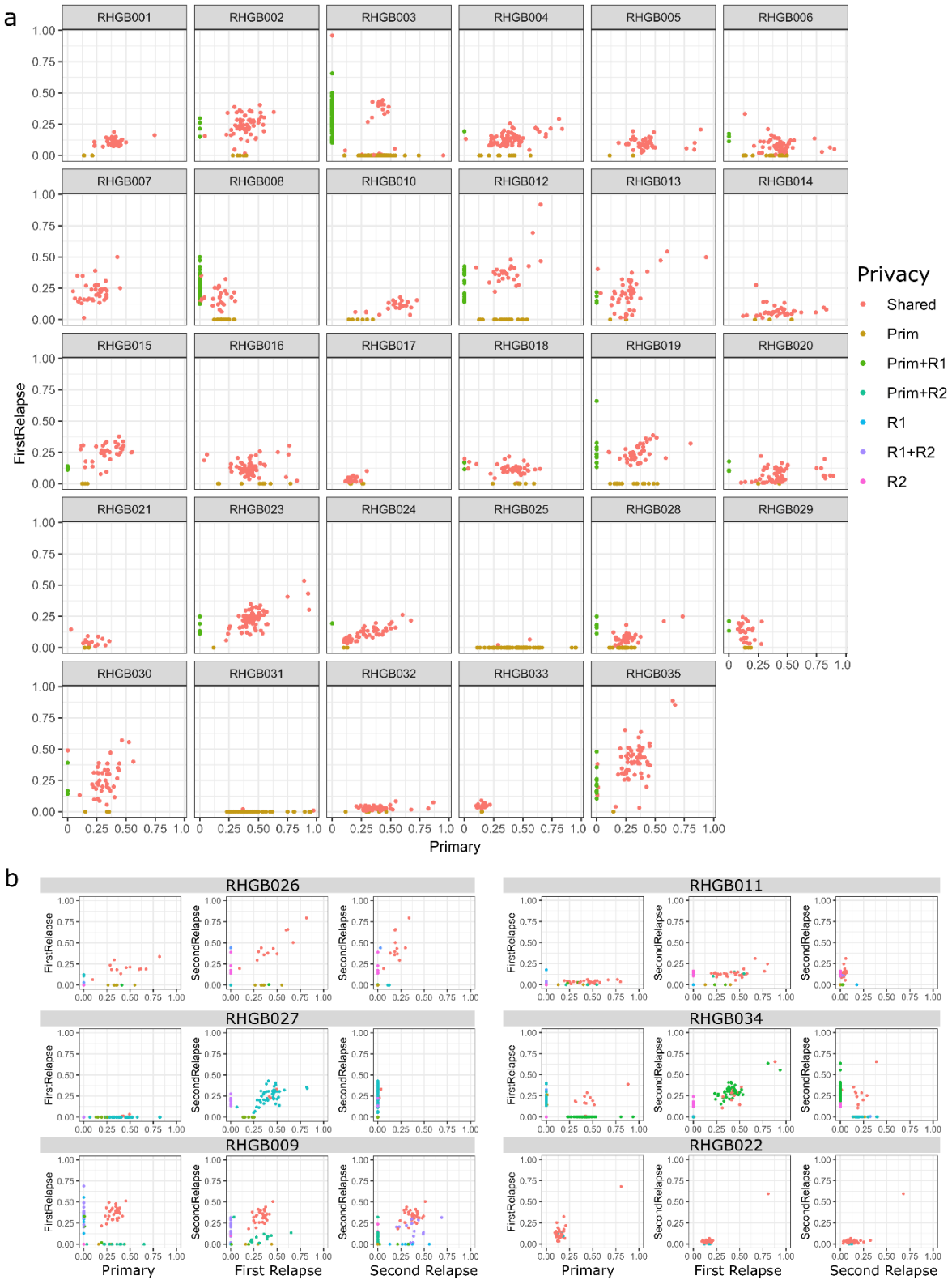

Supplementary figure S2. Comparison of variant allele frequencies (VAFs) for variants found across paired specimens in cases with primary and a single (a) or (b) paired relapse. Colors indicate the privacy status of the variants as found in the primary (Prim), first relapse (R1) or second relapse (R2).

PairedSet	Prim.Raw	R1.Raw	R2.Raw	Prim.PeakVAF	R1.PeakVAF	R2.PeakVAF	Prim.DownSample	R1.DownSample	R2.DownSample	CorrectionFactor	Prim.Corrected	R1.Corrected	R2.Corrected	Note
RHGB035	65	77		0,366441812	0,418277857		65	75		1,03	67	77		
RHGB003	79	127		0,42856429	0,395272552		78	127		1,01	79	129		
RHGB012	48	46		0,348923952	0,37814793		48	46		1	48	46		
RHGB009	49	57	62	0,358342062	0,367138262	0,322785804	46	56	62	1,04	49	57	65	
RHGB030	47	46		0,386993682	0,32233517		46	46		1,02	47	48		
RHGB027	54	3	57	0,460672385 NA		0,30071293	51 NA		57	1,06	54 NA			61 R2 Below Purity threshold for correction
RHGB015	40	42		0,326222253	0,266468814		40	42		1	40	42		
RHGB002	66	63		0,366728944	0,24367402		65	63		1,02	66	64		
RHGB023	68	73		0,435305844	0,243195709		67	73		1,01	68	75		
RHGB007	37	37		0,267095298	0,230750195		37	37		1	37	37		
RHGB019	59	54		0,350865928	0,227292604		56	54		1,05	59	57		
RHGB013	45	47		0,283768393	0,198419005		43	47		1,05	45	50		
RHGB008	52	81		0,175700187	0,193045193		52	81		1	52	81		
RHGB026	19	15	19	0,346254147	0,191720951	0,393135587	18	15	14 1.2/1.35		19	19	19	
RHGB034	59	42	64	0,421475447	0,181694413	0,286536945	56	42	63 1.03/1.02		59	44	64	
RHGB029	28	26		0,141556246	0,14806098		28	26		1	28	26		
RHGB011	33	43		0,452087099	0,137723592		23	43		1,43	33	62		
RHGB004	81	72		0,387929737	0,136303283		70	72		1,16	81	84		
RHGB024	53	52		0,32	0,125		35	52		1,51	53	79		
RHGB018	47	43		0,458977907	0,11788075		36	43		1,31	47	57		
RHGB020	61	63		0,424355964	0,115834233		49	63		1,24	61	79		
RHGB016	65	56		0,430555506	0,11365162		57	56		1,14	65	64		
RHGB010	29	23		0,578836459	0,111993691		19	23		1,53	29	36		
RHGB022	42	42	39	0,132709395	0,09708352	0,029700403	42	42 NA		1	42	42 NA		R2 Below Purity threshold for correction
RHGB001	41	37		0,39607896	0,09319402		34	37		1,21	41	45		
RHGB005	52	50		0,430451079	0,08776159		40	50		1,3	52	65		
RHGB028	62	42		0,24230701	0,07798636		56	42		1,11	62	47		
RHGB006	71	58		0,445013718	0,07241952									R1 Below Purity threshold for correction
RHGB014	43	40		0,395843179	0,05386542									R1 Below Purity threshold for correction
RHGB017	33	28		0,151344743	0,04841804									R1 Below Purity threshold for correction
RHGB021	18	15		0,167311561	0,03962486									R1 Below Purity threshold for correction
RHGB033	20	18		0,154689641	0,03879157									R1 Below Purity threshold for correction
RHGB032	51	46		0,408511537	0,02336695									R1 Below Purity threshold for correction
RHGB025	71	2												Too Few Mutations in Relapse 1
RHGB031	45	2												Too Few Mutations in Relapse 1

Supplementary table ST3. List of included samples and variant allele frequency (VAF). Excluded samples for TMB comparison, is highlighted in red. Unadjusted TMB scores are listed in the column called “Raw” and adjusted TMB scores are listed in the column called “Corrected”. Abbreviations: Prim: primary; R1: first relapse surgery; R2: second relapse surgery

STUDY III

Cell-free DNA in newly diagnosed patients with glioblastoma – a clinical prospective feasibility study

Dorte Schou Nørøxe[1,2], Olga Østrup[3], Christina Westmose Yde[3], Lise Barlebo Ahlborn[3], Finn Cilius Nielsen[3], Signe Regner Michaelsen[1], Vibeke Andrée Larsen[4], Jane Skjøth-Rasmussen[5], Jannick Brennum[5], Petra Hamerlik[6], Hans Skovgaard Poulsen[1,2] and Ulrik Lassen[2]

[1]Department of Radiation Biology, Rigshospitalet, 2100 Copenhagen, Denmark

[2]Department of Oncology, Rigshospitalet, 2100 Copenhagen, Denmark

[3]Center for Genomic Medicine, Rigshospitalet, 2100 Copenhagen, Denmark

[4]Department of Neuroradiology, Rigshospitalet, 2100 Copenhagen, Denmark

[5]Department of Neurosurgery, Rigshospitalet, 2100 Copenhagen, Denmark

[6]Danish Cancer Society, 2100 Copenhagen, Denmark

***Correspondence to**: Dorte Schou Nørøxe, **email:** anne.dorte.schou.noeroexe@regionh.dk*

***Keywords:** glioblastoma; liquid biopsy; cell-free DNA; fragment length; base-pair*

Received:** March 10, 2019 **Accepted:** May 29, 2019 **Published:

ABSTRACT

Background: Glioblastoma (GB) is an incurable brain cancer with limited treatment options. The aim was to test the feasibility of using cell-free DNA (cfDNA) to support evaluation of treatment response, pseudo-progression and whether progression could be found before clinical and/or radiologic progression.

Results: CfDNA fluctuated during treatment with the highest levels before diagnostic surgery and at progression. An increase was seen in 3 out of 4 patients at the time of progression while no increase was seen in 3 out of 4 patients without progression. CfDNA levels could aid in 3 out of 3 questionable cases of pseudo-progression.

Methods: Eight newly diagnosed GB patients were included. Blood samples were collected prior to diagnosis, before start and during oncologic treatment until progression. Seven patients received concurrent radiotherapy/Temozolomide with adjuvant Temozolomide with one of the patients included in a clinical trial with either immunotherapy or placebo as add-on. One patient received radiation alone. CfDNA concentration was determined for each blood sample.

Conclusions: It was feasible to measure cfDNA concentration. Despite the limited cohort size, there was a good tendency between cfDNA and treatment course and -response, respectively with the highest levels at progression.

INTRODUCTION

Glioblastoma (GB) is a highly malignant brain tumor with limited treatment options. With standard treatment, median overall survival (OS) is 16–22 months [1]. The standard method for monitoring a treatment response is by clinical evaluation of the patient and by magnetic resonance imaging (MRI) at defined intervals ranging from two to six months using Response Assessment in Neuro Oncology criteria (RANO) [2]. However, pseudo-progression is seen in approximately 20% of patients [3, 4] and can be difficult to distinguish from true progression. Only surgery with following pathological confirmation of vital tumor cells in the lesion can verify the progressive state. For cases in which only treatment related changes are found, the surgery could have been futile with valuable time lost in which a

different treatment could have been effectuated. Or worse, the surgery will leave the patient clinically unfit for further treatment. Therefore, a less time consuming and non-invasive method for treatment monitoring is needed and a blood-based biopsy seems promising. Several methods exist to monitor liquid-based alterations [5–9] that includes circulating tumor cells (CTCs) or alterations detected in cerebrospinal fluid (CSF). CTCs can be detected in blood in up to 39% of GB patients [10] in experimental settings, using antibodies to target epithelial cell adhesion molecules or by detecting the malaria protein VAR2CSA which is expressed in GB-cell lines [11]. Alterations detected in CSF have been identified in 49.4% of glioma patients with neurologic symptoms [12]. Another more accessible tumor source is circulating cell-free DNA (cfDNA) and specifically circulating tumor DNA (ctDNA). CtDNA is more fragmented than normal cfDNA making size selection strategies usable to indicate tumor fraction [13–16]. The fraction of ctDNA in cancer patients accounts for 3–93% of the total cfDNA [17], thus cfDNA can be used as a surrogate marker of tumor activity/burden. The shedding of tumor DNA has been found to be increased according to tumor burden, necrosis and apoptosis but can also be caused by normal cell degradation from e.g. infection, stroke, renal failure or even strong exercise [18–21]. Elevated cfDNA levels have been detected in patients with severe brain injury which is proof-of-principle that cfDNA is shed from the brain to the blood stream during cell degradation [22, 23] and ctDNA has been detected in patients with brain cancer [24–26]. In this study, we aimed to test the feasibility of detecting cfDNA in patients with GB and to investigate if cfDNA fluctuations could support evaluation of treatment response, pseudo-progression and whether progression could be found before clinical and/or radiologic progression.

RESULTS

Included patients and their clinical course

A total of eight patients were included for further analyses. One patient was treated with 34 Gy/10F and seven patients received RT/TMZ with adjuvant TMZ. One of these seven patients was treated in an experimental trial with a Programmed Death1 inhibitor (PD1i) or placebo as add-on to the standard treatment. (Table 1) At time of data lock four patients had progressed and of the four patients without progression, two were still on-treatment and two were in a follow-up (FU)-program.

cfDNA fluctuated during treatment with the highest value at progression

It was feasible to collect blood samples in patients with GB before, during and after planned treatment. As shown in Table 2 the mean cfDNA before surgery was 12.5 ng/ml (range 2.4–63) and dropped to 7.9 (range 0.3–26.4) one month after, just before start on RT/TMZ. The mean cfDNA then reached 8.3 ng/ml (range 4.1–13.8) at the highest individual value during RT and decreased to 4.9 ng/ml (range 1.5–6.9) after RT/TMZ just before start on adjuvant TMZ. The highest value at all time points was at progression with a mean of 23.4 ng/ml (range 2.4–73.4). During RT/TMZ, a mean cfDNA at the highest individual level was 8.3 (range 4.1–13.8). During RT/TMZ, four patients had the highest concentrations after 20 Gy, one after 30 Gy and one after 40 Gy but levels were relative constant between 0.3–10.5 ng/ml except for GB1 who had a constant decrease. (Supplementary Figure 1).

cfDNA increased before or at radiologic progression in three out of four patients

For the four patients who progressed during the study period (GB1-4), cfDNA concentration and selected MRI´s as related to treatment and time from diagnosis, is shown in Figure 2A–2E. We could detect an increase in cfDNA in GB1, day 155 and GB2, day 345 before radiologic progression. An increase at progression was seen in GB4, day 205. GB3 did not have an increase in cfDNA before radiologic progression. Unfortunately, the blood sample before progression could not be analyzed why a potential increase prior to radiologic progression could not be determined. A detailed description of all eight patients is given in Supplementary Table 1.

cfDNA did not increase in three out of four patients without progression

For the four patients who did not progress during the study period (GB5-8), cfDNA concentration, selected MRI´s and one computed tomography (CT)-scan as related to treatment and time from diagnosis, is shown in Figure 3A–3E. At time of data-lock, GB5-6 were in a FU-program and GB7-8 were still on-treatment. No increase in the latest cfDNA concentrations were noted in GB6-8. GB5 had an increase in the latest measurements and will be further discussed below.

Pseudo-progression was supported by cfDNA in three out of three patients

Three patients were suspected of pseudo-progression based on MRI, one of whom had true progression. GB1 was suspected of progression (Figure 2B, MRI 3) with a simultaneously increase in cfDNA, day 155. He was scheduled for relapse surgery showing no vital tumor cells in the specimen, but an MRI performed two months after confirmed progressive disease in the tumor cavity (Figure 2B, MRI 4). GB2 was suspected of progression (MRI not shown) with a small decrease in cfDNA at day 252 but progression was found unlikely at the multidisciplinary

Table 1: Overview of included patient

Patient	Age	Gender	IDH/MGMT-status	Treatment	Pseudo-progression	Complications during study period	Progression
GB1	52	Male	*IDH*-WT/ MGMT-WT	RT/TMZ	Yes		Yes
GB2	59	Female	*IDH*-WT/ MGMT-meth	RT/TMZ	Yes	Meningitis	Yes
GB3	46	Male	*IDH*-WT/ MGMT-WT	RT/TMZ	No		Yes
GB4	77	Male	*IDH*-WT/ MGMT-meth	34 Gy/10 F	No		Yes
GB5	59	Female	*IDH*WT/ MGMT-WT	RT/TMZ	Yes	The patient declined further treatment after 5 cyc of adj TMZ and was taken off-study.	No. FU-program
GB6	62	Female	*IDH*-WT/ MGMT-meth	RT/TMZ	No	No more blood samples were drawn after two cyc of adj TMZ due to logistics and patient compliance.	No. FU-program
GB7	46	Male	*IDH*-WT/ MGMT-meth	RT/TMZ plus PD1i/placebo	No	Intracerebral bleeding	No, on-treatment
GB8	52	Male	*IDH*-WT/ MGMT-meth	RT/TMZ	No		No, on-treatment

Abbreviations: *IDH*: isocitrate-dehydrogenase; WT: wild type; MGMT: O-6-methyl-guanine-DNA-methyl-transferase; RT/TMZ: radiotherapy/Temozolomide; PD1i: programmed death1 inhibitor; Gy: grey; cyc: cycles; adj: adjuvant; FU; follow-up.

Table 2: Mean concentration of cfDNA (ng/ml plasma) and base pair (bp)-peaks at defined intervals in the study period

Time	Number of evaluable patients	Mean cfDNA ng/ml (range)	Mean bp-peak (range)
Before diagnostic surgery	7	12.5 (2.4–63.0)	153 (136–171)
One month after surgery	7	7.9 (0.3–26.4)	147 (134–166)
During RT (highest individual value)	7	8.3 (4.1–13.8)	148 (138–154)
One month after RT	6	4.9 (1.5–6.9)	153 (147–163)
At progression	4	23.4 (2.4–73.4)	132 (120–144)

The number of evaluable patients at each step is shown.

conference. CfDNA levels later increased on day 345 and 375 before progression was seen on MRI (Figure 2A and 2C, MRI 3). GB5 was suspected of progression day 160 based on an MRI with a stable cfDNA concentration (Figure 3A and 3B, MRI 3). It was interpreted as pseudo-progression and all three cases illustrate a potential connection between pseudo-progression and cfDNA concentration.

Bp-peaks and clinical course

All samples but four (5%) had corresponding bp-peaks of ≤ 166 (Figures 2A and 3A). Of the four samples with bp-peak > 166, three of the measurements were in patient GB7; one before diagnosis with a 69 × 47 mm large, partly necrotic/apoptotic tumor (Figure 3D, MRI 1) and two during RT/TMZ plus PD1i/placebo. Due to tumor size and -location, he had only partial resection done at diagnosis with tumor and necrotic/apoptotic tissue left in the brain (Figure 3D, MRI 2). Concerning the higher levels during RT, a higher mean bp-peak of 150 (110–178) was seen across all patient samples during the RT as compared to the samples taken during the adjuvant setting of 139 (108–160). The last sample with bp-peak > 166 was observed in patient GB2 after RT/TMZ (Figure 2A) at the time she was diagnosed

with meningitis and treated with high dose antibiotics intravenously for three months before she could start on the adjuvant TMZ. Majority of bp-analyses came out with two peaks; one with a low and high bp-fragment size distribution, respectively (Figure 1C). The curve with the highest percentage of measured fragment sizes, were in all cases the short fragment size distribution with a median bp-peak of 147 (108–247) and the curve with a smaller percentage of measured fragment size distribution, had a median bp-peak of 371 (268–2954). A calculated ratio between cfDNA and bp-peaks is shown in Supplementary Figure 2.

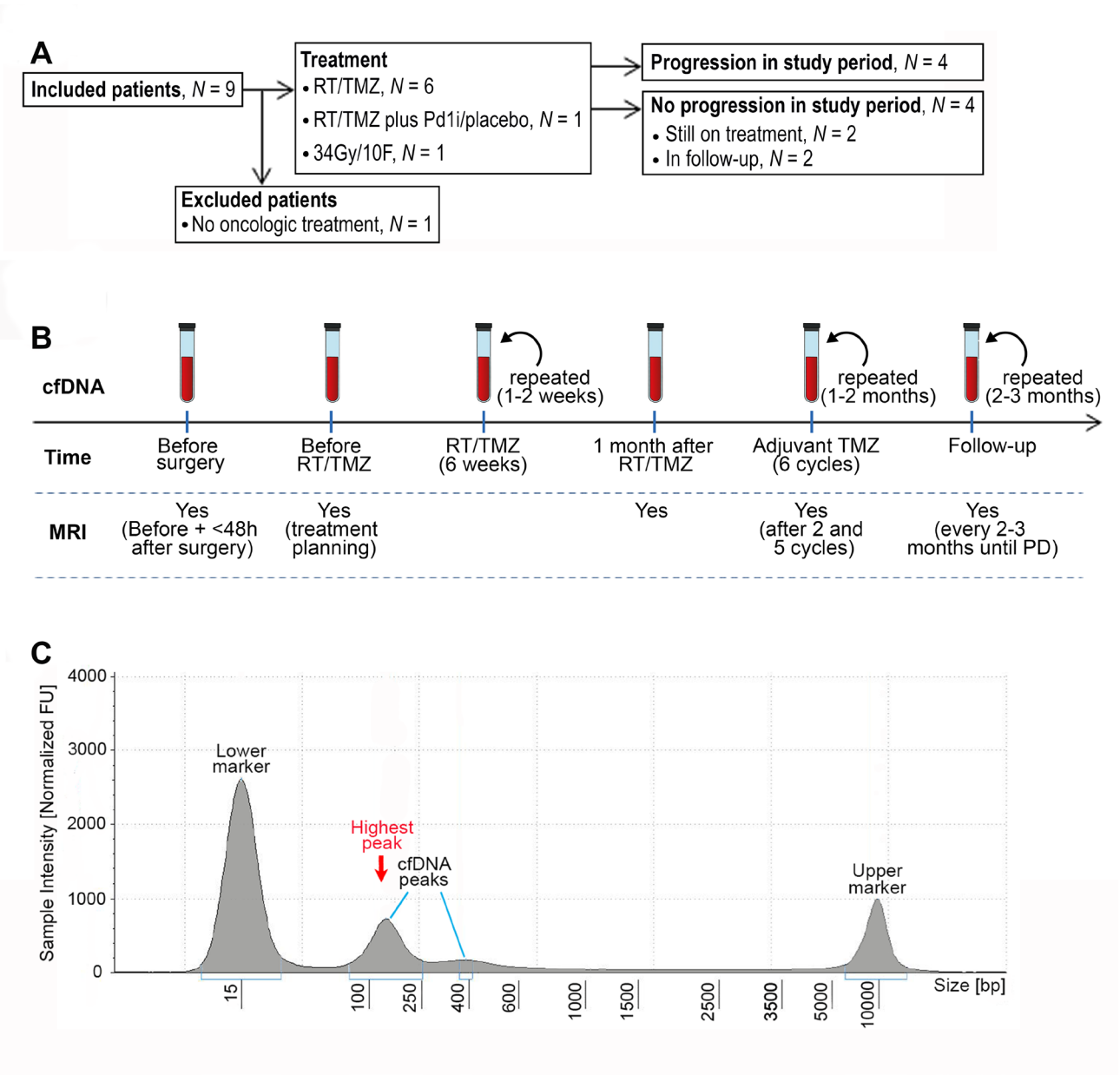

Figure 1: CONSORT diagram, workflow and example of fragment size analysis. (**A**) CONSORT diagram of included patients. Abbreviations: RT/TMZ: radiotherapy/Temozolomide (concurrent RT/TMZ plus adjuvant TMZ); RT/TMZ plus PD1i/placebo: (concurrent RT/TMZ plus Programmed Death1 inhibitor/placebo followed by adjuvant TMZ plus PD1i/placebo). (**B**) Illustration of work flow. First sample was taken the day before or on the day of diagnostic surgery. If the diagnosis of glioblastoma was confirmed, the next sample was taken one month after surgery at first visit to the oncologic department, every 1–2 weeks during RT/TMZ, throughout the adjuvant TMZ with 1–2 months interval and in the follow-up period with approximately 2–3 months interval until progressive disease (PD). Magnetic resonance imaging (MRI) was performed before surgery, ≤48 hours after surgery, for treatment planning of RT/TMZ, one month after RT/TMZ, after two and five cycles of adjuvant TMZ and then every 2-3 months until progression. (**C**) An example of a result from the fragment analysis assessed using the Tape Station instrument. CfDNA fragments were visualized using a higher and lower ladder as reference, respectively. The peak of the curve with the highest % of fragments, was defined as the highest peak.

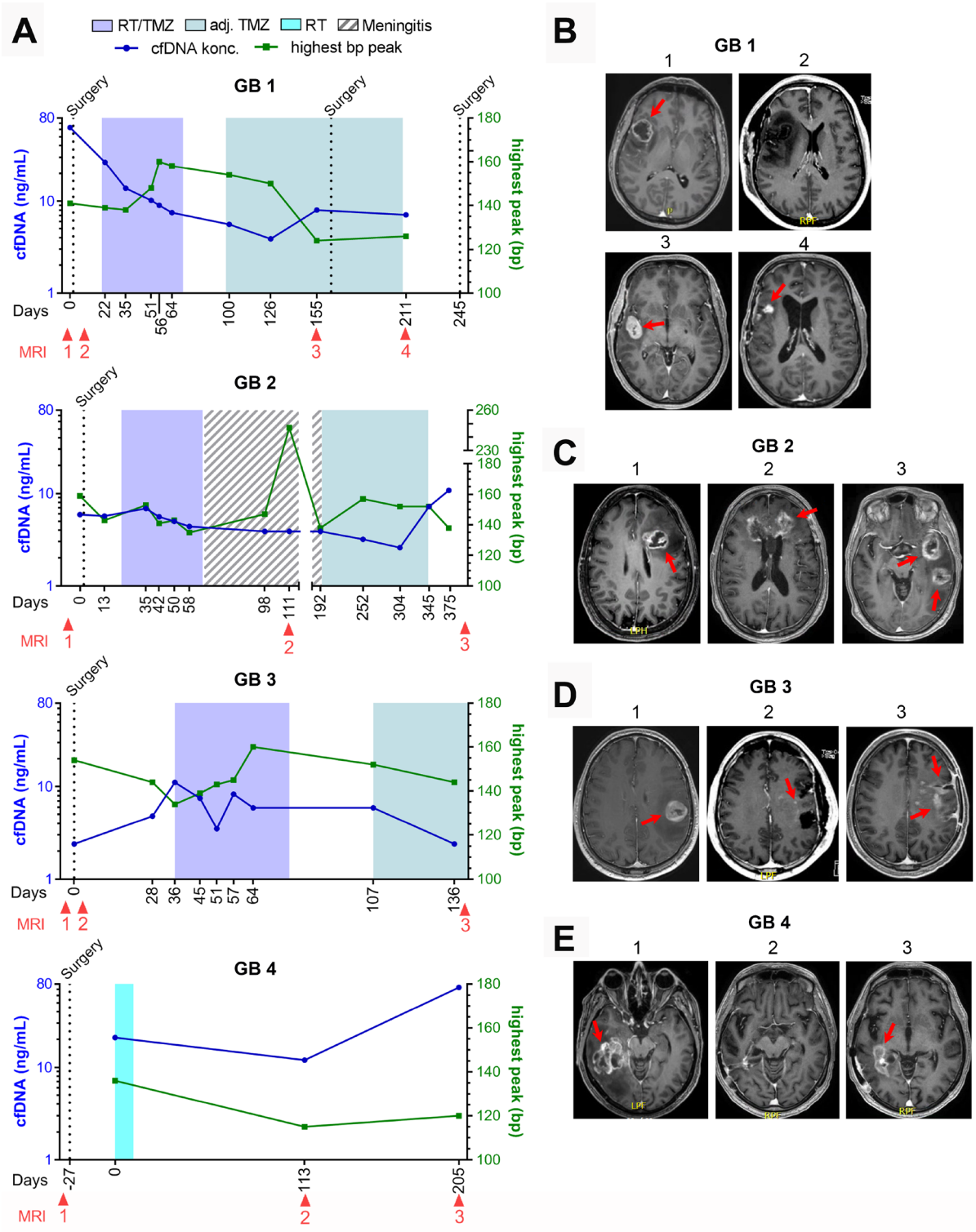

Figure 2: GB1-4 with progression. (**A**) Fluctuations in cell-free DNA (cfDNA) during study period at different treatment times with correlated basepar (bp) peaks. (**B**–**E**) Selected magnetic resonance imaging (MRI) during treatment period. (B) Patient GB1. B1: 30 × 29 mm contrast-enhanced (CE) tumor at diagnosis, B2: <48 hours after surgery with no residual tumor left, B3: 32 × 18 mm CE tumor, B4: progression in tumor cavity including new lesions to a total of 515 mm^3 CE tumor. (C) Patient GB2. C1: 32 × 23 mm CE tumor at diagnosis, C2: During meningitis treatment showing growth of known CE tumor, including new lesions to a total of 2099 mm^3 CE tumor, C3: Progression of all tumor lesions to a total 3863 mm^3. (D) Patient GB3. D1: 28 × 27 mm CE tumor at diagnosis, D2: <48 hours after surgery showing no measurable residual tumor but two punctate CE-lesions, D3: Progression to a 21 × 12 mm CE tumor and new non-measurable lesions. (E) Patient GB4. E1: 49 × 39 mm CE tumor at diagnosis. E2: No measurable CE tumor. E3: Progression with a 62 × 20 mm CE tumor.

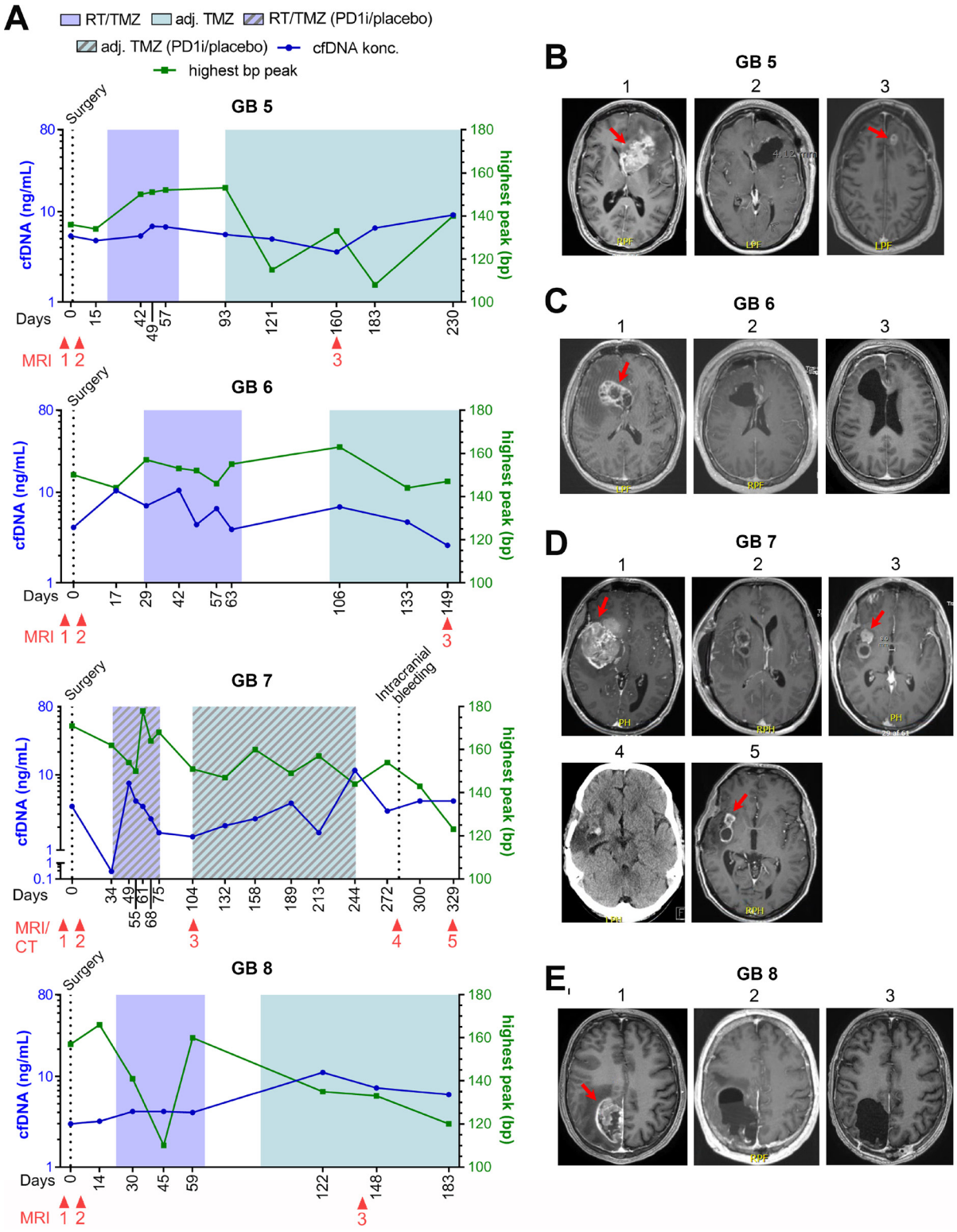

Figure 3: GB5-8 without progression. (**A**) Fluctuations in cell-free DNA (cfDNA) during study period at different treatment times with correlated base pair (bp) peaks. (**B–E**) Selected magnetic resonance imaging (MRI) during treatment period. (B) Patient GB5. B1: 65x36 mm contrast-enhanced (CE) tumor at diagnosis, B2: <48 hours after surgery with no residual tumor, B3: 17 × 12 mm CE tumor (pseudo-progression). (C) Patient GB6. C1: 46 × 29 mm CE tumor at diagnosis, <48 hours after surgery showing a small non-measurable CE lesion, C3: stable disease with non-measurable CE lesion. (D) Patient GB7. D1: 69 × 47 mm CE tumor at diagnosis, D2: <48 hours after surgery showing residual CE tumor of 1040 mm^3, D3: Regression to 20 × 16 mm CE tumor, D4: A computed tomography (CT) scan showing an intracerebral bleeding in the tumor cavity, D5: Further regression to a total of 243 mm^3 CE tumor. (E) GB8. E1: 56 × 33 mm CE tumor at diagnosis, E2: <48 hours after surgery with no residual tumor, E3: Stable disease with no tumor.

cfDNA did not correlate with tumor size

A table and simple scatter plot of tumor size and corresponding cfDNA concentrations is shown in Supplementary Table 2 and Supplementary Figure 3. We had 31 paired measurements, excluding one during meningitis in GB2. We did not find a correlation between tumor size and cfDNA when performing a Spearman´s correlation analysis.

DISCUSSION

We have shown that sequential monitoring of cfDNA-levels in blood samples before diagnosis of GB and during treatment until progression is feasible and detectable. At our institution, the patients arrive at the hospital the night before surgery, leaving a limited time frame for information, collection of the informed consent and the blood sample prior to surgery in a situation where the patients were especially vulnerable due to upcoming high-risk surgery and without a diagnosis. In addition, the blood sampling had to be performed at our institution due to sample preservation and processing. These logistic matters complicated the setup. We observed that cfDNA concentrations fluctuated during treatment with the second highest mean level before diagnosis and the highest at progression. We would expect a high cfDNA concentration before diagnosis due to disruption of the blood brain barrier in combination with high tumor burden and hence shedding of tumor cells in the circulation. As expected, the mean cfDNA concentration decreased one month after surgery due to surgical removal of the tumor burden [21]. The stable levels or increase in cfDNA during RT can be caused by tumor and normal tissue necrosis as was also shown in a recent study with non-small-cell lung cancer (NSCLC) patients [27]. Approximately one month after RT and with no other interventions, the mean level decreased again which could be due to decrease of RT-induced edema and inflammation. In three out of four patients with progression, we saw an increase from the previous sample before or at radiologic progression and the opposite was the case with three out of four patients without progression and without an increase in their latest measurements. In all three questionable cases of pseudo-progression, cfDNA levels could potentially aid in deciding whether it was true progression or not. These findings have potential clinical impact since selected MRI´s in the FU period might be replaced with cfDNA, or the information could aid in determining whether a patient should undergo relapse surgery or not. Due to a small number of patients in this cohort, larger studies are needed to clarify this potential. The corresponding bp-peak of ≤ 166 in all samples but four, suggests that the monitored DNA can include tumor-specific DNA, but this has not been verified in the present study, e.g. by mutation specific sequencing, and is only hypothesis generating. It has been shown that selecting short DNA fragments can increase the fraction of ctDNA however a standardized procedure does not exist [16]. A study in hepatocellular carcinoma defined a cut-off for primarily tumor origin at < 166 bp and a negative correlation between tumor DNA and bp > 180 [28]. Others found different fragment lengths according to different tumor types with bp-length between 134–144 for GB xenografts, 110–140 for melanoma, a bp-peak at 277 in lung cancer or bp-length <100 in advanced colorectal cancer together with an equal distribution of tumor and normal cell DNA between 100–150, respectively [13, 14]. There is a distinct difference between the detection levels for e.g. colorectal- and brain cancer [29] and a ctDNA cut-off has not been defined for brain cancer patients. We found that other factors like RT, infection and necrosis/apoptosis may influence fragment size distribution as has also been shown in other studies [14, 17, 30]. We did not find a correlation between tumor size and cfDNA concentrations in our study even though we had 31 paired measurements. Tumor size was defined using CE, measurable lesions, but non-CE, non-measurable lesions can also shed cfDNA. We did not standardize time of sampling but since ctDNA has a half-life of minutes to 2.5 hours [31–33], the optimal time of sampling needs to be investigated further. Several studies have shown that increased levels of a specific mutation in the blood can be found significantly earlier than a radiologic or clinical progression [34–36] and *IDH* R132H mutation, *TERT* promotor mutation, and MGMT promotor methylation has been detected in brain cancer [24–26]. Therefore, to develop the technique further, it would be meaningful to perform targeted sequencing in plasma for specific mutations found in each patient´s tumor in a personalized strategy.

MATERIALS AND METHODS

Patients

Patients were screened during clinical working hours by one neuro surgeon from her outpatient clinic. The only screening criteria were suspicion of GB with subsequent diagnostic confirmation and eligibility for maximum safe surgery. A total of nine patients were identified and all were included at Rigshospitalet, Copenhagen University, Denmark, between November 2017 and June 2018. One patient decided not to receive further oncologic treatment after surgery and was excluded (Figure 1A). Each patient gave signed informed consent prior to diagnostic surgery. End of study was defined at progression, but each patient was followed until death or time of data lock (13.12.2018). All patients underwent surgery and standard pathological examination according to the World Health Organization (WHO) diagnostic criteria for brain tumors 2016 [37]. All included patients were diagnosed with GB, isocitrate dehydrogenase (*IDH)*-wildtype (WT), as assessed by

Multiplex Ligation-dependant Probe Amplification (MLPA), and five patients had a O-6-methyl-guanine-DNA-methyl-transferase (MGMT)-methylated tumor, measured by promoter methylation using a cut-off of 10%. Standard oncologic treatment after surgery was offered according to the patient´s clinical status at the first visit at Department of Oncology. Each patient had MRI performed before surgery, ≤48 hours after surgery, after two and five cycles of adjuvant TMZ and then every three months until progression. If a patient was clinically stable but the MRI showed a possible progression, we could perform a ^{18}Fluoro-*O*-(2) fluoroethyl-l-tyrosine/positron-emission-tomography (FET/PET) scan for further confirmation. The case was then discussed at a multidisciplinary meeting with neuro surgeons, -radiologists, -pathologists and -oncologists. Peripheral blood was collected prior to initial surgery, before oncologic therapy, during concurrent radiotherapy (RT)/Temozolomide (TMZ) plus adjuvant TMZ until progression (Figure 1B). The project was carried out in accordance with the Declaration of Helsinki and with approval from Ethics Committee (Journal number: H-17019401) and Danish Data Protection Agency (Journal number: RH-2017-269, I-Suite number: 05801).

Blood sample collection, cfDNA determination and base pair detection

Peripheral blood was collected in cell-stabilizing Blood Collection Tubes (BCT; Streck Laboratories, Omaha, NE, USA). Total cfDNA was extracted from 4 ml plasma using the QIAsymphony Circulating DNA Kit (Qiagen, Hilden, Germany) according to the manufacturer's instructions using an elution volume of 60µl. Quantification of cfDNA was performed using the dsDNA HS Assay Kit on a Qubit Fluorometer (Thermo Fisher Scientific, Waltham, MA) detecting double stranded DNA (> 10 pg/ µL) using intercalating fluorescent dyes. CfDNA fragment distribution was assessed using the Agilent 4200 TapeStation System (D5000). This system uses electrophoresis to separate DNA fragments from 100–5000 bp. The peak of the curve with the highest % of fragments, was defined as the highest peak (Figure 1C). To investigate the relation between cfDNA and bp-peaks further, we calculated a ratio between the two using the formula: cfDNA/(bp-peak/100)^2.

Tumor size determination

A trained, senior neuro radiologist noted contrast enhanced (CE), measurable tumor of each MRI. We paired cfDNA concentration with tumor size if both were performed within 14 days of each other except for the MRI performed <48 hours after surgery which was paired with the cfDNA concentration one month after surgery without any treatment initiated.

Limitations and strengths

Our study has several limitations. It is a small study with eight patients and results need to be validated in a larger cohort. Some blood samples were not taken or could not be analyzed due to logistic challenges and patient compliance. We measured only cfDNA and not ctDNA due to the scope of the study. It is a strength that it is a prospective study with GB, *IDH*-WT and multiple blood sampling throughout the planned treatment. All included patients completed the radiation course and seven out of eight patients moved to the adjuvant setting.

CONCLUSIONS

We found that it was possible to detect cfDNA concentrations in patients with GB in sequential blood sampling. CfDNA concentrations increased at progression in three out of four patients but did not increase in three out of four patients without progression. CfDNA levels could potentially aid in three out of three questionable cases of pseudo-progression.

Abbreviations

GB: Glioblastoma; CTC: Circulating tumor cell; CSF: Cerebrospinal fluid; CfDNA: Cell-free DNA; CtDNA: Circulating tumor DNA; Bp: Base Pair; RT: Radio Therapy; TMZ: Temozolomide; OS: Overall survival; PFS: Progression-free survival; MRI: Magnetic resonance imaging; RANO: Response Assessment in Neuro Oncology; WHO: World Health Organization; MLPA: Multiplex Ligation-dependant Probe Amplification; IDH: Isocitrate Dehydrogenase; MGMT: O-6-methyl-guanine-DNA-methyl-transferase; TERT: Telomerase Reverse Transcriptase; FET/PET: ^{18}Fluoro-*O*-(2) fluoroethyl-l-tyrosine/positron-emission-tomography; CE: Contrast Enhanced; PD1i: Programmed Death 1 inhibitor; NSCLC: Non-Small-Cell Lung Cancer.

Author contributions

Concepted the study: DSN, UL and HSP. Identification and inclusion of patients: JSR and DSN. Review of MRI´s: VAL. Analyzing data: DSN, OØ, LBA, SRM and CWY. Figures: SRM and DSN. Writing of manuscript: DSN. Critical review of manuscript: OØ, LBA, SRM and CWY. Valuable feedback: UL, HSP, JB and FCN. All authors have read and approved the final manuscript.

ACKNOWLEDGMENTS

The authors wish to thank Miriam Yan Juk Gou and Aseeba Ayub for performing the cfDNA concentration- and fragment analyses and a special thanks to the included patients.

CONFLICTS OF INTEREST

The authors declare no conflicts of interest.

FUNDING

Danish Cancer Society.

REFERENCES

1. Hegi ME, Diserens AC, Gorlia T, Hamou MF, de Tribolet N, Weller M, Kros JM, Hainfellner JA, Mason W, Mariani L, Bromberg JE, Hau P, Mirimanoff RO, et al. MGMT gene silencing and benefit from temozolomide in glioblastoma. N Engl J Med. 2005; 352:997–1003. https://doi.org/10.1056/NEJMoa043331. [PubMed]
2. Wen PY, Chang SM, Van den Bent MJ, Vogelbaum MA, Macdonald DR, Lee EQ. Response Assessment in Neuro-Oncology Clinical Trials. J Clin Oncol. 2017; 35:2439–49. https://doi.org/10.1200/JCO.2017.72.7511. [PubMed]
3. Taal W, Brandsma D, de Bruin HG, Bromberg JE, Swaak-Kragten AT, Smitt PA, van Es CA, van den Bent MJ. Incidence of early pseudo-progression in a cohort of malignant glioma patients treated with chemoirradiation with temozolomide. Cancer. 2008; 113:405–10. https://doi.org/10.1002/cncr.23562. [PubMed]
4. Gerstner ER, McNamara MB, Norden AD, Lafrankie D, Wen PY. Effect of adding temozolomide to radiation therapy on the incidence of pseudo-progression. J Neurooncol. 2009; 94:97–101. https://doi.org/10.1007/s11060-009-9809-4. [PubMed]
5. Diaz LA Jr, Bardelli A. Liquid biopsies: genotyping circulating tumor DNA. J Clin Oncol. 2014; 32:579–86. https://doi.org/10.1200/JCO.2012.45.2011. [PubMed]
6. Fassunke J, Ihle MA, Lenze D, Lehmann A, Hummel M, Vollbrecht C, Penzel R, Volckmar AL, Stenzinger A, Endris V, Jung A, Lehmann U, Zeugner S, et al. EGFR T790M mutation testing of non-small cell lung cancer tissue and blood samples artificially spiked with circulating cell-free tumor DNA: results of a round robin trial. Virchows Arch. 2017; 471:509–20. https://doi.org/10.1007/s00428-017-2226-8. [PubMed]
7. Nilsson RJ, Karachaliou N, Berenguer J, Gimenez-Capitan A, Schellen P, Teixido C, Tannous J, Kuiper JL, Drees E, Grabowska M, van Keulen M, Heideman DA, Thunnissen E, et al. Rearranged EML4-ALK fusion transcripts sequester in circulating blood platelets and enable blood-based crizotinib response monitoring in non-small-cell lung cancer. Oncotarget. 2016; 7:1066–75. https://doi.org/10.18632/oncotarget.6279. [PubMed]
8. Bottoni P, Scatena R. The Role of CA 125 as Tumor Marker: Biochemical and Clinical Aspects. Adv Exp Med Biol. 2015; 867:229–44. https://doi.org/10.1007/978-94-017-7215-0_14. [PubMed]
9. Das V, Kalita J, Pal M. Predictive and prognostic biomarkers in colorectal cancer: A systematic review of recent advances and challenges. Biomed Pharmacother. 2017; 87:8–19. https://doi.org/10.1016/j.biopha.2016.12.064. [PubMed]
10. Sullivan JP, Nahed BV, Madden MW, Oliveira SM, Springer S, Bhere D, Chi AS, Wakimoto H, Rothenberg SM, Sequist LV, Kapur R, Shah K, Iafrate AJ, et al. Brain tumor cells in circulation are enriched for mesenchymal gene expression. Cancer Discov. 2014; 4:1299–309. https://doi.org/10.1158/2159-8290.CD-14-0471. [PubMed]
11. Agerbæk MO, Bang-Christensen SR, Yang MH, Clausen TM, Pereira MA, Sharma S, Ditlev SB, Nielsen MA, Choudhary S, Gustavsson T, Sorensen PH, Meyer T, Propper D, et al. The VAR2CSA malaria protein efficiently retrieves circulating tumor cells in an EpCAM-independent manner. Nat Commun. 2018; 9:3279. https://doi.org/10.1038/s41467-018-05793-2. [PubMed]
12. Miller AM, Shah RH, Pentsova EI, Pourmaleki M, Briggs S, Distefano N, Zheng Y, Skakodub A, Mehta SA, Campos C, Hsieh WY, Selcuklu SD, Ling L, et al. Tracking tumour evolution in glioma through liquid biopsies of cerebrospinal fluid. Nature. 2019; 565:654–58. https://doi.org/10.1038/s41586-019-0882-3. [PubMed]
13. Underhill HR, Kitzman JO, Hellwig S, Welker NC, Daza R, Baker DN, Gligorich KM, Rostomily RC, Bronner MP, Shendure J. Fragment Length of Circulating Tumor DNA. PLoS Genet. 2016; 12:e1006162. https://doi.org/10.1371/journal.pgen.1006162. [PubMed]
14. Mouliere F, Robert B, Arnau Peyrotte E, Del Rio M, Ychou M, Molina F, Gongora C, Thierry AR. High fragmentation characterizes tumour-derived circulating DNA. PLoS One. 2011; 6:e23418. https://doi.org/10.1371/journal.pone.0023418. [PubMed]
15. Thierry AR, Mouliere F, Gongora C, Ollier J, Robert B, Ychou M, Del Rio M, Molina F. Origin and quantification of circulating DNA in mice with human colorectal cancer xenografts. Nucleic Acids Res. 2010; 38:6159–75. https://doi.org/10.1093/nar/gkq421. [PubMed]
16. Mouliere F, Chandrananda D, Piskorz AM, Moore EK, Morris J, Ahlborn LB, Mair R, Goranova T, Marass F, Heider K, Wan JC, Supernat A, Hudecova I, et al. Enhanced detection of circulating tumor DNA by fragment size analysis. Sci Transl Med. 2018; 10:eaat4921. https://doi.org/10.1126/scitranslmed.aat4921. [PubMed]
17. Jahr S, Hentze H, Englisch S, Hardt D, Fackelmayer FO, Hesch RD, Knippers R. DNA fragments in the blood plasma of cancer patients: quantitations and evidence for their origin from apoptotic and necrotic cells. Cancer Res. 2001; 61:1659–65. [PubMed]
18. Beiter T, Fragasso A, Hudemann J, Niess AM, Simon P. Short-term treadmill running as a model for studying cell-free DNA kinetics *in vivo*. Clin Chem. 2011; 57:633–36. https://doi.org/10.1373/clinchem.2010.158030. [PubMed]
19. Tovbin D, Novack V, Wiessman MP, Abd Elkadir A, Zlotnik M, Douvdevani A. Circulating cell-free DNA in

hemodialysis patients predicts mortality. Nephrol Dial Transplant. 2012; 27:3929–35. https://doi.org/10.1093/ndt/gfs255. [PubMed]

20. Destouni A, Vrettou C, Antonatos D, Chouliaras G, Traeger-Synodinos J, Patsilinakos S, Kitsiou-Tzeli S, Tsigas D, Kanavakis E. Cell-free DNA levels in acute myocardial infarction patients during hospitalization. Acta Cardiol. 2009; 64:51–57. https://doi.org/10.2143/AC.64.1.2034362. [PubMed]

21. Schwarzenbach H, Hoon DS, Pantel K. Cell-free nucleic acids as biomarkers in cancer patients. Nat Rev Cancer. 2011; 11:426–37. https://doi.org/10.1038/nrc3066. [PubMed]

22. Macher H, Egea-Guerrero JJ, Revuelto-Rey J, Gordillo-Escobar E, Enamorado-Enamorado J, Boza A, Rodriguez A, Molinero P, Guerrero JM, Dominguez-Roldán JM, Murillo-Cabezas F, Rubio A. Role of early cell-free DNA levels decrease as a predictive marker of fatal outcome after severe traumatic brain injury. Clin Chim Acta. 2012; 414:12–17. https://doi.org/10.1016/j.cca.2012.08.001. [PubMed]

23. Regner A, Meirelles LD, Ikuta N, Cecchini A, Simon D. Prognostic utility of circulating nucleic acids in acute brain injuries. Expert Rev Mol Diagn. 2018; 18:925–38. https://doi.org/10.1080/14737159.2018.1535904. [PubMed]

24. Boisselier B, Gállego Pérez-Larraya J, Rossetto M, Labussière M, Ciccarino P, Marie Y, Delattre JY, Sanson M. Detection of IDH1 mutation in the plasma of patients with glioma. Neurology. 2012; 79:1693–98. https://doi.org/10.1212/WNL.0b013e31826e9b0a. [PubMed]

25. Majchrzak-Celińska A, Paluszczak J, Kleszcz R, Magiera M, Barciszewska AM, Nowak S, Baer-Dubowska W. Detection of MGMT, RASSF1A, p15INK4B, and p14ARF promoter methylation in circulating tumor-derived DNA of central nervous system cancer patients. J Appl Genet. 2013; 54:335–44. https://doi.org/10.1007/s13353-013-0149-x. [PubMed]

26. Zachariah MA, Oliveira-Costa JP, Carter BS, Stott SL, Nahed BV. Blood-based biomarkers for the diagnosis and monitoring of gliomas. Neuro Oncol. 2018; 20:1155–61. https://doi.org/10.1093/neuonc/noy074. [PubMed]

27. Kageyama SI, Nihei K, Karasawa K, Sawada T, Koizumi F, Yamaguchi S, Kato S, Hojo H, Motegi A, Tsuchihara K, Akimoto T. Radiotherapy increases plasma levels of tumoral cell-free DNA in non-small cell lung cancer patients. Oncotarget. 2018; 9:19368–78. https://doi.org/10.18632/oncotarget.25053. [PubMed]

28. Jiang P, Chan CW, Chan KC, Cheng SH, Wong J, Wong VW, Wong GL, Chan SL, Mok TS, Chan HL, Lai PB, Chiu RW, Lo YM. Lengthening and shortening of plasma DNA in hepatocellular carcinoma patients. Proc Natl Acad Sci U S A. 2015; 112:E1317–25. https://doi.org/10.1073/pnas.1500076112. [PubMed]

29. Bettegowda C, Sausen M, Leary RJ, Kinde I, Wang Y, Agrawal N, Bartlett BR, Wang H, Luber B, Alani RM, Antonarakis ES, Azad NS, Bardelli A, et al. Detection of circulating tumor DNA in early- and late-stage human malignancies. Sci Transl Med. 2014; 6:224ra24. https://doi.org/10.1126/scitranslmed.3007094. [PubMed]

30. Suzuki N, Kamataki A, Yamaki J, Homma Y. Characterization of circulating DNA in healthy human plasma. Clin Chim Acta. 2008; 387:55–58. https://doi.org/10.1016/j.cca.2007.09.001. [PubMed]

31. Diehl F, Schmidt K, Choti MA, Romans K, Goodman S, Li M, Thornton K, Agrawal N, Sokoll L, Szabo SA, Kinzler KW, Vogelstein B, Diaz LA Jr. Circulating mutant DNA to assess tumor dynamics. Nat Med. 2008; 14:985–90. https://doi.org/10.1038/nm.1789. [PubMed]

32. Wan JC, Massie C, Garcia-Corbacho J, Mouliere F, Brenton JD, Caldas C, Pacey S, Baird R, Rosenfeld N. Liquid biopsies come of age: towards implementation of circulating tumour DNA. Nat Rev Cancer. 2017; 17:223–38. https://doi.org/10.1038/nrc.2017.7. [PubMed]

33. Yao W, Mei C, Nan X, Hui L. Evaluation and comparison of *in vitro* degradation kinetics of DNA in serum, urine and saliva: A qualitative study. Gene. 2016; 590:142–48. https://doi.org/10.1016/j.gene.2016.06.033. [PubMed]

34. Ahlborn LB, Tuxen IV, Mouliere F, Kinalis S, Schmidt AY, Rohrberg KS, Santoni-Rugiu E, Nielsen FC, Lassen U, Yde CW, Oestrup O, Mau-Sorensen M. Circulating tumor DNA as a marker of treatment response in BRAF V600E mutated non-melanoma solid tumors. Oncotarget. 2018; 9:32570–79. https://doi.org/10.18632/oncotarget.25948. [PubMed]

35. El Messaoudi S, Mouliere F, Du Manoir S, Bascoul-Mollevi C, Gillet B, Nouaille M, Fiess C, Crapez E, Bibeau F, Theillet C, Mazard T, Pezet D, Mathonnet M, et al. Circulating DNA as a Strong Multimarker Prognostic Tool for Metastatic Colorectal Cancer Patient Management Care. Clin Cancer Res. 2016; 22:3067–77. https://doi.org/10.1158/1078-0432.CCR-15-0297. [PubMed]

36. Gray ES, Rizos H, Reid AL, Boyd SC, Pereira MR, Lo J, Tembe V, Freeman J, Lee JH, Scolyer RA, Siew K, Lomma C, Cooper A, et al. Circulating tumor DNA to monitor treatment response and detect acquired resistance in patients with metastatic melanoma. Oncotarget. 2015; 6:42008–18. https://doi.org/10.18632/oncotarget.5788. [PubMed]

37. Louis DN, Perry A, Reifenberger G, von Deimling A, Figarella-Branger D, Cavenee WK, Ohgaki H, Wiestler OD, Kleihues P, Ellison DW. The 2016 World Health Organization Classification of Tumors of the Central Nervous System: a summary. Acta Neuropathol. 2016; 131:803–20. https://doi.org/10.1007/s00401-016-1545-1. [PubMed]

APPENDIX 1

ESMO Open Cancer Horizons

Hallmarks of glioblastoma: a systematic review

Dorte Schou Nørøxe, Hans Skovgaard Poulsen, Ulrik Lassen

► Prepublication history is available. To view please visit the journal (http://dx.doi.org/10.1136/esmoopen-2016-000144).

To cite: Nørøxe DS, Poulsen HS, Lassen U. Hallmarks of glioblastoma: a systematic review. *ESMO Open* 2016;**1**:e000144. doi:10.1136/esmoopen-2016-000144

Received 09 December 2016
Revised 30 December 2016
Accepted 04 January 2017

Department of Radiation Biology, The Finsen Center, Rigshospitalet, Copenhagen, Denmark

Correspondence to
Dr Dorte Schou Nørøxe, The Finsen Center, Rigshospitalet, Blegdamsvej 9, Copenhagen 2100, Denmark; anne.dorte.schou.noeroexe@regionh.dk

ABSTRACT

Despite decades of intense research, the complex biology of glioblastoma (GBM) is not completely understood. Progression-free survival and overall survival have remained unchanged since the implementation of the STUPP regimen in 2005 with concomitant radio-/chemotherapy and adjuvant chemotherapy with temozolomide.

In the context of Hanahan and Weinberg's six hallmarks and two emerging hallmarks of cancer, we discuss up-to-date status and recent research in the biology of GBM. We discuss the clinical impact of the research results with the most promising being in the hallmarks 'enabling replicative immortality', 'inducing angiogenesis', 'reprogramming cellular energetics' and 'evading immune destruction'. This includes the importance of molecular diagnostics according to the new WHO classification and how next generation sequencing is being implemented in the clinical daily life. Molecular results linked together with clinical outcome have revealed the importance of the prognostic biomarker isocitratedehydrogenase (IDH), which is now part of the diagnostic criteria in brain tumours. IDH is discussed in the context of the hallmark 'reprogramming cellular energetics'. O-6-methylguanine-DNA methyltransferase status predicts a more favourable response to treatment and is thus a predictive marker. Based on genomic aberrations, Verhaak *et al* have suggested a division of GBM into three subgroups, namely, proneural, classical and mesenchymal, which could be meaningful in the clinic and could help guide and differentiate treatment decisions according to the specific subgroup.

The information achieved, will develop and improve precision medicine in the future.

INTRODUCTION

Glioblastoma (GBM) has a complex biology and despite decades of research, much is still unknown. The incidence is 3.2/100 000,[1] and GBM is the most malignant brain tumour.

GBM separates from lower grade gliomas by expressing necrosis and/or microvascular proliferation[2] and is characterised by rapid, infiltrating growth. GBM can arise either as a primary tumour or as a secondary tumour, the latter as a malignant transformation from a lower grade brain tumour and/or with mutation in the isocitrate dehydrogenase (IDH) gene.

Treatment in patients with a good performance status is multimodal with surgery, radiation and chemotherapy. However, in spite of the intensive treatment, patients have a poor prognosis with a progression-free survival (PFS) of 7–8 months, a median survival of 14–16 months and 5-year overall survival (OS) of 9.8%.[3 4]

The diagnosis of gliomas has historically been by histopathological examination. Recent advances have indicated the importance of molecular subtyping. As such, a new WHO classification of GBM into GBM, IDH-wildtype, GBM, IDH-mutant and GBM not otherwise specified (NOS) was recently presented.[2] This raises the dilemma of contradiction between the histological/phenotypic diagnosis and the molecular/genomic diagnosis. The genomic diagnosis will then overrule and dictate the diagnosis. There has been suggestion of a further subdivision based on the molecular changes by Verhaak *et al*[5 6] and table 1. However, today, this subdivision has no role in diagnostics and treatment decisions but might help overcome some of the heterogeneity in GBM and improve treatment.

The predictive factor O-6-methylguanine-DNA methyltransferase (MGMT) is now used in treatment decisions due to results with median OS in patients with MGMT-methylated tumour of 22–26 months compared with non-MGMT-methylated tumours of 12–15 months, respectively.[7]

Hanahan and Weinberg[8] have made an impressive work, investigating the similarities in cancer and explaining these from six hallmarks and two emerging hallmarks. In the following below, we discuss these hallmarks in the context of GBM.

METHODS

We searched PubMed with no limitation to time. Only articles in English were used.

Sustaining proliferative signalling

Normal cell growth is regulated through a number of growth signals and paracrine signalling that sustains a cell in a healthy, normal homeostasis.

Table 1 Subclassification in glioblastoma.

Classical	Mutated in EGFR with high expression. Lacks P53 mutation. CDKN2A deleted which causes inactivation of the RB pathway. Amplification of chromosome 7 and deletion of chromosome 10. Classical O-6-methylguanine-DNA methyltransferase (MGMT)-methylated tumours respond significantly better to aggressive treatment as compared with non-MGMT-methylated classical tumours. Astrocytic-like.
Mesenchymal	Mutated in *NF* which activates the PI3K/Akt pathway. Mutated in *PTEN* which activates the RAS pathway. Expression of YKL-40 and MET which can cause epithelial-to-mesenchymal transition. Inflammatory and necrotic. MGMT-methylated mesenchymal tumours seem to respond better to aggressive treatment than non-MGMT-methylated tumours, but this is not significant. Astrocytic-like.
Proneural	Mutated in *PDGFRA* which activates the PI3K pathway and the RAS pathway. Mutated in *P53*, *IDH* and *PDGFRA*. If *PDGFRA* is mutated, then *IDH* will not be mutated and opposite. No difference in response to aggressive treatment when stratified for MGMT status. Often secondary glioblastoma. Oligodendrocytic-like.

Modified and simplified from Verhaak et al,[5] Cancer Genome Atlas Research Network,[9] Murat et al,[32]
EGFR, epidermal growth factor; IDH, isocitrate dehydrogenase; RAS, rat sarcoma.

A cancer cell has evolved mechanisms to sustain this proliferative signalling by aberrations in the gene signature. Examples of activating and inactivating mutations can be seen in table 2, and a list of the top 20 mutated genes in GBM can be seen in figure 1.

The Cancer Genome Atlas (TCGA) group first investigated the genomic characterisation in GBM in 2008.[9] Two hundred and six specimens of GBM tissue were analysed, and significant findings were done in the following three core pathways: receptor tyrosine kinase (RTK)/rat sarcoma (RAS)/PI3K, p53 and RB with alterations in 88%, 78% and 87%, respectively.

The most significant alteration in the RTK/RAS/PI3K pathway was in epidermal growth factor receptor (EGFR) in 45%. EGFR can be altered in a number of ways[10], and mutation in the *EGFR* gene results in overexpression of EGFR in GBM as seen in the classical subtype. In total, activating alterations were found in 70% in the RTKs.

The most significant inactivating alteration was found in the *PTEN* gene in 36%, thereby losing the negative feedback to PI3K causing proliferation and decreased apoptosis. RAS was only mutated in 2% of the specimens, but this is of importance due to the role as a key activator and the influence on several proteins downstream.

In the p53 pathway, the most significant findings were in 49% of *CDKN2A* and 35% in *TP53*.

In the RB pathway, *CDKN2A* and *CDKN2B* were inactivated in 52% and 47%, respectively and the gene *RB* was homozygote deleted in 11%.

In 2013, the same specimens were analysed with next-generation sequencing (NGS) and another 337 specimens were added, ending up with 543 tumours.[11] Seventy-one significantly mutated genes (SMGs) were found, which many of them corresponded with previous findings. In long-term survivors, aberrations in *EGFR*, *CDK4* and *CDKN2A* were less frequent. Focus should therefore be on the three pathways described.

Evading growth suppressors

Loss of function in tumour suppressor genes such as *NF2*, *LKB1*, *RB* or *TP53* is essential. The latter two genes play a crucial role in the G1 phase in the cell cycle, having the ability to delay entrance into the S-phase to repair the damage detected or ultimately cause apoptosis of the cell.

NF2 codes for Merlin which cause binding of cell adhesion molecules such as E-cadherin on the transmembrane RTK in the cytoplasm, making the cell adhesion stronger and more dense thereby limiting the ability to bind growth factors.[12 13]

Table 2 Examples of oncogenes and tumour suppressor genes

Activating (oncogenes)	Inactivating (tumour suppressor genes)
B-RAF	Tumour protein (*TP53*)
Phosphoinositide 3-kinase (*PI3K*) isoforms	Retinoblastoma associated (*RB*)
Rat sarcoma (*RAS*)	Mammalian target of rapamycin (*mTOR*)
Epidermal growth factor receptor (*EGFR*)	Phosphatase and tensin homolog (*PTEN*)
Platelet derived growth factor receptor A (PDGFRA)	Breast cancer1 (BRCA1)

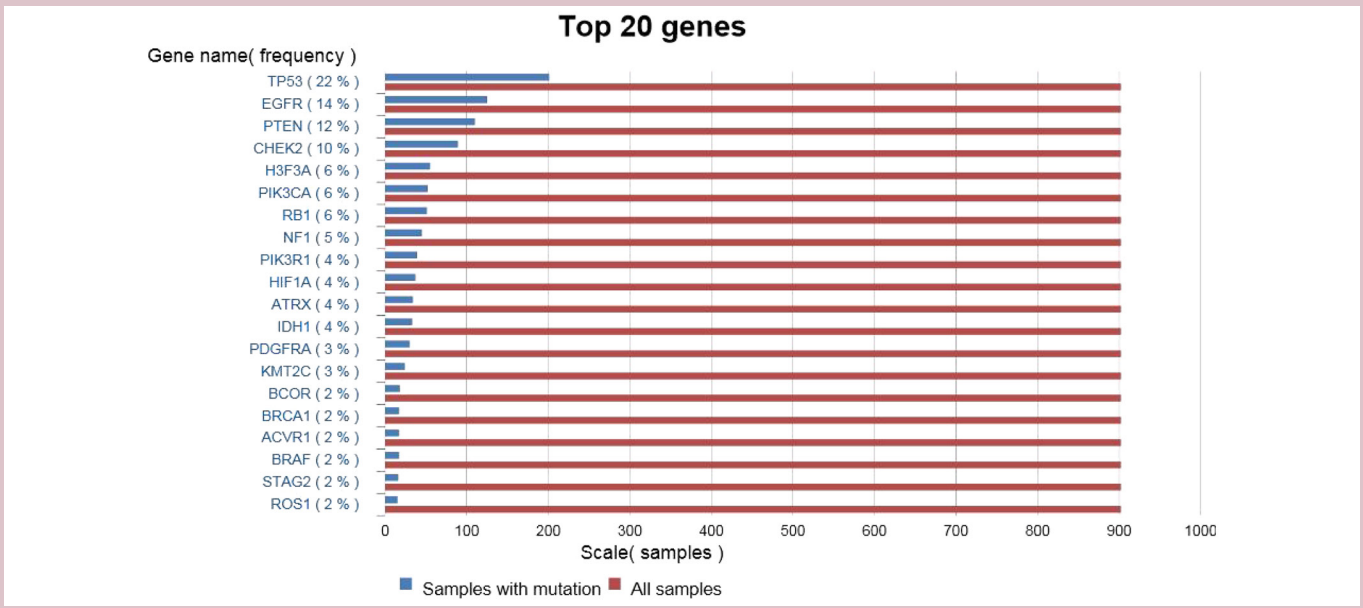

Figure 1 Top 20 mutated genes in glioblastoma based on 712 samples of astrocytoma grade IV.[16]

LKB1 is a key activator of mTOR and acts by altering and stabilising the epithelial architecture.[14]

Mutation in the *RB* gene is not as common as mutations in the protein (p)RB. *RB* is mutated in most other cancers but only 6%–11% in GBM.[15 16] PRB acts on extracellular signals, and inactivation of pRB can happen in a number of ways in the malignant cell; CDK 4 and 6 can phosphorylate pRB, making it inactive and thus allowing the cell to enter the G1 phase in the cell cycle or the gene can be deleted by mutation. The proteins of the gene *CDKN2A* work by inhibiting CDK4 and 6. When *CDKN2A* function is lost by mutation, this indirectly inhibits the function of pRB. It is therefore important to know whether RB insufficiency is due to *RB* mutation or due to aberrations in the pathway. The latter makes the cancer cell responsive to anti-pathway treatment, whereas the first makes it resistant to the same drugs. Studies in breast[17] and bladder[18] cancers have shown that loss of pRB makes the cancer more susceptible to radiotherapy and chemotherapy, suggesting pRB loss as a predictive marker of response to such.

The p53 pathway acts on intracellular signals. *TP53* is mutated in 27%–33.8% of GBM[16 19] and is more correlated to astrocytomas than to oligodendrogliomas. A total of 10 isoforms of *TP53* have been identified resulting in different expression of p53[20–22], and it seems that mutations in *TP53* are not tumour-type specific but are shared across tumour types.[23] It also seems that mutations in *TP53* do not change with chemotherapy.[24] Other isoforms have been identified in patients with breast and ovary cancers and acute myeloid leukaemia.[20] The different isoforms showed different response to treatment and PFS.

This suggests that *TP53* may be used as a prognostic biomarker in some cancers but not in GBM. In the COSMIC-database, the prognostic value has been investigated. In brain cancer, three studies found a positive predictive value, whereas two studies did not and four studies were not related to outcome. Only studies with more than 50 patients were included.[16]

The above shows that knowledge is being obtained concerning tumour suppressor genes, but it is yet too scarce to target these in clinical protocols.

Activating invasion and metastasis

The ability of communication between cancer cells and the periphery, the neoplastic stroma, is proving more important in terms of invasive growth and metastases.

Since extracranial metastases are extremely rare in GBM,[25] invasion and migration are the main features of GBM spreading.

Three major ways of invasion, migration and metastases have been identified, which will be discussed next; the collective invasiveness, where the cancer cell invades to nearby tissue through existing interstices in the extracellular matrix, thereby expanding from the primary tumour but without directly detachment. Connexin 43 (cnx43) plays a role in the tight junctions between cells. GBM cells can downregulate cnx43, thereby causing lesser adherence and communication between the cells and making possible invasion to nearby tissue.[26]

Another way is invasion by inflammatory cells where protumoural immune cells produce extracellular matrix degrading enzymes in the periphery, making way for the cancer cell and creating an imbalance between tissue inhibitor of metalloproteinases and metalloproteinases. Hypoxia also causes an increase in proinflammatory proteins and cancer stem cells.[27] The proinflammatory

proteins allow for cancer stem cells to differentiate, causing gliomagenesis.

Finally, epithelial-to-mesenchymal transition (EMT)[28] can occur. The heterogenous GBM cell can display epithelial features, and EMT has been observed in GBM.[29] For EMT to happen, E-cadherin is often lacking.[30] E-cadherin normally forms junctions between adjacent epithelial cells, thereby assisting senescence and diminishing the ability to grow and invade. When impaired, this causes disruption of the normal cell–cell contact and cell polarity, enabling cell motility. The cell can then undergo epigenetic changes, resulting in dedifferentiation and acquisition of stem cell features.

Hypoxia can also recruit myeloid cells. They cause upregulation of transforming growth factor (TGF)-β, epithelial growth factor, platelet-derived growth factor (PDGFRA) and TWIST, which secretes transcription factors like N-cadherin that is necessary for EMT. Expression of TGF-β and TWIST is higher in necrotic areas and so is the expression of the stem cell marker CD133. Expression of TGF-β in necrotic areas and expression of CD133 are correlated to poorer survival.[31 32]

Enabling replicative immortality

The gene telomerase reverse transcriptase (*TERT*) causes expression of telomerase that can add lengths to the telomeres. Telomerase is almost absent in normal cells but is abundantly represented in cancer cells, and the gene has been found mutated in 51% of GBM.[16] This enables the cell to avoid telomere shortening and causing an otherwise doomed cell to reverse into immortality.

In the 2013 TCGA study,[11] expression of *TERT* was found in 21/25 cases accessible for investigation. In the remaining four samples, mutations were found in the transcriptional regulator gene alpha thalassaemia mental retardation (*ATRX*). These alterations were not expressed concurrently. They implied that either *TERT* or *ATRX* is responsible for the telomere lengthening. *ATRX* was expressed concurrently with mutations in *TP53* and *IDH1*, representing secondary GBM.

Ceccarelli *et al* found that *ATRX* mutation was associated with lengthening of telomeres while, on the other hand, *TERT* mutated tumours did not have a difference in telomere length compared with normal tissue controls.[33]

To support the latter, the authors of a recently published abstract presented at American Society of Oncology (ASCO) 2016 investigated 303 patients and found human TERT (h*TERT*) mutation in 75% of the patients. In substratification based on h*TERT* status and MGMT methylation, patients with h*TERT* mutation lived significantly longer with median OS of 28.3 months in methylated tumours and 15.9 months in non-MGMT-methylated tumours. No difference was observed with h*TERT* non-mutation regardless of MGMT methylation. This was validated in a TCGA cohort.[34] Whether this means that *TERT* plays a role in the better prognosis in MGMT-methylated tumours, is yet to be fully discovered.

Inducing angiogenesis

Vascular endothelial growth factor (VEGF) A gene stimulates angiogenesis and is rather constant. Angiogenesis can be stimulated in a variety of ways, for example, by oncogenes such as *RAS* and *MYC* or by inflammatory reactions. Bone marrow–derived cells (BMDCs) such as macrophages, neutrophils, mast cells and myeloid progenitors are recruited due to the peritumoural oedema. Some of the recruited vascular progenitor cells can transform into pericytes or endothelial cells, protecting and stabilising the newly formed vessel.[35] Bevacizumab (BEV) is a humanised monoclonal antibody that targets the vascular endothelial growth factor receptor.[36] It can only cross the blood–brain barrier (BBB) where this is destroyed, as seen in GBM. BEV was approved in 2009 by the Food and Drug Administration (FDA) for treatment of recurrent GBM.

A meta-analysis,[37] including two large phase III studies, the AvaGlio[38] and the RTOG085,[39] have demonstrated an increase in PFS but no influence on OS in newly diagnosed GBM patients treated with BEV.

Mechanisms of resistance to BEV are partly due to immunogenic disturbances. The BEV-induced hypoxia recruits proangiogenic BMDCs, mainly tumour-associated macrophages,[40] thereby ignoring the effect of BEV.

Hypoxia and BMDCs can enable EMT, as mentioned above, causing a transformation to the more infiltratory mesenchymal subtype.[41] Urup *et al* investigated whether proneural and mesenchymal subtype showed predictiveness towards response to BEV and found that this was not the case. They found that low gene expression of angiotensinogen and high expression of human leucocyte antigen (HLA) class II were predictive markers of response to BEV,[42] but this needs to be validated.

Resisting cell death

There are three mechanisms of cell death: apoptosis, autophagy and death by necrosis. The mechanisms are listed hierarchically.

In a normal cell, apoptosis can be divided into an extrinsic part (death receptor mediated) and an intrinsic part (mitochondria-mediated) (figure 2). Aberrations in these subtle mechanisms can lead to avoidance of apoptosis, which can also be achieved by loss of *TP53* and *RB*. PI3K, AKT and mTOR can block apoptosis and autophagy when survival signals are abundant.

Another aspect is autophagy, which happens with metabolic stress, nutrient limitation or dysfunction of organelles, thereby decreasing the activity of the cell. The metabolites produced can be used as energy, also in a cancer cell where energy is sparse. This represents a dilemma as autophagy in the early stage cancer can be tumour degrading and in late-stage cancer, can be tumour enhancing.

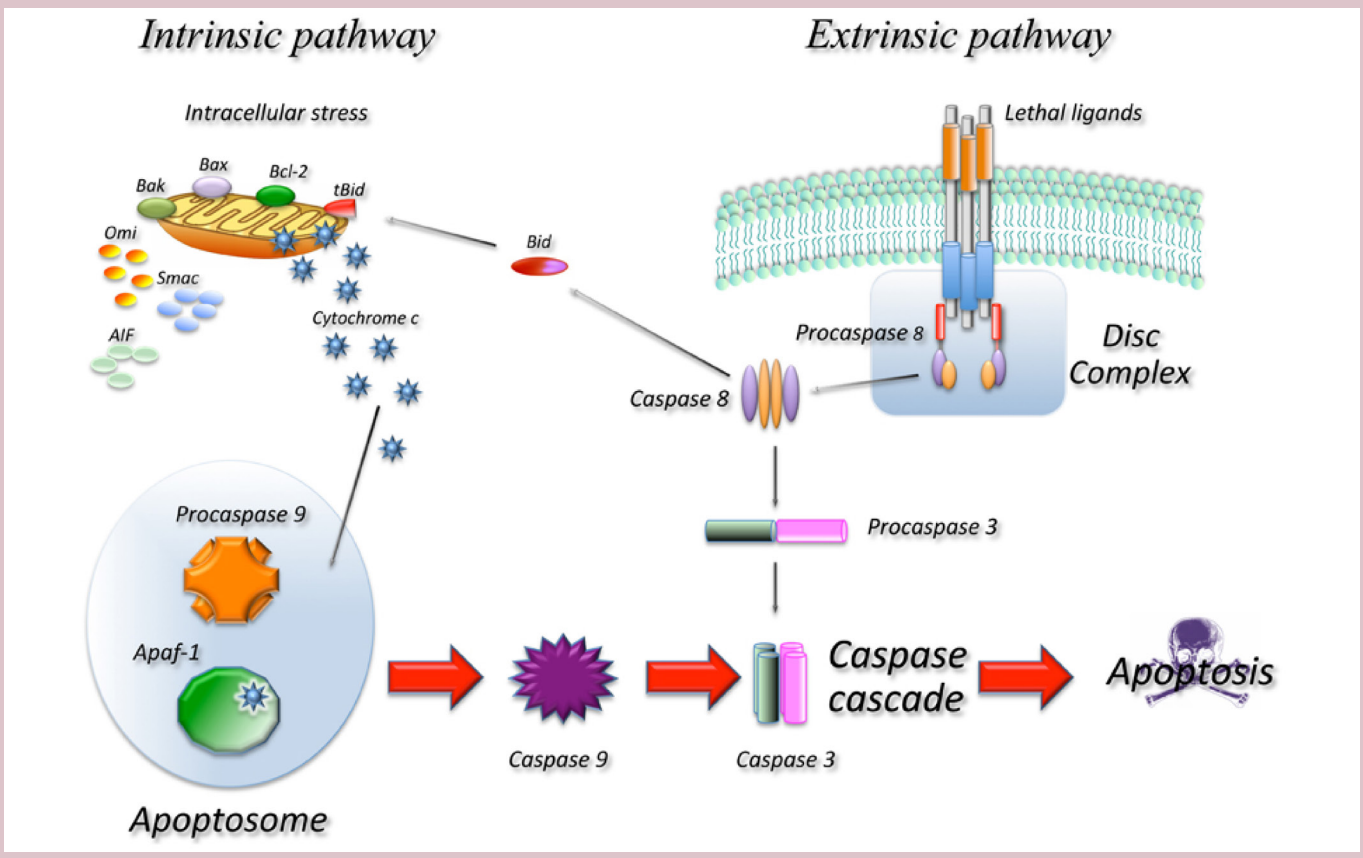

Figure 2 The intrinsic apoptotic pathway is a balance between proapoptotic proteins, for example, Bax and Bak and antiapoptotic proteins. The latter works by inhibiting Bax and Bak. When the inhibition stops, Bax and Bak change the mitochondrial outer membrane, causing release of cytochrome C, which triggers the Caspases and causes apoptosis.[87]

Cell death by necrosis mediates a proinflammatory response in the microenvironment. This activates the adaptive immune response with recruitment of BMDCs. Therefore, cell death by necrosis is considered as collateral damage for a tumour cell. Hence, if autophagy is impaired together with a defective apoptosis, a cell can become tumourigenic or die by necrosis and inflammation, causing even more space for tumourigenesis and a poor prognosis.[43]

In GBM, it seems that the cells are more prone to death by necrosis or autophagy as they are in a large extent resistant to death by apoptosis due to impairment of *TP53* or *RB*.[44 45] As an example, temozolomide induces death by autophagy.[46] Selective autophagy may be a potential target, and the importance of autophagy was highlighted by the recognition of 2016 Nobel Prize winner in medicine, cell biologist Yoshinori Ohsumi.[47]

In a study of 350 specimens of astrocytomas WHO grades I–IV, it was found that autophagy is enhanced in astrocytomas regardless of WHO grade and prognosis, casting light once again on the microenvironment.[48]

Evading immune destruction

The immune system is constantly surveilling the homeostasis and an immune competent person is able to eradicate many cancers in the making.[49] Experiments in immune incompetent mice where cytotoxic T-lymphocytes (CTLs) and natural killer cells were depleted showed an increasing tendency towards developing cancer.[50]

GBM cells are able to avoid an immune response due to a limited number of antigens and an ability to recruit myeloid-derived suppressor cells. However, GBM causes leaks in the astrocytic end feet that are part of the BBB.[51]

Presently, the main focus is on peptide and dendritic cell vaccines and checkpoint inhibitors.

Rindopepimut is an EGFRvIII peptide vaccine conjugated to an immunogenic carrier protein and admixed with the adjuvant granulocyte macrophage colony-stimulating factor.[52] Rindopepimut was investigated in the phase II trial ReACT for patients with relapse of GBM.[53] They were randomised to BEV plus Rindopepimut or control. Preliminary results presented at ASCO 2015 showed a significant OS of 11.3 months in the Rindopepimut group compared with 9.3 in the control group and an objective response rate of 23%–30% vs 9%–18%, respectively. In the single arm phase II trial, ACT III, for patients with newly diagnosed GBM, a median PFS and OS of 9.2 and 21.8 months were found, respectively. The results were better for patients with MGMT methylation.[54] A double-blind phase III trial, the ACT IV was then initiated. However, the protocol has been stopped, since it was found that the study would not meet its primary OS endpoint. Noteworthy was that the control group

lived longer than predicted based on historical-matched control groups and thus might have masked the effect of Rindopepimut. Patients treated with the drug prior to termination of the protocol are still offered treatment in compassionate use programmes.[55]

Another study investigating actively personalised peptide vaccination (GAPVAC) is being performed in newly diagnosed patients and is now closed for inclusion.[56]

A dendritic cell vaccine works by acting as an antigen-presenting cell. It is possible either to extract autologous antigen-specific T cells, expand them ex vivo and re-infuse into patients or by vaccination with an antigen together with an adjuvant.[57]

A phase I/II trial including 22 patients with grade II–IV gliomas, showed a positive immunological response in 13 patients.[58] The procedure, though, is time consuming and it seems that only 4% of the injected vaccine arrive at the draining lymph node.[59] Other studies have shown increased effect by prestimulation of the injection site.[60]

CTL-4 and programmed death 1 (PD1) are receptors on the T-cell causing apoptosis of the T-cell when abundant and inappropriate, thereby preventing development of autoimmune diseases. Cancer cells can bind to these receptors, causing apoptosis of the T-cell. A CTL-4 inhibitor revolutionised the treatment of unresectable malignant melanoma when Ipilimumab was approved by FDA in 2011.[61]

A PD1 inhibitor is a monoclonal antibody that binds to and occupies the PD1 receptor. PD1 inhibitors are now being investigated in first-line settings of GBM.[62 63] A combination with CTL-4 and PD1 inhibitors are also being performed and immune checkpoint inhibitors could potentially be more effective with prepriming of the immune system with a dendritic cell vaccine or a peptide vaccine.[64]

Another promising field of research is in the oncolytic viro therapy where poliovirus is genetically engineered with rhinovirus (PVSRIPO). PVSRIPO binds to the Ig superfamily adhesion molecule CD155 or Necl5, which GBM cells express.[65] The effect is local and cytotoxic.[66] A trial with 22 GBM patients with relapse is being performed at Preston Robert Tisch Brain Tumor Center at Duke University, USA. The treatment is promising and phase II/III trials are being planned.

Autologous lymphoid effector cells specific against tumour cells (ALECSAT) in recurrent GBM have also been tested. No increase in PFS or OS was found, and the study was stopped prematurely.[67] It has been suggested that the negative results could be explained due to the fact that patients in the ALECSAT group started treatment 28 days after standard treatment with BEV and Irinotecan in the control group[68] and different set-up may be investigated.

Reprogramming cellular energetics

Cancer cells can reprogram their metabolism into favouring anaerob glycolysis followed by lactate acid fermentation in the cytosol,[69] thereby producing only two-three molecules of ATP per molecule glucose instead of the 38 accomplished through mitochondrial oxidative phosphorylation. This is overcome by upregulating the number of glucose uptake receptors, namely GLUT1, a trade achieved by *RAS*, *MYC* and *TP53*. The anaerobic glycolysis produces intermediates used to facilitate other biosynthetic pathways.

Five metabolic IDH genes have been defined, coding for three IDH enzymes. The enzymes are responsible for the oxidative carboxylation of isocitrate to α-ketoglutarate producing nicotinamide adenine dinucleotide phosphate (NADPH).

IDH1 is localised in the cytosol and peroxisome, delivering energy to production of peroxisomal enzymes thereby affecting many metabolic pathways. IDH2 and IDH3 are localised in the mitochondria, functioning in the tricarboxylic acid cycle, supporting cell growth.[70]

Only *IDH1* and *IDH2* are found mutated in GBM; they exert the same mutagenic effect[71] and are settled prognostic markers for lower grade gliomas and secondary GBM.[72] *IDH* is found mutated in 70% of lower grade gliomas and secondary GBM and up to 5% in primary GBM.[71]

IDH mutations decrease the normal IDH activity by approximately 50%, thereby producing less α-ketoglutarate and NADPH and instead produce the onco-metabolite 2-hydroxyglutarate (2-HG) using NADPH, which lowers NADPH further.[73] 2-HG is an inhibitor of α-ketoglutarate-dependent dioxygenases, which may cause epigenetic changes, including hypermethylation in human gliomas.[74] It can also induce an increased removal of an insulator protein, which enables increased contact to *PDGFRA*, thereby further inducing gliomagenesis.[75]

With the impaired function of the mitochondria, the production of bioenergy and intermediates is decreased hence the growth of the cancer cell is lowered when compared with IDH-WT gliomas.[76] Preliminary data suggest that inhibition of glutaminase which is necessary for production of 2-HG cause slow-down of glioma cell growth[77 78], but the data are still immature for therapeutic use.

Studies are emerging though, with the purpose to target *IDH* mutations. Hence, preliminary data for the AG120[79] trial in the glioma expansion cohort with recurrence or progression of GBM showed a response in 2% and stable disease in 83%. (Mellinghoff IK *et al* Abstract ACTR-46, SNO 2016). A phase I study AG881 with a pan inhibitor of IDH[80] is being evaluated, and another phase I study, the NOA16, is investigating treatment in grade III and IV gliomas with an IDH1 peptide vaccine targeting the IDH1R132H.[81]

In a study of 105 specimens of GBM, 12% had mutations in *IDH1* and in these, 83% had mutations in *TP53* as opposed to only 27% in the IDH1-WT tumours. None of the IDH1 mutated tumours had mutations in *PTEN*, *RB1*, *EGFR* or *NF1* as opposed to 60% in IDH1-WT tumours. The IDH mutated patients had more favourably clinical

features regarding median age at diagnosis, frequency of recurrent GBM, secondary GBM and median OS.[82]

In a meta-analysis including 24 studies with GBM and IDH1 and −2 status, it was found that IDH mutations were prognostic factors for a better OS and PFS. A total of 15 studies included data for OS. The HR was 0.36 (95% CI 0.26 to 0.49, p<0.001) favouring IDH mutations. Out of the 15 studies, eight included data for PFS, and the HR was 0.32 (95% CI 0.24 to 0.46, p<0.001) favouring IDH mutations.[83]

IDH mutations have been identified in a number of other cancer types with the highest frequency in GBM and melanoma.[84–86]

CONCLUSION AND PERSPECTIVES

The most promising next steps are in the hallmarks 'enabling replicative immortality', 'inducing angiogenesis', 'reprogramming cellular energetics' and 'evading immune destruction' where the challenge is not to find differences but to find similarities in GBM. The hallmark with the greatest clinical impact is in 'evading immune destruction', where immune therapy might actually represent a similarity in cancer treatment. Promising results have been achieved both in first-line and second-line settings, and development of clinical trials with combination therapy with different immunogenic therapies and/or radiotherapy together with predictive markers might improve results even further. Defining and developing prognostic and predictive markers for better patient selection and treatment response is important. Such could be *TERT* mutation combined with MGMT methylation, which have showed improved OS or high HLA and low angiotensinogen for treatment response with BEV. Development of liquid biopsies for these markers will increase the clinical usability. The metabolism of GBM is another promising field with the role of IDH which represents epigenetic changes and thus a possibility to target the trunk of GBM instead of the branches where the complexity increases.

More individual treatment is warranted. This is becoming even more evident with the new WHO classification. Research in the three subclasses also represents the molecular focus. The SMGs identified in each subclass has significance in each of the six hallmarks and two emerging hallmarks. Different responses to aggressive treatment together with stratification for MGMT status in each subclass have been demonstrated. This indicates that a patient with, for example, subclass proneural, MGMT non-methylated, perhaps should not be offered STUPP regimen, but rather another 1st line treatment and one might hypothesise that a patient with a mesenchymal tumour and hence more inflammation and death by necrosis might respond better to immune therapy. All this needs further validation but is a clinical meaningful way of thinking.

NGS is expanding, and the handling of and interpretation of big data from these analyses should be carefully evaluated and validated. NGS may provide a more detailed information on GBM to help overcome some of the heterogeneity that challenges today's treatment, as today's treatment is not differentiated according to, for example, molecular aberrations except *IDH* status and MGMT methylation status. This will have increased importance in the future.

With the economical accessibility, more laboratories will be performing NGS with different equipment and experience. Therefore, development of quality assessments and reproducibility is important, and NGS should only be performed in laboratories with the necessary requirements for this. The challenge is well illustrated by tests for MGMT methylation where this can be performed either by immunohistochemistry or PCR. The latter is considered the most reproducible and independent of interobserver variability, and the first is the most accessible for the community but still there is not consensus on this field.

International cooperation with data sharing is necessary in order to enter the era of precision medicine.

Contributors DSN is the main author and is responsible for the overall content of the review. HSP and UL contributed equally to the supervision process. All three authors have read the manuscript and participated in the editing process and all three authors have approved of the content.

Competing interests None declared.

Provenance and peer review Not commissioned; externally peer reviewed.

REFERENCES

1. Ostrom QT, Gittleman H, Fulop J, *et al*. CBTRUS statistical report: primary brain and central nervous system tumors diagnosed in the United States in 2008-2012. *Neuro Oncol* 2015;17(suppl 4):iv1–iv62.
2. Louis DN, Perry A, Reifenberger G, *et al*. The 2016 World Health Organization classification of tumors of the central nervous system: a summary. *Acta Neuropathol* 2016;131:803–20.
3. Stupp R, Hegi ME, Mason WP, *et al*; European Organisation for Research and Treatment of Cancer Brain Tumour and Radiation Oncology Groups National Cancer Institute of Canada Clinical Trials Group. Effects of radiotherapy with concomitant and adjuvant temozolomide versus radiotherapy alone on survival in glioblastoma in a randomised phase III study: 5-year analysis of the EORTC-NCIC trial. *Lancet Oncol* 2009;10:459–66.
4. Michaelsen SR, Christensen IJ, Grunnet K, *et al*. Clinical variables serve as prognostic factors in a model for survival from glioblastoma multiforme: an observational study of a cohort of consecutive non-selected patients from a single institution. *BMC Cancer* 2013;13:402.
5. Verhaak RG, Hoadley KA, Purdom E, *et al*; Cancer Genome Atlas Research Network. Integrated genomic analysis identifies clinically relevant subtypes of glioblastoma characterized by abnormalities in PDGFRA, IDH1, EGFR, and NF1. *Cancer Cell* 2010;17:98–110.
6. BioRxiv the present server for biology. http://biorxiv.org/content/early/2016/08/13/052076 (accessed on 29 Dec 2016).
7. Hegi ME, Diserens AC, Gorlia T, *et al*. MGMT gene silencing and benefit from temozolomide in glioblastoma. *N Engl J Med* 2005;352:997–1003.
8. Hanahan D, Weinberg RA. Hallmarks of cancer: the next generation. *Cell* 2011;144:646–74.
9. Cancer Genome Atlas Research Network. Comprehensive genomic characterization defines human glioblastoma genes and core pathways. *Nature* 2008;455:1061–8.

10. Zandi R, Larsen AB, Andersen P, *et al*. Mechanisms for oncogenic activation of the epidermal growth factor receptor. *Cell Signal* 2007;19:2013–23.
11. Brennan CW, Verhaak RG, McKenna A, *et al*; TCGA Research Network. The somatic genomic landscape of glioblastoma. *Cell* 2013;155:462–77.
12. Guerrero PA, Yin W, Camacho L, *et al*. Oncogenic role of merlin/NF2 in glioblastoma. *Oncogene* 2015;34:2621–30.
13. Houshmandi SS, Emnett RJ, Giovannini M, *et al*. The neurofibromatosis 2 protein, merlin, regulates glial cell growth in an ErbB2- and Src-dependent manner. *Mol Cell Biol* 2009;29:1472–86.
14. Shackelford DB, Shaw RJ. The LKB1-AMPK pathway: metabolism and growth control in tumour suppression. *Nat Rev Cancer* 2009;9:563–75.
15. Knudsen ES, Knudsen KE. Tailoring to RB: tumour suppressor status and therapeutic response. *Nat Rev Cancer* 2008;8:714–24.
16. Bamford S, Dawson E, Forbes S, *et al*. The COSMIC (Catalogue of Somatic Mutations in Cancer) database and website. *Br J Cancer* 2004;91:355–8.
17. Derenzini M, Donati G, Mazzini G, *et al*. Loss of retinoblastoma tumor suppressor protein makes human breast cancer cells more sensitive to antimetabolite exposure. *Clin Cancer Res* 2008;14:2199–209.
18. Agerbaek M, Alsner J, Marcussen N, *et al*. Retinoblastoma protein expression is an independent predictor of both radiation response and survival in muscle-invasive bladder cancer. *Br J Cancer* 2003;89:298–304.
19. Xiu J, Piccioni D, Juarez T, *et al*. Multi-platform molecular profiling of a large cohort of glioblastomas reveals potential therapeutic strategies. *Oncotarget* 2016;7:21556–69.
20. Marcel V, Dichtel-Danjoy ML, Sagne C, *et al*. Biological functions of p53 isoforms through evolution: lessons from animal and cellular models. *Cell Death Differ* 2011;18:1815–24.
21. Bouaoun L, Sonkin D, Ardin M, *et al*. TP53 variations in human cancers: New lessons from the IARC TP53 database and genomics data. *Hum Mutat* 2016;37:865–76.
22. Marcel V, Palmero EI, Falagan-Lotsch P, *et al*. TP53 PIN3 and MDM2 SNP309 polymorphisms as genetic modifiers in the Li-Fraumeni syndrome: impact on age at first diagnosis. *J Med Genet* 2009;46:766–72.
23. Petitjean A, Mathe E, Kato S, *et al*. Impact of mutant p53 functional properties on TP53 mutation patterns and tumor phenotype: lessons from recent developments in the IARC TP53 database. *Hum Mutat* 2007;28:622–9.
24. Wong TN, Ramsingh G, Young AL, *et al*. Role of TP53 mutations in the origin and evolution of therapy-related acute myeloid leukaemia. *Nature* 2015;518:552–5.
25. Johansen MD, Rochat P, Law I, *et al*. Presentation of two cases with early extracranial metastases from glioblastoma and review of the literature. *Case Rep Oncol Med* 2016;2016:1–5.
26. Sin WC, Crespin S, Mesnil M. Opposing roles of connexin43 in glioma progression. *Biochim Biophys Acta* 1818;2012:2058–67.
27. Tafani M, Di Vito M, Frati A, *et al*. Pro-inflammatory gene expression in solid glioblastoma microenvironment and in hypoxic stem cells from human glioblastoma. *J Neuroinflammation* 2011;8:32.
28. Hollier BG, Evans K, Mani SA. The epithelial-to-mesenchymal transition and cancer stem cells: a coalition against cancer therapies. *J Mammary Gland Biol Neoplasia* 2009;14:29–43.
29. Iser IC, Pereira MB, Lenz G, *et al*. The Epithelial-to-Mesenchymal transition-like process in glioblastoma: an updated systematic review and in silico investigation. *Med Res Rev* 2016.
30. Guarino M, Rubino B, Ballabio G. The role of epithelial-mesenchymal transition in cancer pathology. *Pathology* 2007;39:305–18.
31. Iwadate Y, Matsutani T, Hirono S, *et al*. Transforming growth factor-β and stem cell markers are highly expressed around necrotic areas in glioblastoma. *J Neurooncol* 2016;129:101–7.
32. Murat A, Migliavacca E, Gorlia T, *et al*. Stem cell-related "self-renewal" signature and high epidermal growth factor receptor expression associated with resistance to concomitant chemoradiotherapy in glioblastoma. *J Clin Oncol* 2008;26:3015–24.
33. Ceccarelli M, Barthel FP, Malta TM, *et al*; TCGA Research Network. Molecular profiling reveals biologically discrete subsets and pathways of progression in diffuse glioma. *Cell* 2016;164:550–63.
34. Nguyen HN, Lie HN, Li HN, et al. Human TERT promoter mutation enables survival advantage from MGMT promoter methylation in IDH1 wild-type primary glioblastoma treated by standard chemoradiotherapy. *Neuro Oncol* 2016. Epub ahead of print: 29 Aug 2016.
35. Patenaude A, Parker J, Karsan A. Involvement of endothelial progenitor cells in tumor vascularization. *Microvasc Res* 2010;79:217–23.
36. Poulsen HS, Urup T, Michaelsen SR, *et al*. The impact of bevacizumab treatment on survival and quality of life in newly diagnosed glioblastoma patients. *Cancer Manag Res* 2014;6:373–87.
37. Fu P, He YS, Huang Q, *et al*. Bevacizumab treatment for newly diagnosed glioblastoma: Systematic review and meta-analysis of clinical trials. *Mol Clin Oncol* 2016;4:833–8.
38. Chinot OL, Wick W, Mason W, *et al*. Bevacizumab plus radiotherapy-temozolomide for newly diagnosed glioblastoma. *N Engl J Med* 2014;370:709–22.
39. Gilbert MR, Dignam JJ, Armstrong TS, *et al*. A randomized trial of bevacizumab for newly diagnosed glioblastoma. *N Engl J Med* 2014;370:699–708.
40. Lu-Emerson C, Snuderl M, Kirkpatrick ND, *et al*. Increase in tumor-associated macrophages after antiangiogenic therapy is associated with poor survival among patients with recurrent glioblastoma. *Neuro Oncol* 2013;15:1079–87.
41. Iwadate Y. Epithelial-mesenchymal transition in glioblastoma progression. *Oncol Lett* 2016;11:1615–20.
42. Urup T, Michaelsen SR, Olsen LR, *et al*. Angiotensinogen and HLA class II predict bevacizumab response in recurrent glioblastoma patients. *Mol Oncol* 2016;10:1160–8.
43. Degenhardt K, Mathew R, Beaudoin B, *et al*. Autophagy promotes tumor cell survival and restricts necrosis, inflammation, and tumorigenesis. *Cancer Cell* 2006;10:51–64.
44. Jiang H, White EJ, Conrad C, *et al*. Autophagy pathways in glioblastoma. *Methods Enzymol* 2009;453:273–86.
45. Lefranc F, Kiss R. Autophagy, the Trojan horse to combat glioblastomas. *Neurosurg Focus* 2006;20:E7.
46. Kanzawa T, Germano IM, Komata T, *et al*. Role of autophagy in temozolomide-induced cytotoxicity for malignant glioma cells. *Cell Death Differ* 2004;11:448–57.
47. Ohsumi Y. Historical landmarks of autophagy research. *Cell Res* 2014;24:9–23.
48. Jennewein L, Ronellenfitsch MW, Antonietti P, *et al*. Diagnostic and clinical relevance of the autophago-lysosomal network in human gliomas. *Oncotarget* 2016;7:20016–32.
49. Gajewski TF, Schreiber H, Fu YX. Innate and adaptive immune cells in the tumor microenvironment. *Nat Immunol* 2013;14:1014–22.
50. Fuertes MB, Kacha AK, Kline J, *et al*. Host type I IFN signals are required for antitumor CD8+ T cell responses through CD8{alpha}+ dendritic cells. *J Exp Med* 2011;208:2005–16.
51. Watkins S, Robel S, Kimbrough IF, *et al*. Disruption of astrocyte-vascular coupling and the blood-brain barrier by invading glioma cells. *Nat Commun* 2014;5:4196.
52. Gedeon PC, Choi BD, Sampson JH, *et al*. Rindopepimut: anti-EGFRvIII peptide vaccine, oncolytic. *Drugs Future* 2013;38:147–55.
53. A Study of Rindopepimut/GM-CSF in patients with relapsed EGFRvIII-positive glioblastoma. https://clinicaltrials.gov/NCT01498328 (accessed 29 Dec 2016).
54. Schuster J, Lai RK, Recht LD, *et al*. A phase II, multicenter trial of rindopepimut (CDX-110) in newly diagnosed glioblastoma: the ACT III study. *Neuro Oncol* 2015;17:854–61.
55. Phase III Study of Rindopepimut/GM-CSF in patients with newly diagnosed glioblastoma. https://clinicaltrials.gov/NCT01480479 (accessed 29 Dec 2016).
56. GAPVAC phase I trial in newly diagnosed glioblastoma patients. https://clinicaltrials.gov/NCT02149225 (accessed 29 Dec 2016).
57. Palucka K, Banchereau J. Cancer immunotherapy via dendritic cells. *Nat Rev Cancer* 2012;12:265–77.
58. Okada H, Kalinski P, Ueda R, *et al*. Induction of CD8+ T-cell responses against novel glioma-associated antigen peptides and clinical activity by vaccinations with {alpha}-type 1 polarized dendritic cells and polyinosinic-polycytidylic acid stabilized by lysine and carboxymethylcellulose in patients with recurrent malignant glioma. *J Clin Oncol* 2011;29:330–6.
59. Verdijk P, Aarntzen EH, Lesterhuis WJ, *et al*. Limited amounts of dendritic cells migrate into the T-cell area of lymph nodes but have high immune activating potential in melanoma patients. *Clin Cancer Res* 2009;15:2531–40.
60. Martln-Fontecha A, Sebastiani S, Höpken UE, *et al*. Regulation of dendritic cell migration to the draining lymph node: impact on T lymphocyte traffic and priming. *J Exp Med* 2003;198:615–21.

61. Hodi FS, O'Day SJ, McDermott DF, *et al*. Improved survival with ipilimumab in patients with metastatic melanoma. *N Engl J Med* 2010;363:711–23.
62. Study of nivolumab compared to temozolomide, given with radiation therapy, for newly-diagnosed patients with glioblastoma (GBM, a Malignant Brain Cancer). http://www.clinicaltrials.gov/NCT02617589 (accessed 29 Dec 2016).
63. Study of temozolomide plus radiation therapy with nivolumab or placebo, for newly diagnosed patients with glioblastoma (GBM, a Malignant Brain Cancer). http://www.clinicaltrials.gov/NCT02667587 (accessed 29 Dec 2016).
64. Desai R, Suryadevara CM, Batich KA, *et al*. Emerging immunotherapies for glioblastoma. *Expert Opin Emerg Drugs* 2016;21:133–45.
65. Merrill MK, Bernhardt G, Sampson JH, *et al*. Poliovirus receptor CD155-targeted oncolysis of glioma. *Neuro Oncol* 2004;6:208–17.
66. Brown MC, Gromeier M. Cytotoxic and immunogenic mechanisms of recombinant oncolytic poliovirus. *Curr Opin Virol* 2015;13:81–5.
67. Randomized phase 2 study to investigate efficacy of ALECSAT in patients with GBM measured compared to avastin/Irinotecan. http://www.clinicaltrials.gov/NCT02060955 (accessed 29 Dec 2016).
68. http://cytovac.com/clinical-data/brain-cancer (accessed 29 Dec 2016).
69. López-Lázaro M. The warburg effect: why and how do cancer cells activate glycolysis in the presence of oxygen? *Anticancer Agents Med Chem* 2008;8:305–12.
70. Xu X, Zhao J, Xu Z, *et al*. Structures of human cytosolic NADP-dependent isocitrate dehydrogenase reveal a novel self-regulatory mechanism of activity. *J Biol Chem* 2004;279:33946–57.
71. Yan H, Parsons DW, Jin G, *et al*. IDH1 and IDH2 mutations in gliomas. *N Engl J Med* 2009;360:765–73.
72. Brat DJ, Verhaak RG, Aldape KD, *et al*; Cancer Genome Atlas Research Network. Comprehensive, Integrative Genomic Analysis of Diffuse Lower-Grade Gliomas. *N Engl J Med* 2015;372:2481–98.
73. Bleeker FE, Atai NA, Lamba S, *et al*. The prognostic IDH1(R132) mutation is associated with reduced NADP+-dependent IDH activity in glioblastoma. *Acta Neuropathol* 2010;119:487–94.
74. Christensen BC, Smith AA, Zheng S, *et al*. DNA methylation, isocitrate dehydrogenase mutation, and survival in glioma. *J Natl Cancer Inst* 2011;103:143–53.
75. Flavahan WA, Drier Y, Liau BB, *et al*. Insulator dysfunction and Oncogene activation in IDH mutant gliomas. *Nature* 2016; 529:110–4.
76. Zhang C, Moore LM, Li X, *et al*. IDH1/2 mutations target a key hallmark of cancer by deregulating cellular metabolism in glioma. *Neuro Oncol* 2013;15:1114–26.
77. Guo C, Pirozzi CJ, Lopez GY, *et al*. Isocitrate dehydrogenase mutations in gliomas: mechanisms, biomarkers and therapeutic target. *Curr Opin Neurol* 2011;24:648–52.
78. Seltzer MJ, Bennett BD, Joshi AD, *et al*. Inhibition of glutaminase preferentially slows growth of glioma cells with mutant IDH1. *Cancer Res* 2010;70:8981–7.
79. Study of orally administered AG-120 in subjects with advanced solid tumors, including glioma, With an IDH1 mutation. https://clinicaltrials.gov/NCT02073994 (accessed 29 Dec 2016).
80. Study of orally administered AG-881 in patients with advanced solid tumors, including gliomas, with an IDH1 and/or IDH2 mutation. https://clinicaltrials.gov/NCT02481154 (accessed 29 Dec 2016).
81. Phase I trial of IDH1 peptide vaccine in IDH1R132H-mutated grade III-IV gliomas. https://clinicaltrials.gov/NCT02454634 (accessed 29 Dec 2016).
82. Parsons DW, Jones S, Zhang X, *et al*. An integrated genomic analysis of human glioblastoma multiforme. *Science* 2008;321:1807–12.
83. Chen JR, Yao Y, Xu HZ, *et al*. Isocitrate dehydrogenase (IDH)1/2 Mutations as Prognostic Markers in Patients With Glioblastomas. *Medicine* 2016;95:e2583.
84. Kang MR, Kim MS, Oh JE, *et al*. Mutational analysis of IDH1 codon 132 in glioblastomas and other common cancers. *Int J Cancer* 2009;125:353–5.
85. Shen Y, Zhu YM, Fan X, *et al*. Gene mutation patterns and their prognostic impact in a cohort of 1185 patients with acute myeloid leukemia. *Blood* 2011;118:5593–603.
86. Sjöblom T, Jones S, Wood LD, *et al*. The consensus coding sequences of human breast and colorectal cancers. *Science* 2006;314:268–74.
87. Favaloro B, Allocati N, Graziano V et al. Role of Apoptosis in disease. *Aging* 2012;4(5):330–49.